Studies of missing-energy final states focusing on $B^+ \to K^+ \nu\bar{\nu}$ at Belle II

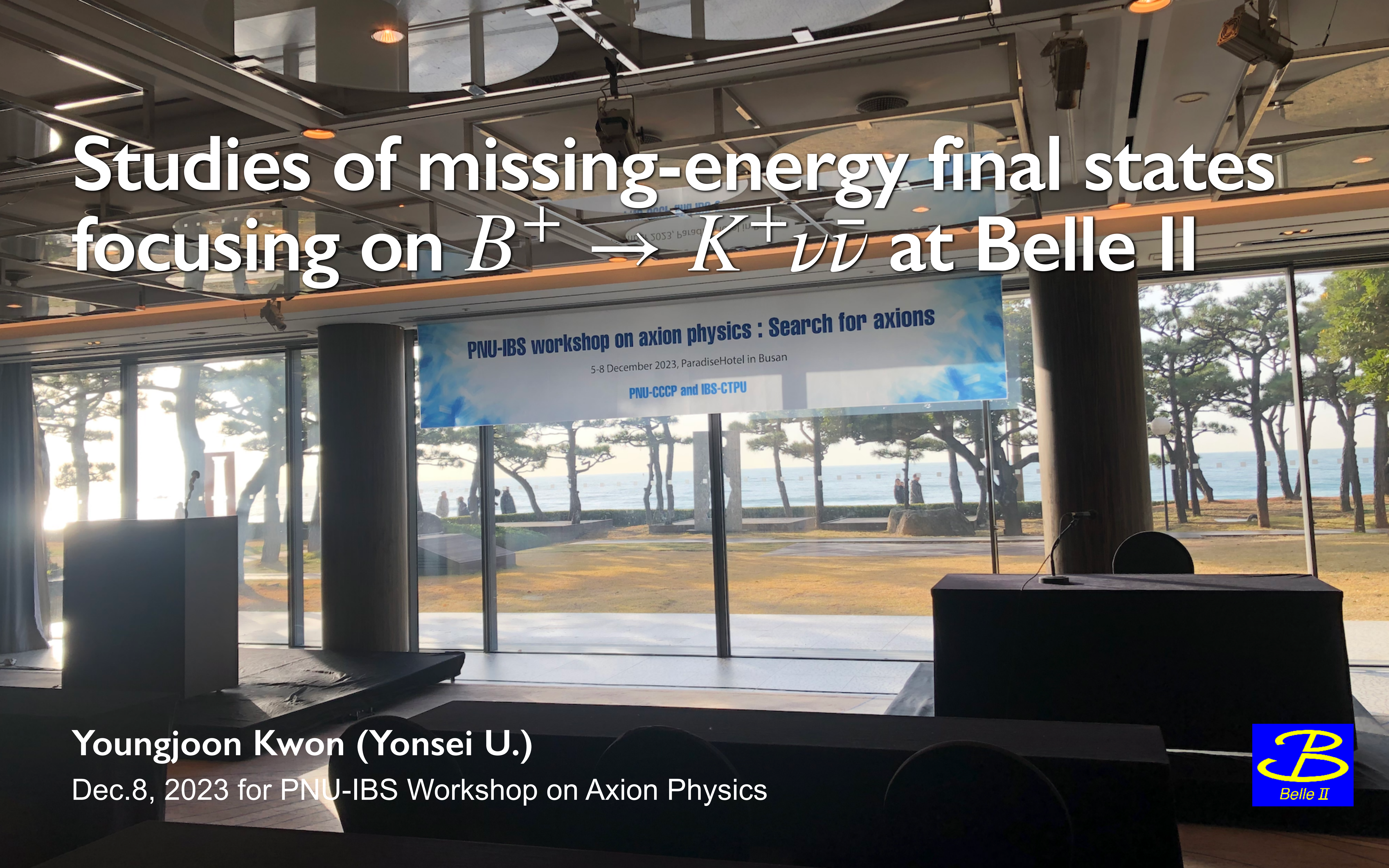

Youngjoon Kwon (Yonsei U.)

Dec.8, 2023 for PNU-IBS Workshop on Axion Physics

Belle II

Overview

- Quick intro. to Belle II
- (起) ALP search at Belle II — **Belle II** PRL 125, 161806 (2020)
- (承) Test of LFU at Belle II
  - Exclusive, $R(D^{(*)})$ — **Belle II** *preliminary* (EPS-HEP 2023)
  - Incluisve, $R(X_{\tau/\ell})$ — **Belle II** arXiv:2311.07248
- (轉) $B^+ \to K^+ \nu \overline{\nu}$ — **Belle II** arXiv:2311.14647
- (結) Closing

SuperKEKB $e^- \xrightarrow{7\text{ GeV}} (\star) \xleftarrow{4\text{ GeV}} e^+$ Belle II

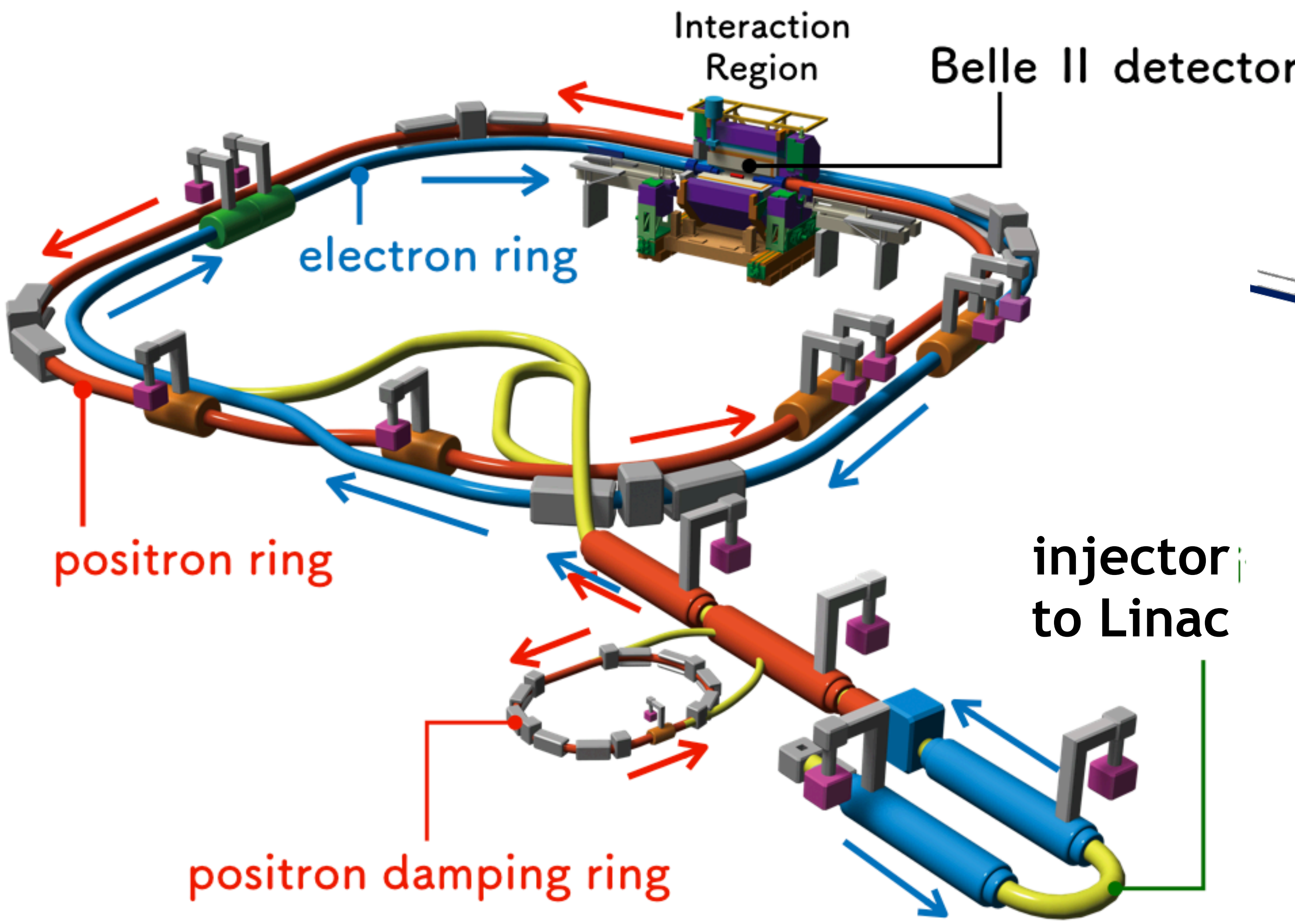

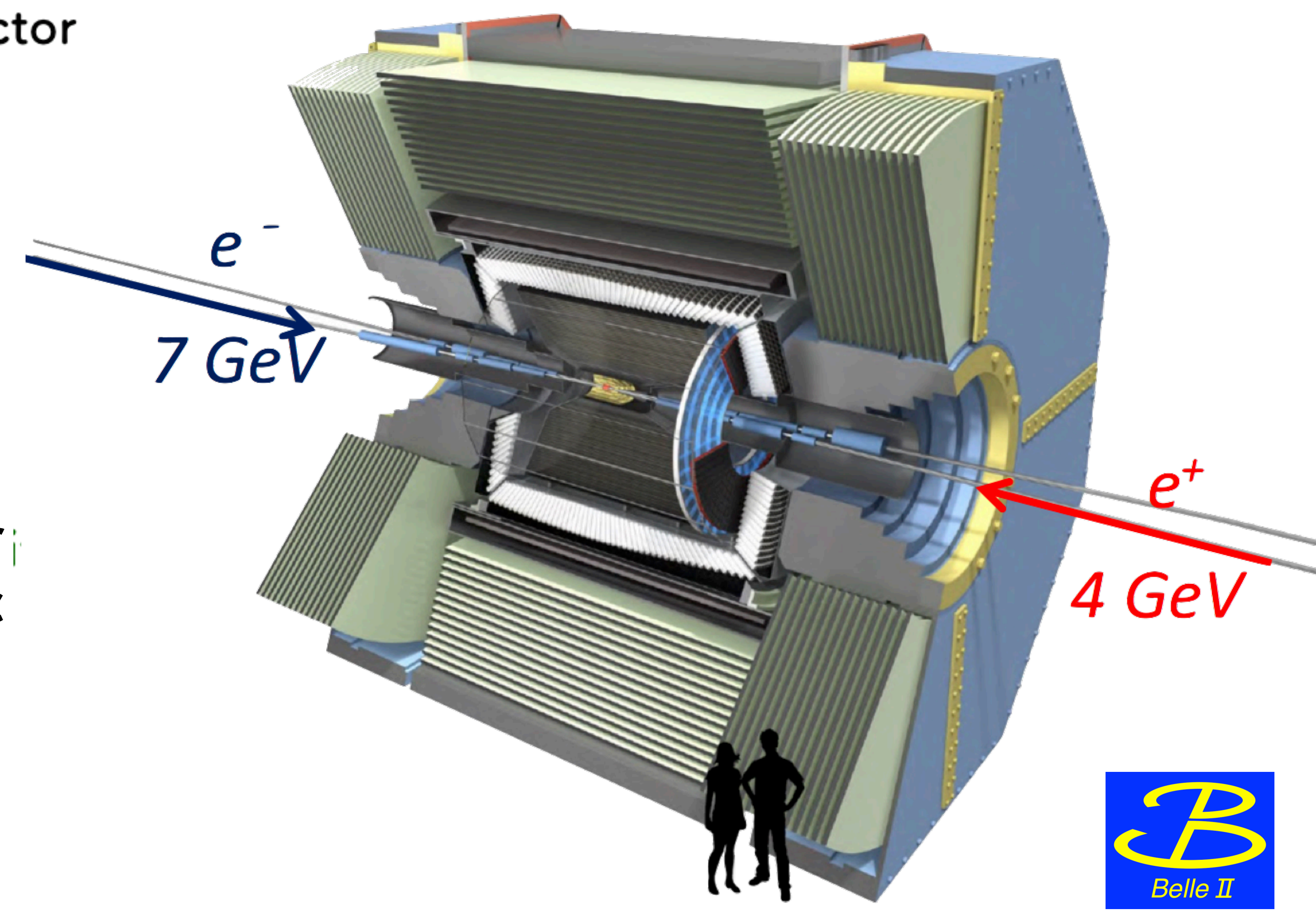

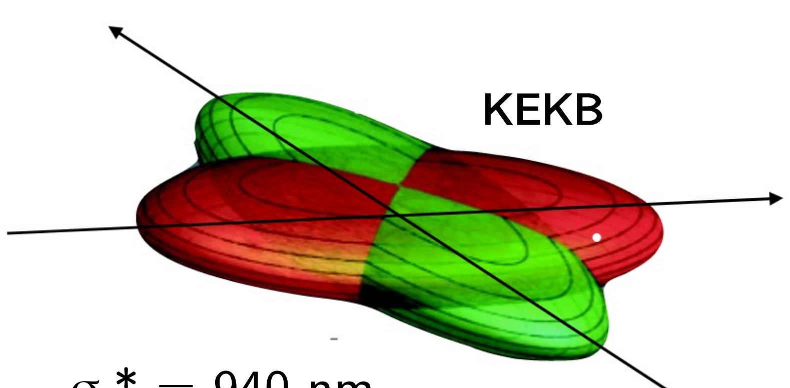

$\sigma_y^* = 940$ nm

$\beta_y^* = 5.9$ mm

$\sigma_x^* = 147/170$ µm

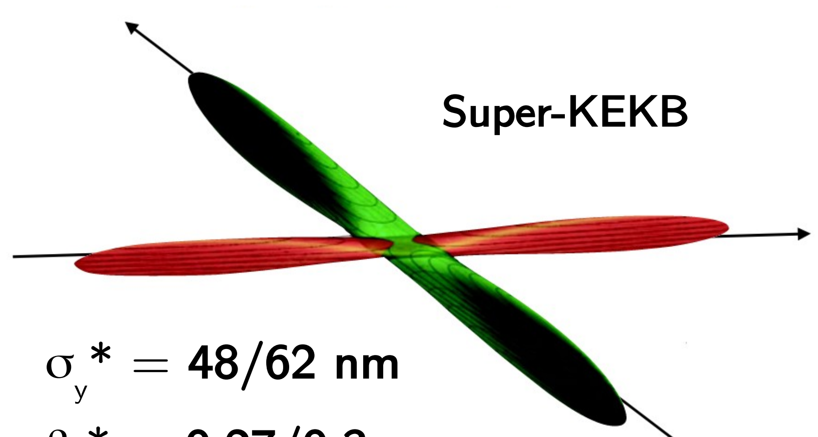

$\sigma_y^* = 48/62$ nm

$\beta_y^* = 0.27/0.3$ mm

$\sigma_x^* = 10.1/10.7$ µm

$$\mathcal{L}_{\rm II}^{\rm peak} \approx 30 \times \mathcal{L}_{\rm I}^{\rm peak}$$

$$\int^{\rm goal} \mathcal{L}_{\rm II}\, dt = 50\ {\rm ab}^{-1} \approx 50 \int \mathcal{L}_{\rm I}\, dt$$

The Belle II Collaboration

26 countries/regions, ~120 institutions, ~1000 collaborators

Belle II Collected luminosity before LS1 (2019-2022)

Belle II has been in operation through the Pandemic era, with modified working mode in accordance with the anti-pandemic policy.

peak luminosity world record

$4.7 \times 10^{34}\ \text{cm}^{-2}\text{s}^{-1}$

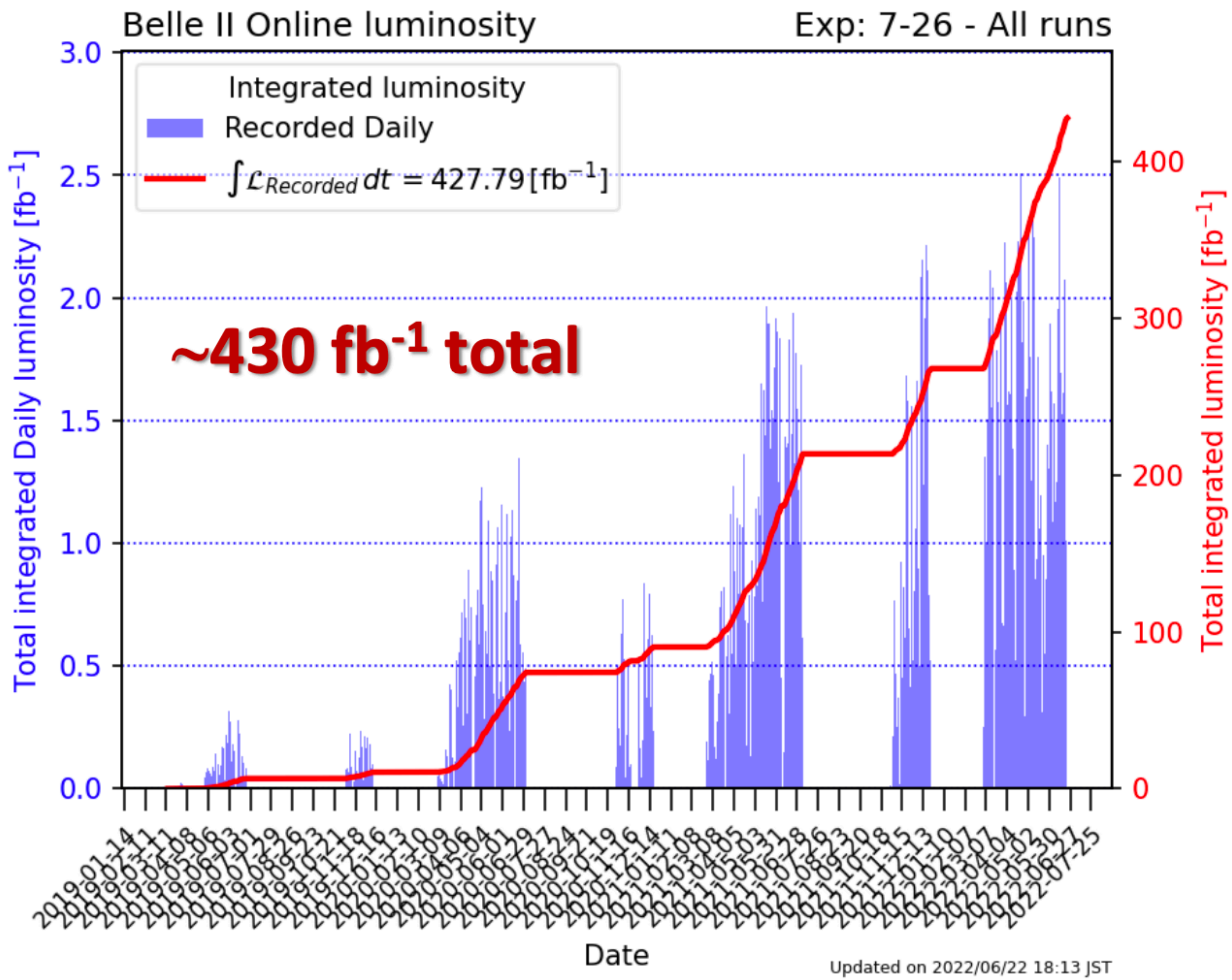

Belle II Physics Mind-map

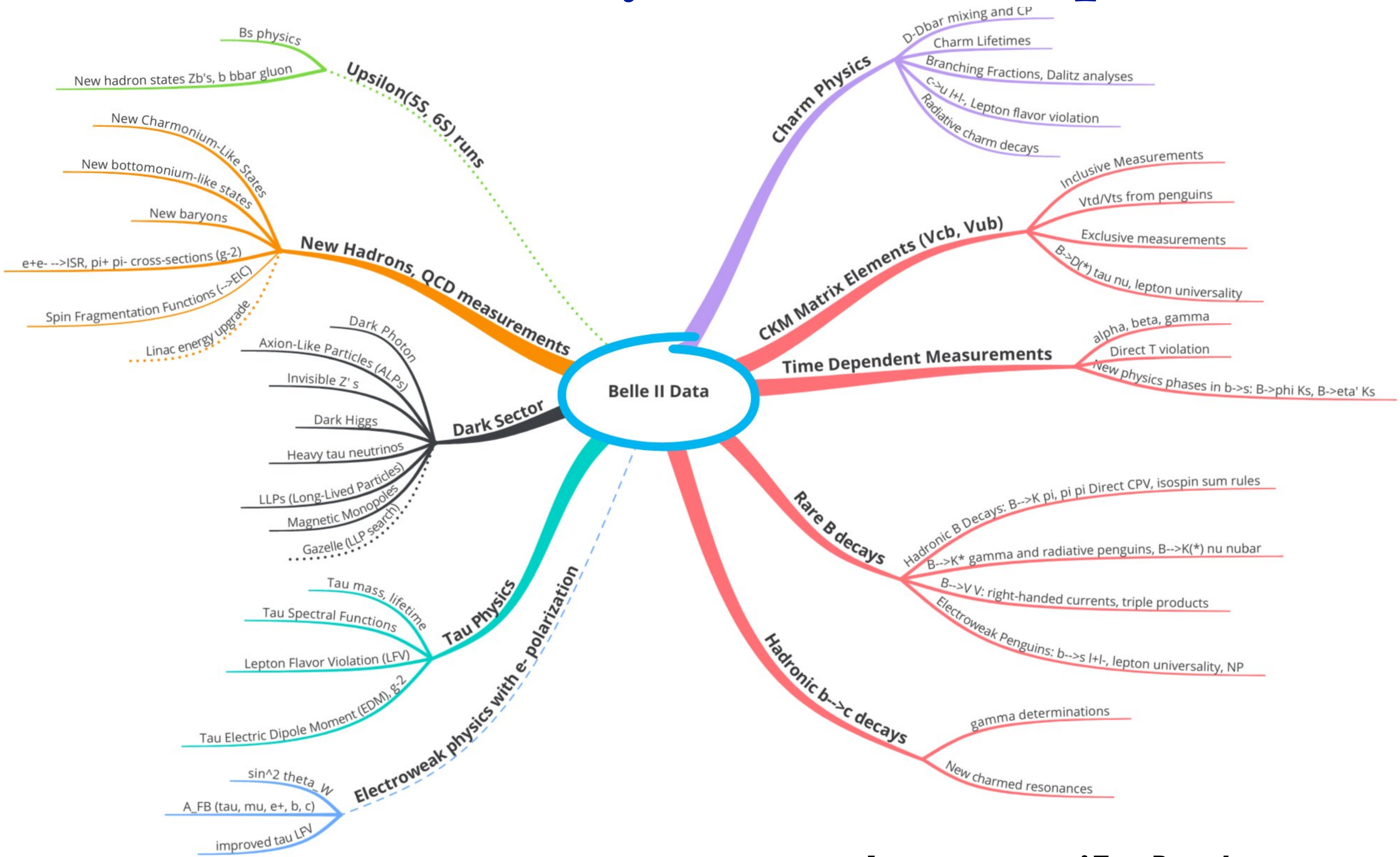

Image courtesy of Tom Browder

Belle II Physics Mind-map

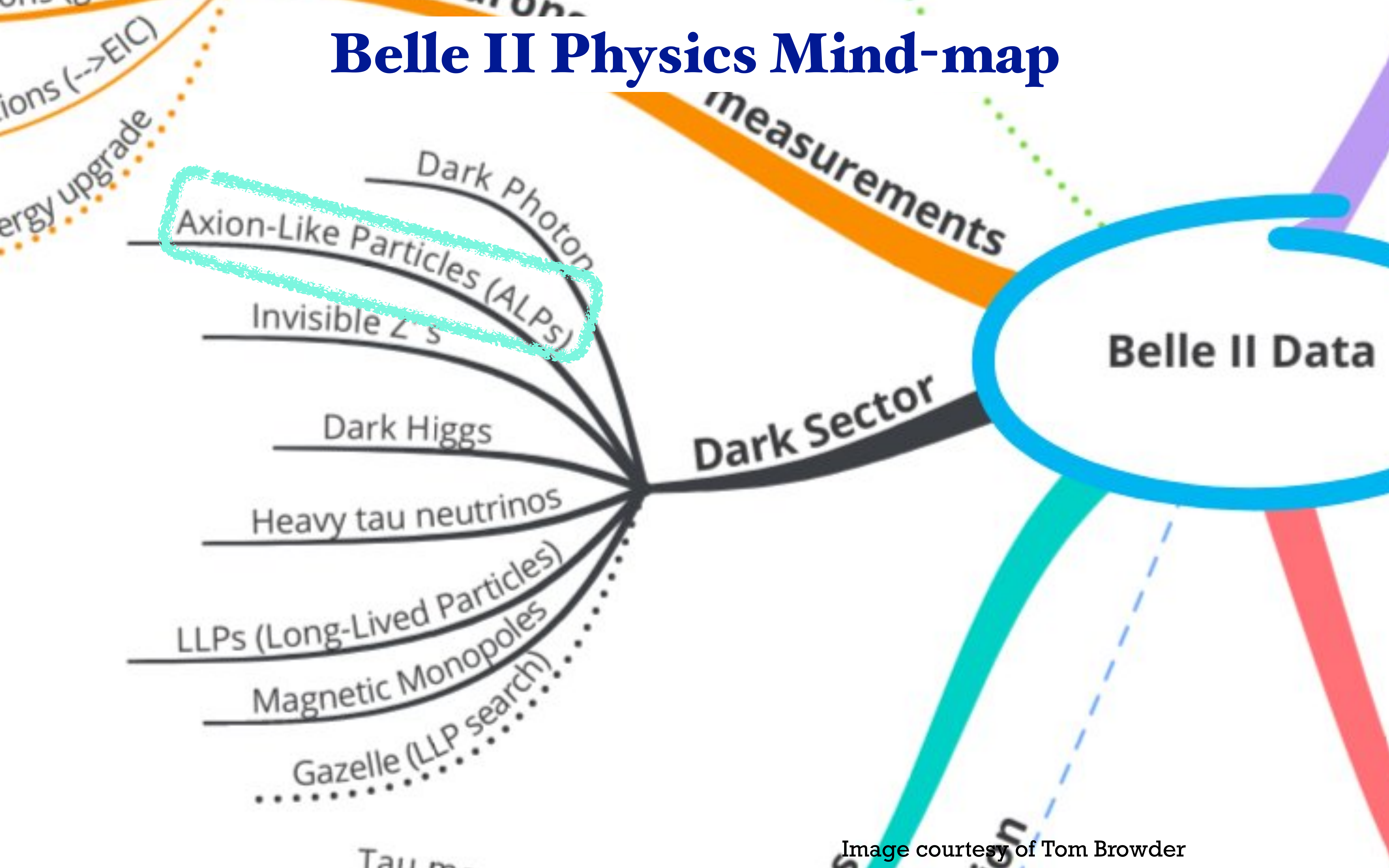

Image courtesy of Tom Browder

Belle II Physics Mind-map

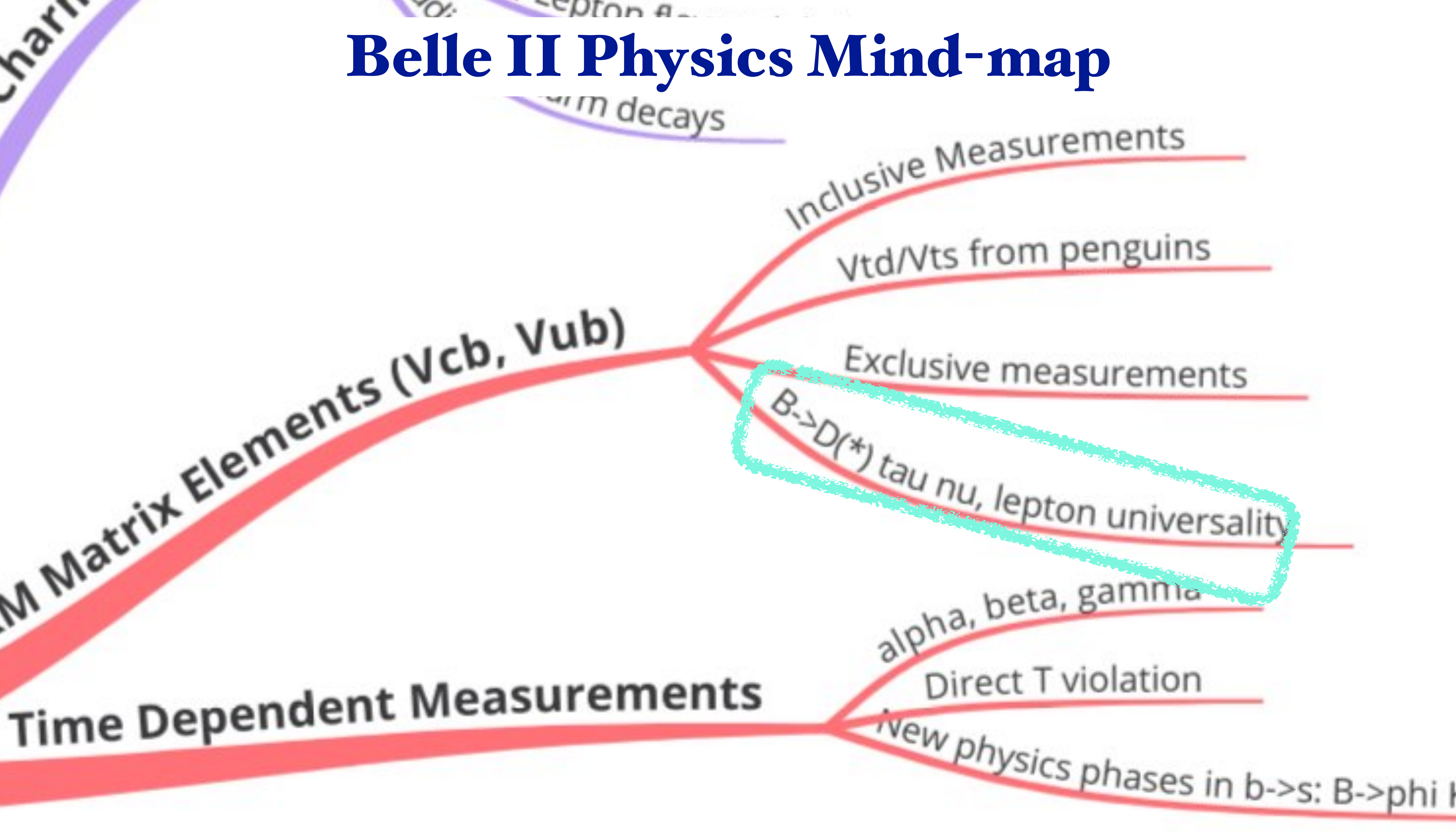

Image courtesy of Tom Browder

Belle II Physics Mind-map

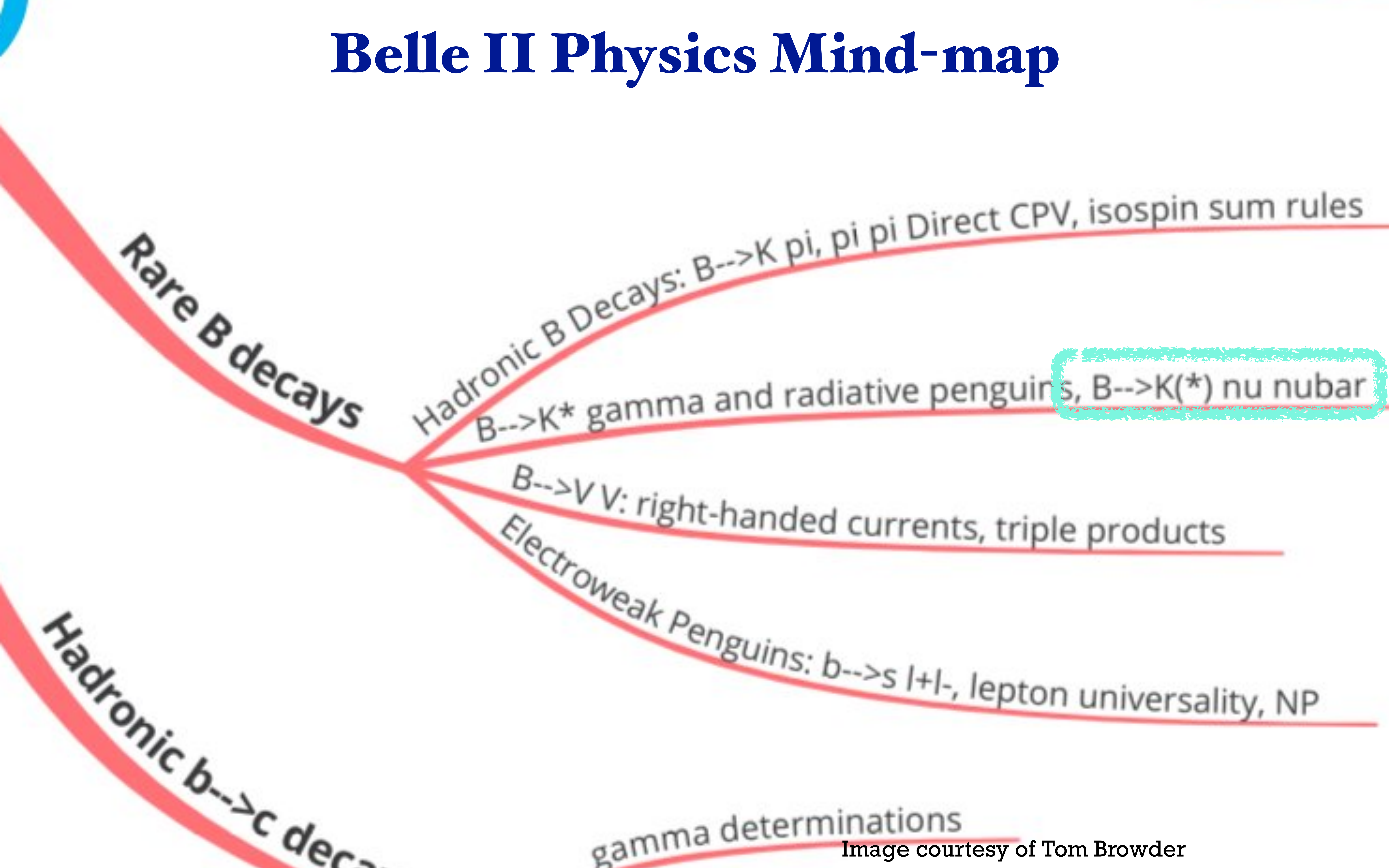

Image courtesy of Tom Browder

How to handle a missing particle at Belle II?

- $e^+e^- \to \Upsilon(4S) \to B\overline{B}$
  - only two B mesons in the final state
  - Since the initial state is clearly determined, fully accounting one B (B_{tag}) makes it possible to constrain the accompanying B (B_{sig})
  - Having a single missing particle (e.g. ν) is usually as clean as getting all particles measured
  - The price to pay is a big drop of efficiency ($< \mathcal{O}(1\%)$)

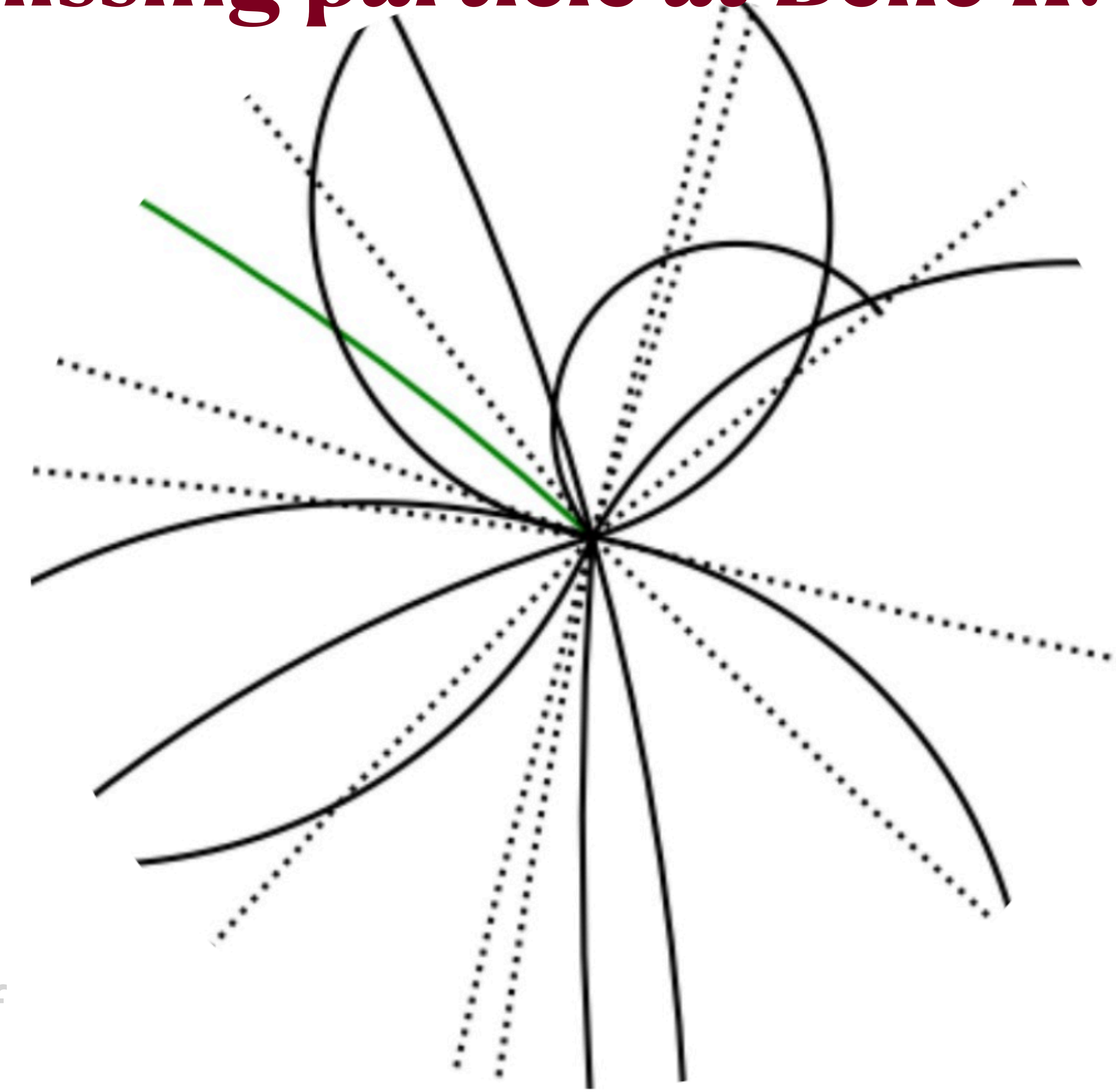

How to handle a missing particle at Belle II?

- $e^+e^- \to \Upsilon(4S) \to B\overline{B}$
  - only two B mesons in the final state
  - Since the initial state is clearly determined, fully accounting one B ($B_{\rm tag}$) makes it possible to constrain the accompanying B ($B_{\rm sig}$)
  - Having a single missing particle (e.g. ν) is usually as clean as getting all particles measured
  - The price to pay is a big drop of efficiency ($< \mathcal{O}(1\%)$)

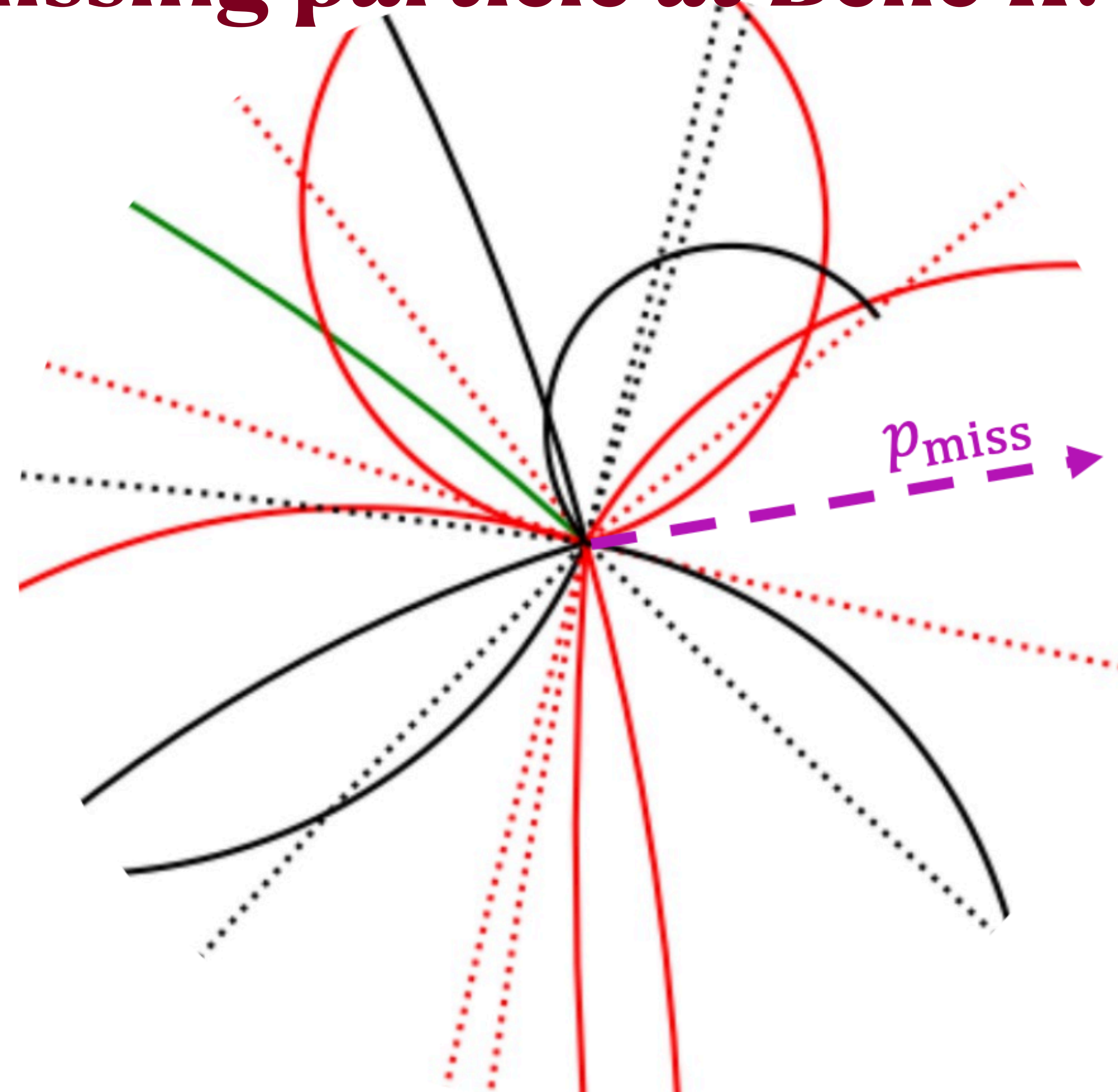

ALP search at Belle II

PHYSICAL REVIEW LETTERS **125,** 161806 (2020)

Search for Axionlike Particles Produced in e^+e^- Collisions at Belle II

F. Abudinén,[42] I. Adachi,[21,18] H. Aihara,[115] N. Akopov,[121] A. Aloisio,[87,35] F. Ameli,[39] N. Anh Ky,[32,11] D. M. Asner,[2] T. Aushev,[23] V. Aushev,[77] V. Babu,[9] S. Baehr,[46] S. Bahinipati,[25] P. Bambade,[96] Sw. Banerjee,[105] S. Bansal,[68] J. Baudot,[97] J. Becker,[46] P. K. Behera,[27] J. V. Bennett,[109] E. Bernieri,[40] F. U. Bernlochner,[99] M. Bertemes,[29] M. Bessner,[102] S. Bettarini,[90,38] V. Bhardwaj,[24] F. Bianchi,[93,41] T. Bilka,[5] S. Bilokin,[52] D. Biswas,[105] M. Bračko,[107,76] P. Branchini,[40] N. Braun,[46] T. E. Browder,[102] A. Budano,[40] S. Bussino,[92,40] M. Campajola,[87,35] G. Casarosa,[90,38] C. Cecchi,[89,37] D. Červenkov,[5] M.-C. Chang,[14] P. Chang,[61] R. Cheaib,[100] V. Chekelian,[55] B. G. Cheon,[20] K. Chilikin,[50] K. Chirapatpimol,[6] H.-E. Cho,[20] K. Cho,[47] S.-J. Cho,[122] S.-K. Choi,[19] D. Cinabro,[119] L. Corona,[90,38] L. M. Cremaldi,[109] S. Cunliffe,[9] N. Dash,[27] F. Dattola,[9] E. De La Cruz-Burelo,[4] G. De Nardo,[87,35] M. De Nuccio,[9] G. De Pietro,[40] R. de Sangro,[34] M. Destefanis,[93,41] A. De Yta-Hernandez,[4] F. Di Capua,[87,35] Z. Doležal,[5] T. V. Dong,[15] K. Dort,[45] D. Dossett,[108] G. Dujany,[97] S. Eidelman,[3,50,64] T. Ferber,[9] D. Ferlewicz,[108] S. Fiore,[39] A. Fodor,[56] F. Forti,[90,38] B. G. Fulsom,[67] E. Ganiev,[94,42] R. Garg,[68] A. Garmash,[3,64] V. Gaur,[118] A. Gaz,[58,59] U. Gebauer,[16] A. Gellrich,[9] T. Geßler,[45] R. Giordano,[87,35] A. Giri,[26] B. Gobbo,[42] R. Godang,[112] P. Goldenzweig,[46] B. Golob,[104,76] P. Gomis,[33] W. Gradl,[44] E. Graziani,[40] D. Greenwald,[79] C. Hadjivasiliou,[67] S. Halder,[78] O. Hartbrich,[102] K. Hayasaka,[63] H. Hayashii,[60] C. Hearty,[100,31] M. T. Hedges,[102] I. Heredia de la Cruz,[4,8] M. Hernández Villanueva,[109] A. Hershenhorn,[100] T. Higuchi,[116] E. C. Hill,[100] H. Hirata,[58] M. Hoek,[44] M. Hohmann,[108] C.-L. Hsu,[114] Y. Hu,[30] K. Inami,[58] G. Inguglia,[29] J. Irakkathil Jabbar,[46] A. Ishikawa,[21,18] R. Itoh,[21,18] P. Jackson,[98] W. W. Jacobs,[28] D. E. Jaffe,[2] E.-J. Jang,[19] S. Jia,[15] Y. Jin,[42] C. Joo,[116] A. B. Kaliyar,[78] J. Kandra,[5] G. Karyan,[121] Y. Kato,[58,59] H. Kichimi,[21] C. Kiesling,[55] C.-H. Kim,[20] D. Y. Kim,[75] H. J. Kim,[49] S.-H. Kim,[72] Y.-K. Kim,[122] T. D. Kimmel,[118] K. Kinoshita,[101] C. Kleinwort,[9] P. Kodyš,[5] T. Koga,[21] S. Kohani,[102] I. Komarov,[9] S. Korpar,[107,76] T. M. G. Kraetzschmar,[55] P. Križan,[104,76] P. Krokovny,[3,64] T. Kuhr,[52] M. Kumar,[54] R. Kumar,[70] K. Kumara,[119] S. Kurz,[9] Y.-J. Kwon,[122] S. Lacaprara,[36] C. La Licata,[116] L. Lanceri,[42] J. S. Lange,[45] I.-S. Lee,[20] S. C. Lee,[49] P. Leitl,[55] D. Levit,[79] P. M. Lewis,[99] C. Li,[51] L. K. Li,[101] Y. B. Li,[69] J. Libby,[27] K. Lieret,[52] L. Li Gioi,[55] Z. Liptak,[102] Q. Y. Liu,[15] D. Liventsev,[119,21] S. Longo,[9] T. Luo,[15]

Search for ALPs at Belle II

- Search for axion-like particles in $e^+e^- \to \gamma a$
  for $a \to \gamma\gamma$ (i.e. 3γ final state) and $a \to$ invisible (i.e. $\gamma + \not{p}$)
- use 2018 data of Belle II with $\int \mathscr{L} dt = (496 \pm 3)\ \mathrm{pb}^{-1}$
  - ✓ use 10% data for optimization and measure with $445\ \mathrm{pb}^{-1}$
- m_a-dependent E_γ threshold
  - ✓ 1.0 GeV for $m_a \leq 4$ GeV, and 0.65 GeV for $m_a > 4$ GeV,
- Require $0.88 \leq M_{3\gamma}/\sqrt{s} \leq 1.03$
  - ✓ study Data sideband with $M_{3\gamma}/\sqrt{s} \leq 0.88$

M^2 resolution

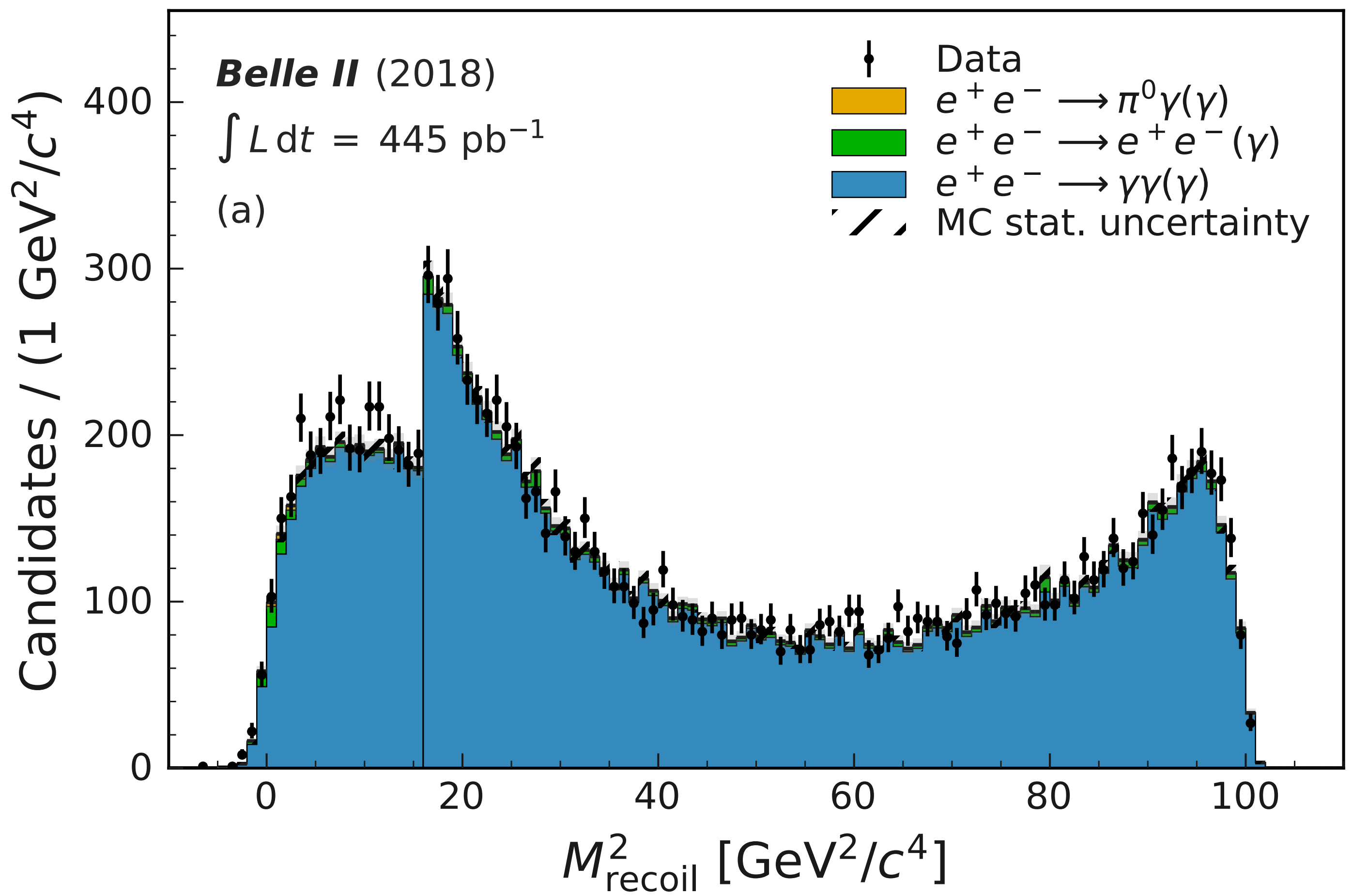

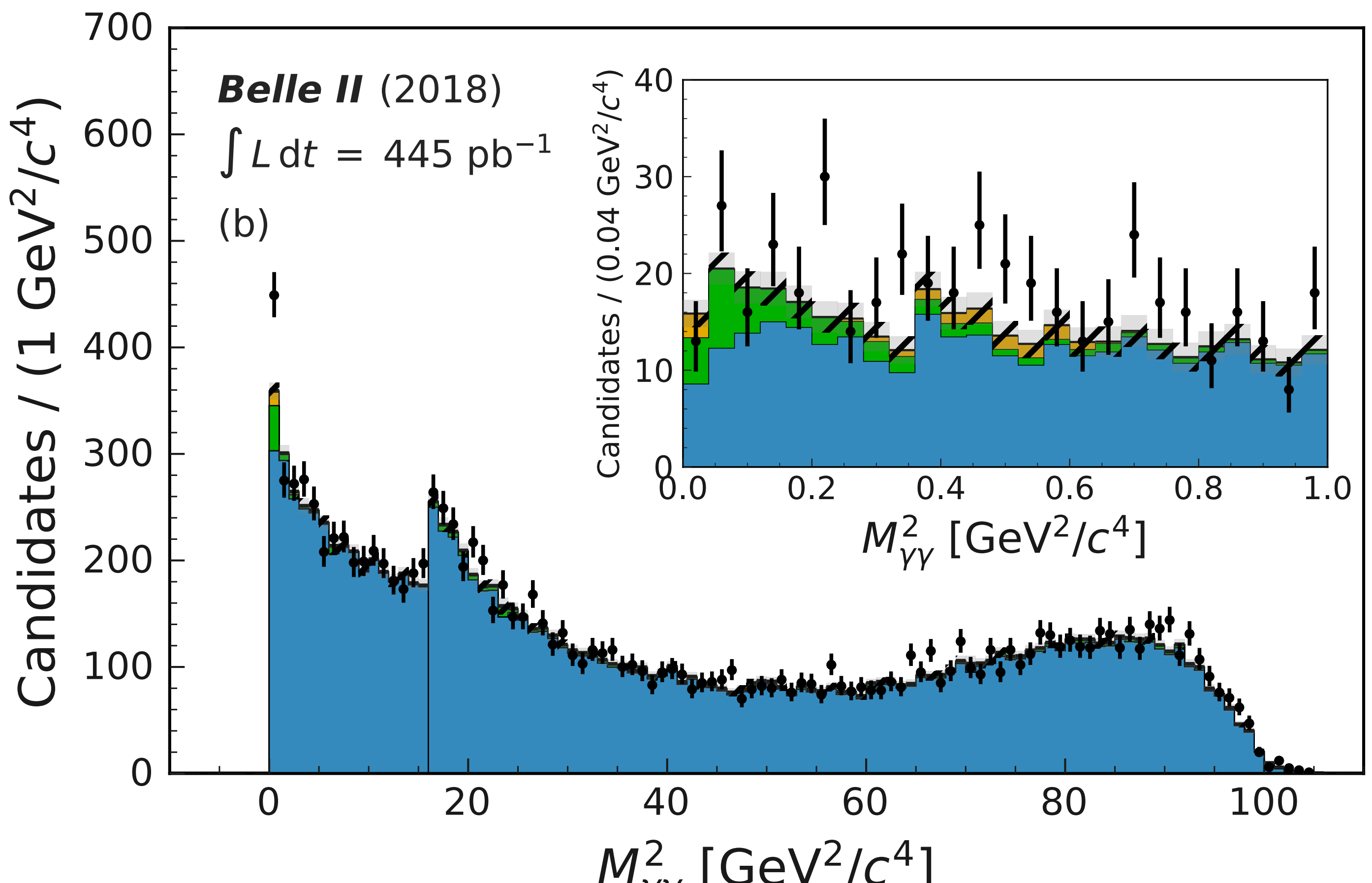

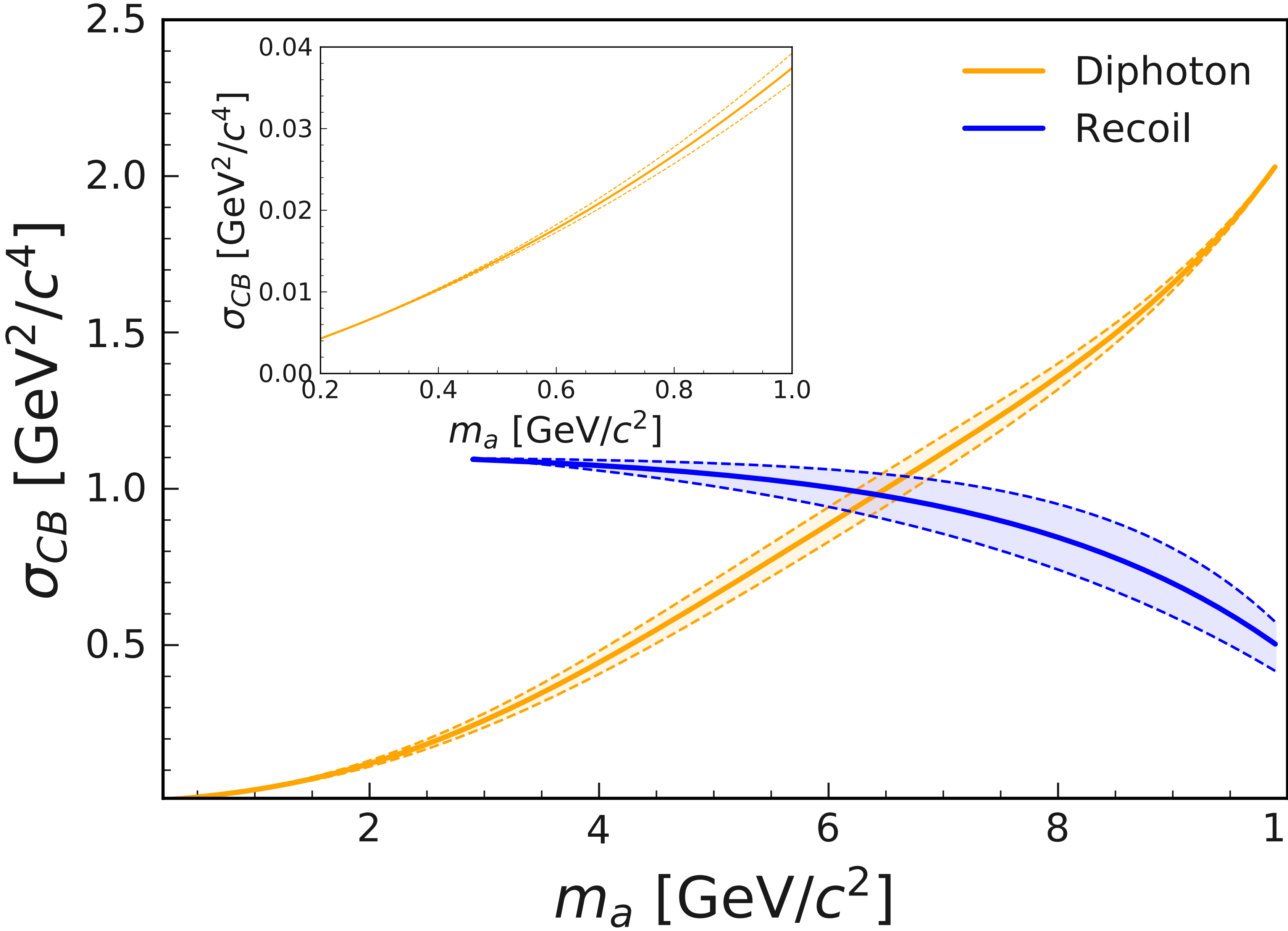

- fit $M^2_{\gamma\gamma}$ for $0.2 < m_a < 6.85$ GeV, and
- fit $M^2_{\rm rec}$ for $m_a > 6.85$ GeV,
- Look for resonance in the fit

ALP significance & limits

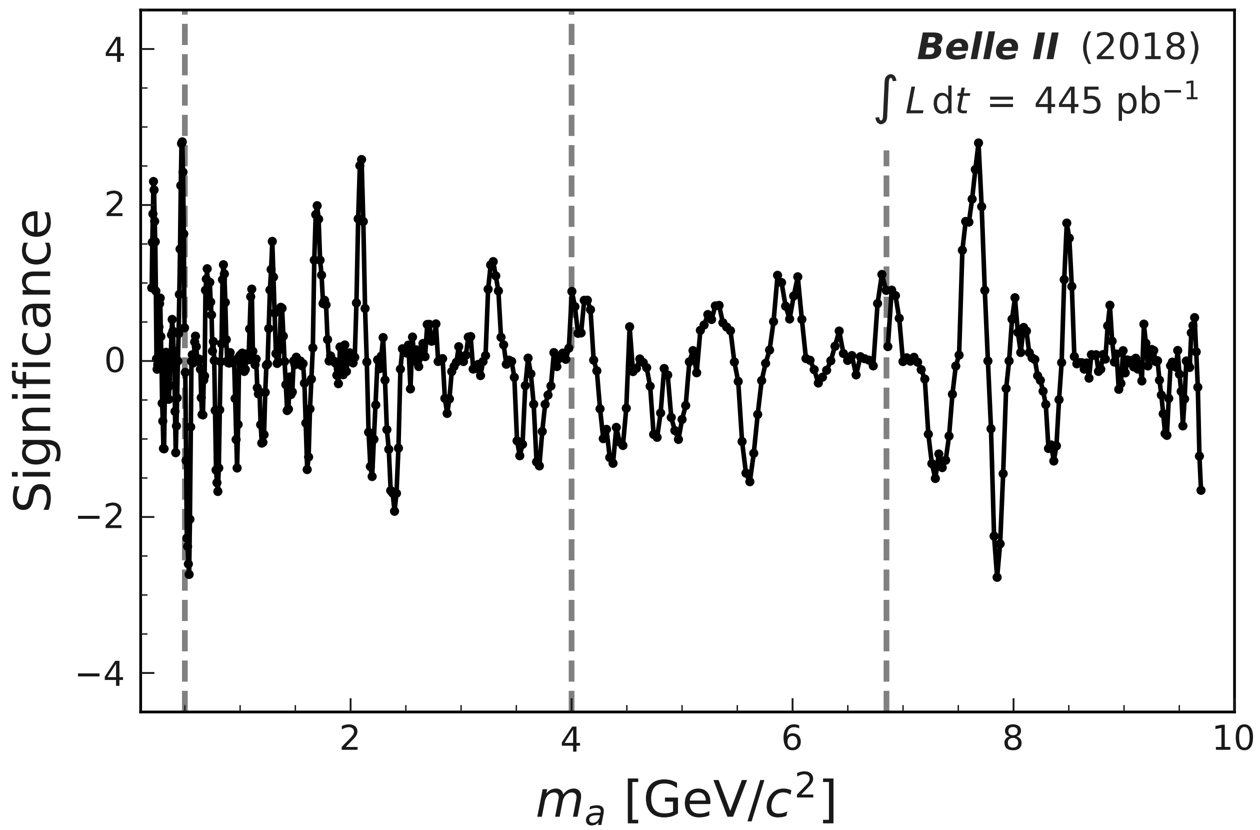

max. local significance of $\mathcal{S} = 2.8$ at
$m_a = 0.477$ GeV

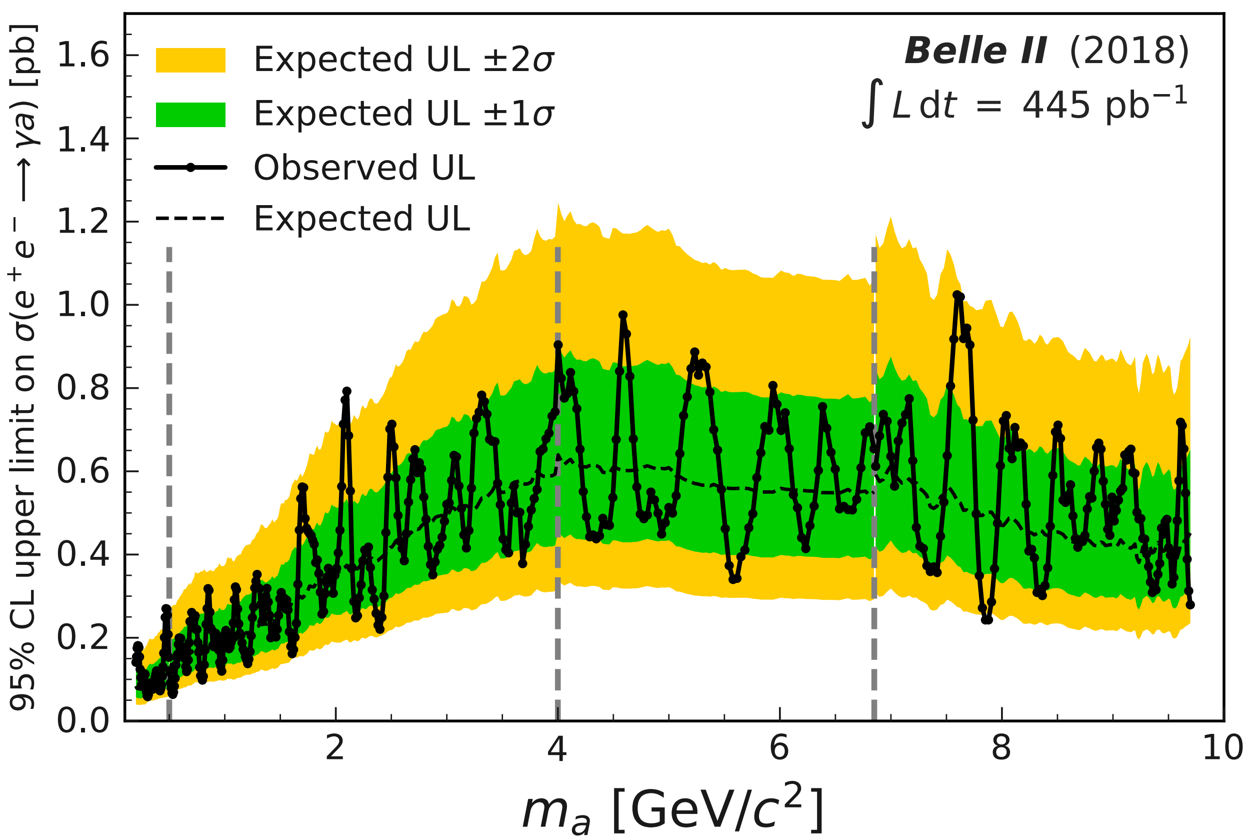

ALP search - UL on $g_{a\gamma\gamma}$

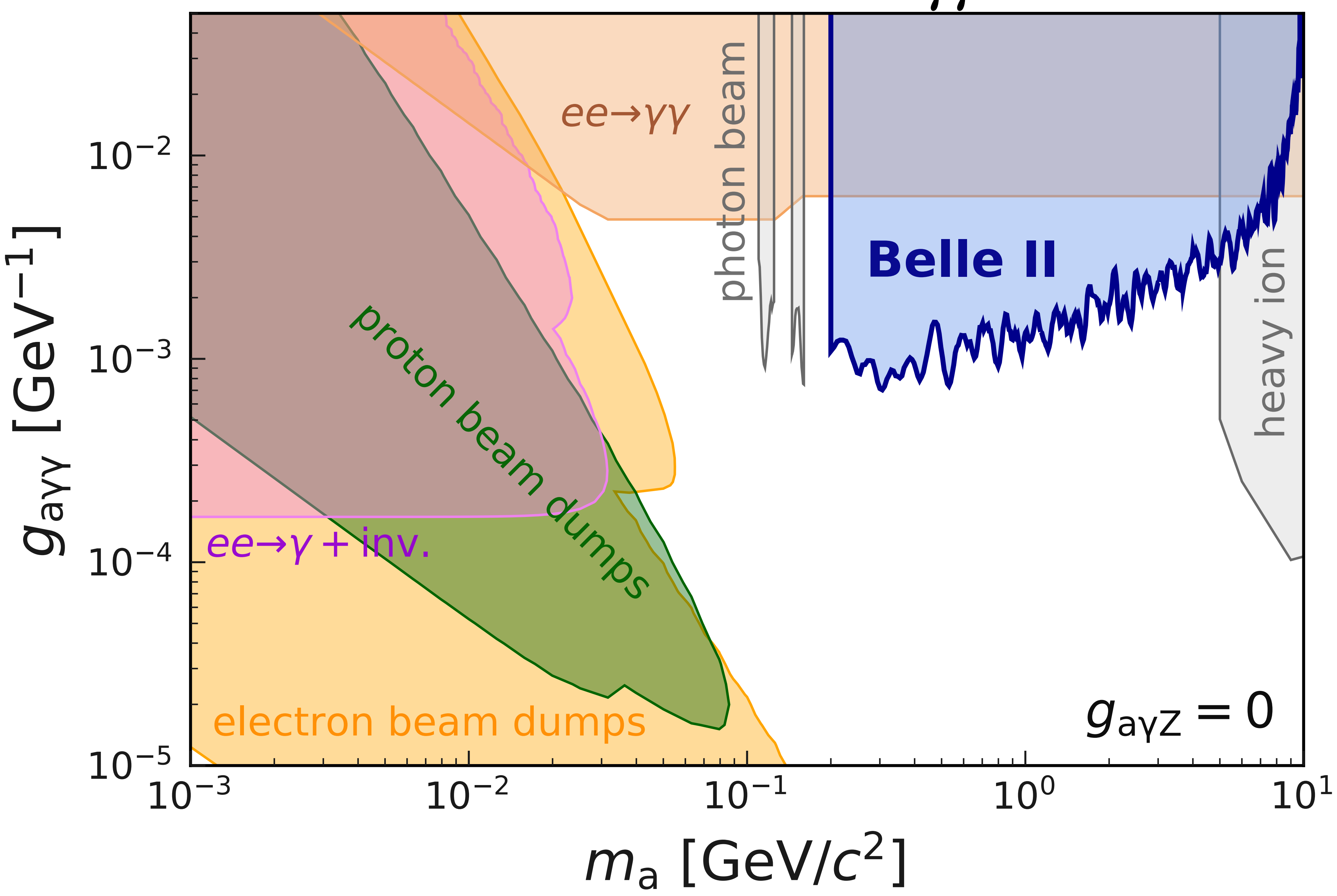

LFU test in Belle II

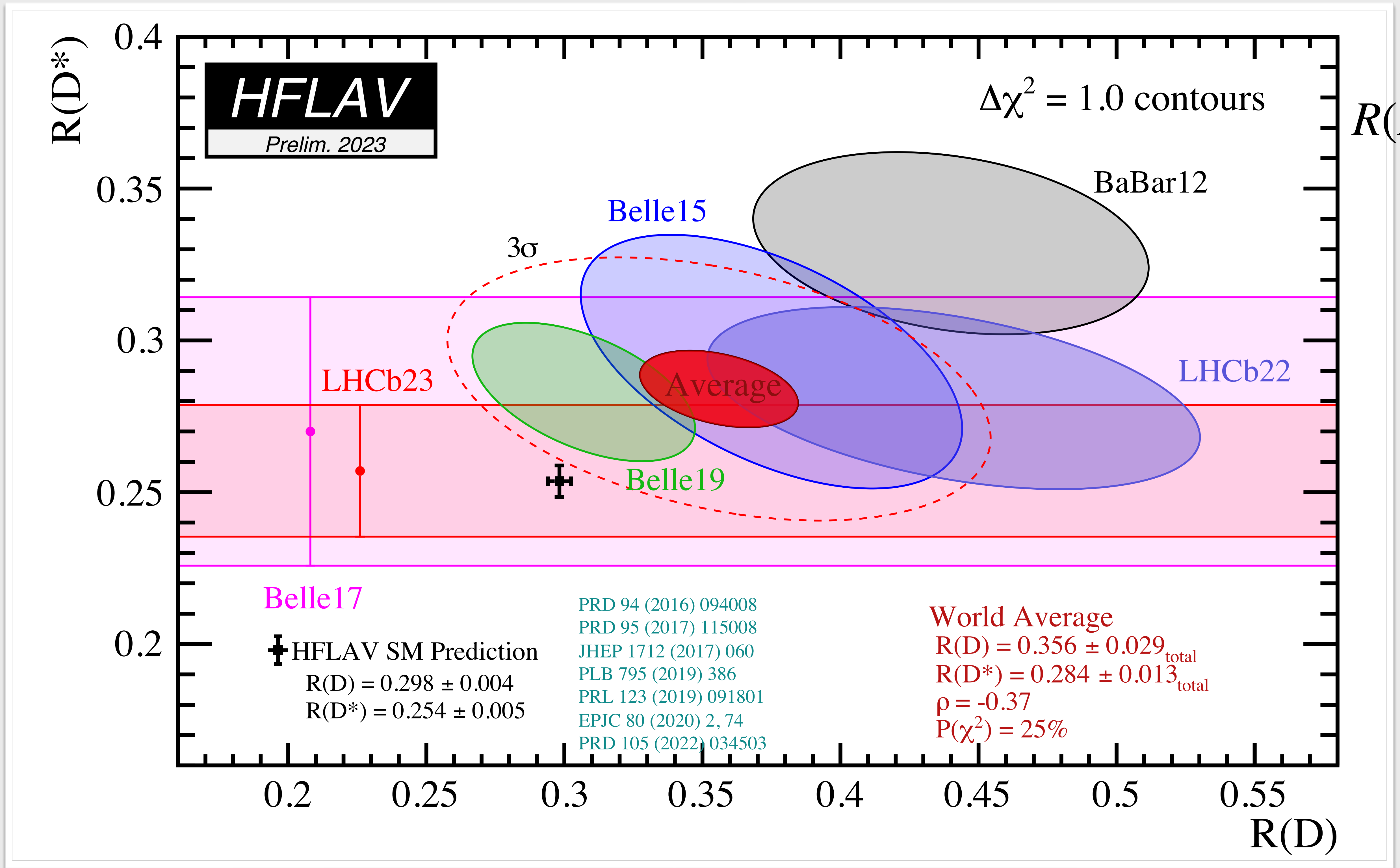

$$R(D^{(*)}) \equiv \frac{\mathscr{B}(B \to D^{(*)}\tau^+\nu)}{\mathscr{B}(B \to D^{(*)}\ell^+\nu)}$$

$R(D^*)$ from Belle II

New for July, 2023
Preliminary

- First $R(D^*)$ result from Belle II

$$R(D^*) \equiv \frac{\mathcal{B}(B \to D^*\tau^+\nu)}{\mathcal{B}(B \to D^*\ell^+\nu)}$$

- Analysis features
  - Use hadronic B-tagging with FEI (slide 64)
  - leptonic τ decays, $\tau^+ \to \ell^+\nu_\ell\bar{\nu}_\tau$
  - three D^* modes: $D^{*+} \to D^0\pi^+$, $D^+\pi^0$ and $D^{*0} \to D^0\pi^0$

- Signal ($B \to D^*\tau^+\nu$) & Normalization ($B \to D^*\ell^+\nu$)
  - extracted simultaneously
  - by fitting 2D $(M^2_{\rm miss}, E_{\rm ECL})$

$$M^2_{\rm miss} \equiv (p_{e^+e^-} - p_{B_{\rm tag}} - p_{D^*} - p_\ell)^2$$

$E_{\rm ECL}$ = extra energy (unmatched) in the EM calorimeter

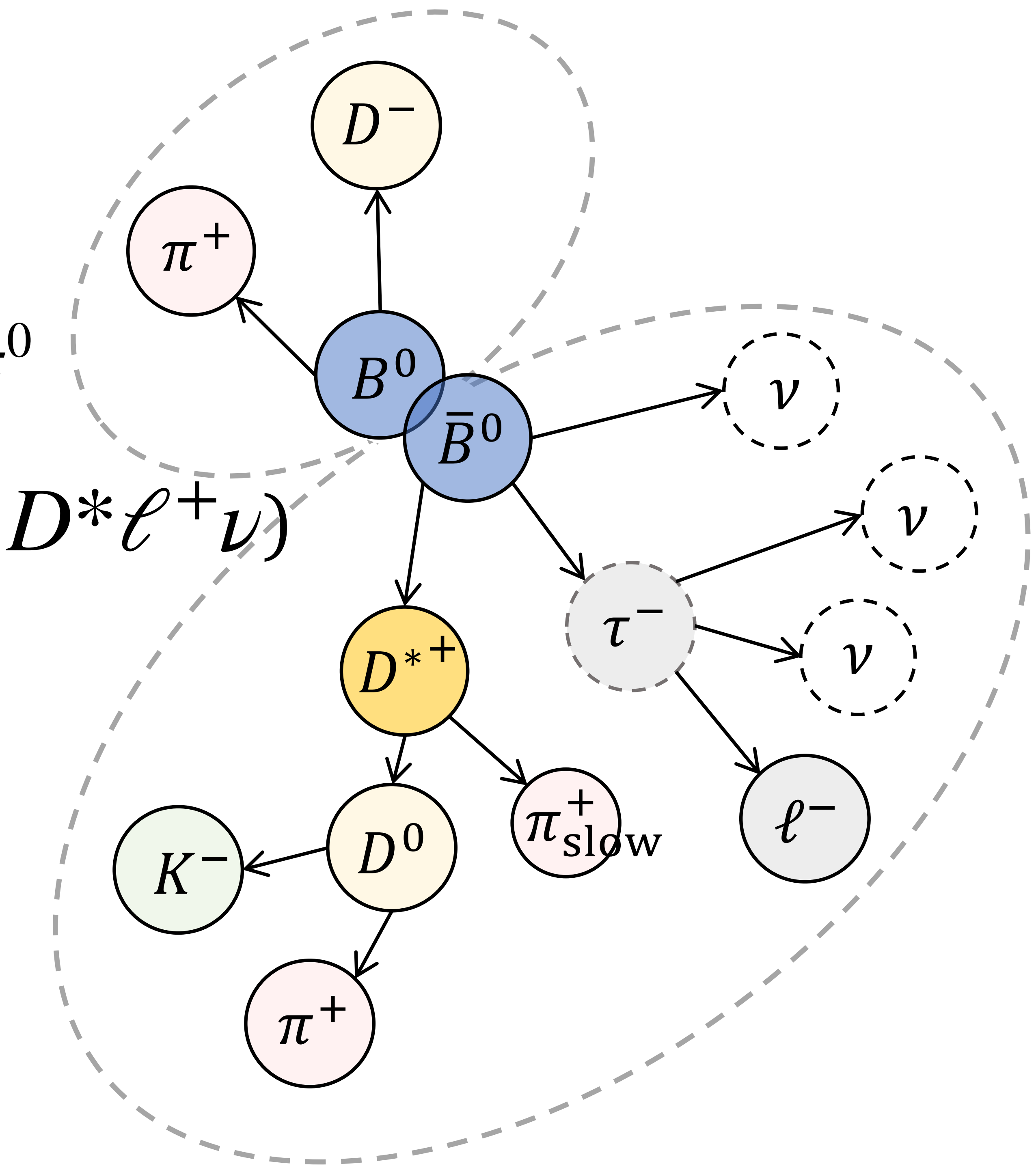

$R(D^*)$ from Belle II

New for July, 2023
Preliminary

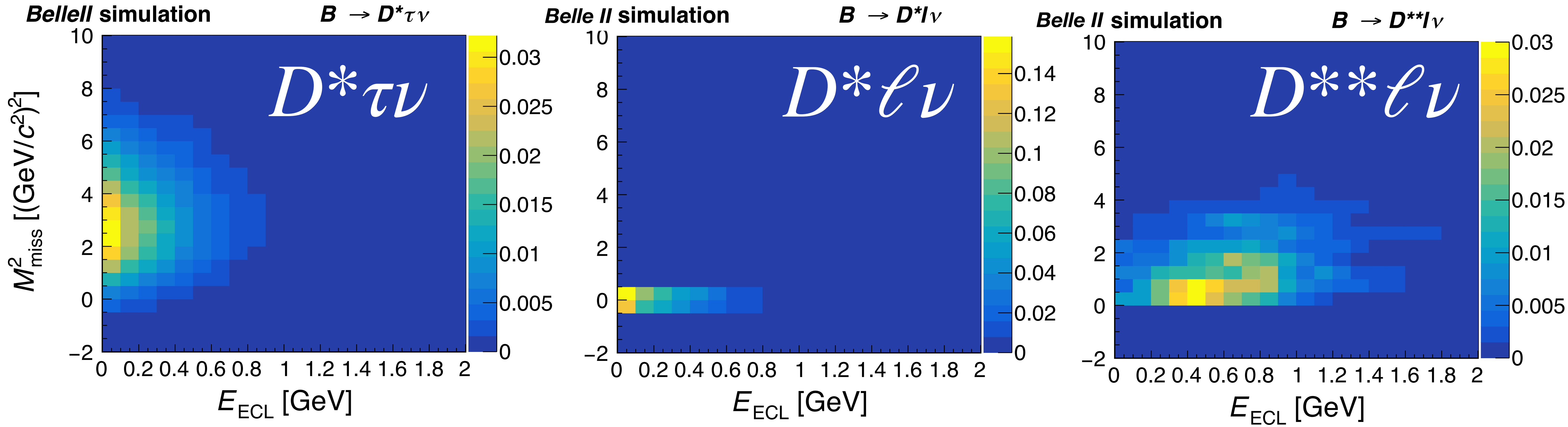

- Signal ($B \to D^*\tau^+\nu$) & Normalization ($B \to D^*\ell^+\nu$)
  - extracted simultaneously
  - by fitting 2D ($M^2_{\rm miss}, E_{\rm ECL}$)

$$M^2_{\rm miss} \equiv (p_{e^+e^-} - p_{B_{\rm tag}} - p_{D^*} - p_\ell)^2$$

$E_{\rm ECL}$ = extra energy (unmatched) in the EM calorimeter

$R(D^*)$ from Belle II

$\mathscr{L}_{\text{int}} = 189\ \text{fb}^{-1}$

New for July, 2023
Preliminary

- Fit projections for the sub-mode $D^{*+} \to D^0\pi^+$

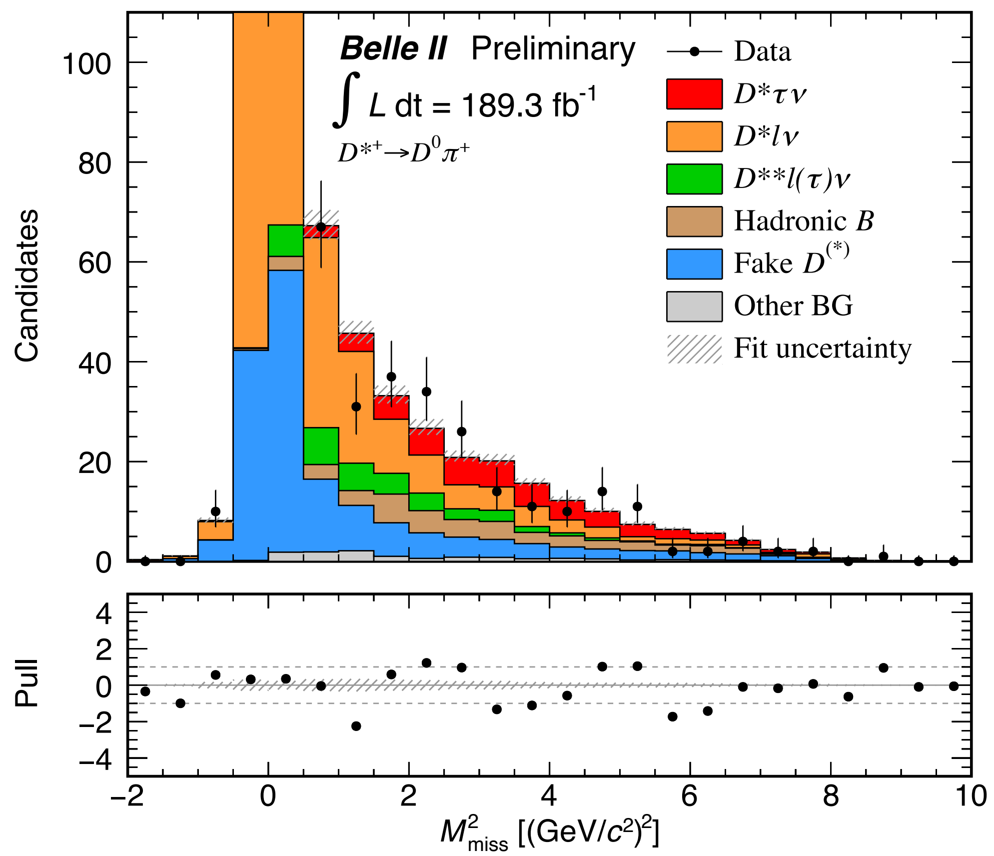

M^2_{miss} (peak-bin yield ~O(600))

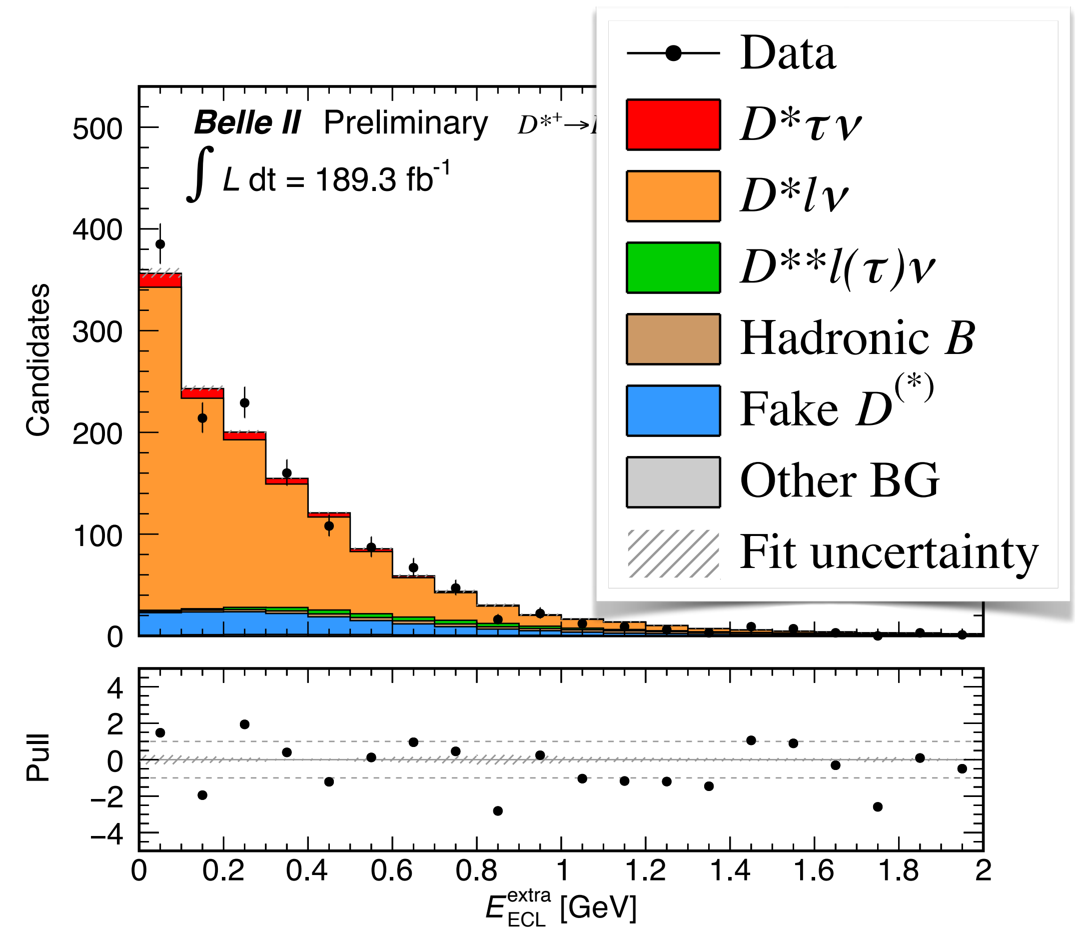

E_{ECL} for entire M^2_{miss} region

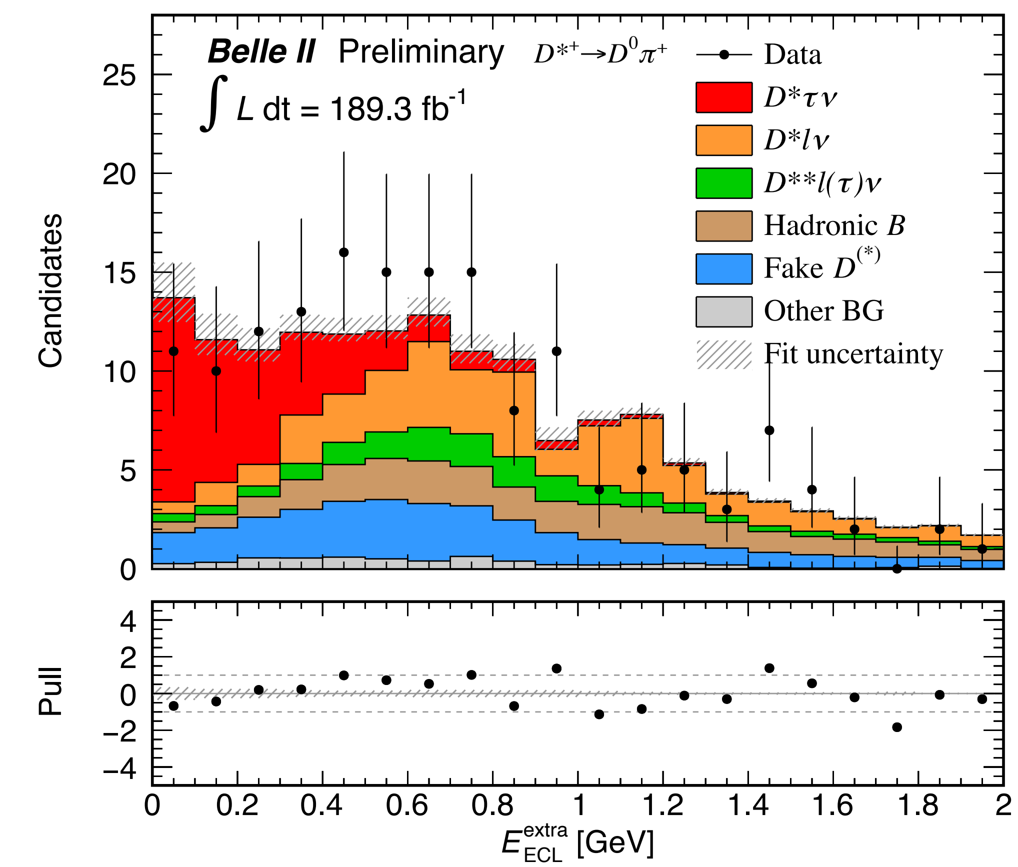

E_{ECL} for signal-enhanced region
$1.5 < M^2_{\text{miss}} < 6.0\ \text{GeV}^2$

$$R(D^*) = 0.267^{+0.041}_{-0.039}{}^{+0.028}_{-0.033}$$

- Systematics
  - dominant sources: E_{ECL} PDF shape, MC statistics

$R(D^*)$ from Belle II

New for July, 2023
Preliminary

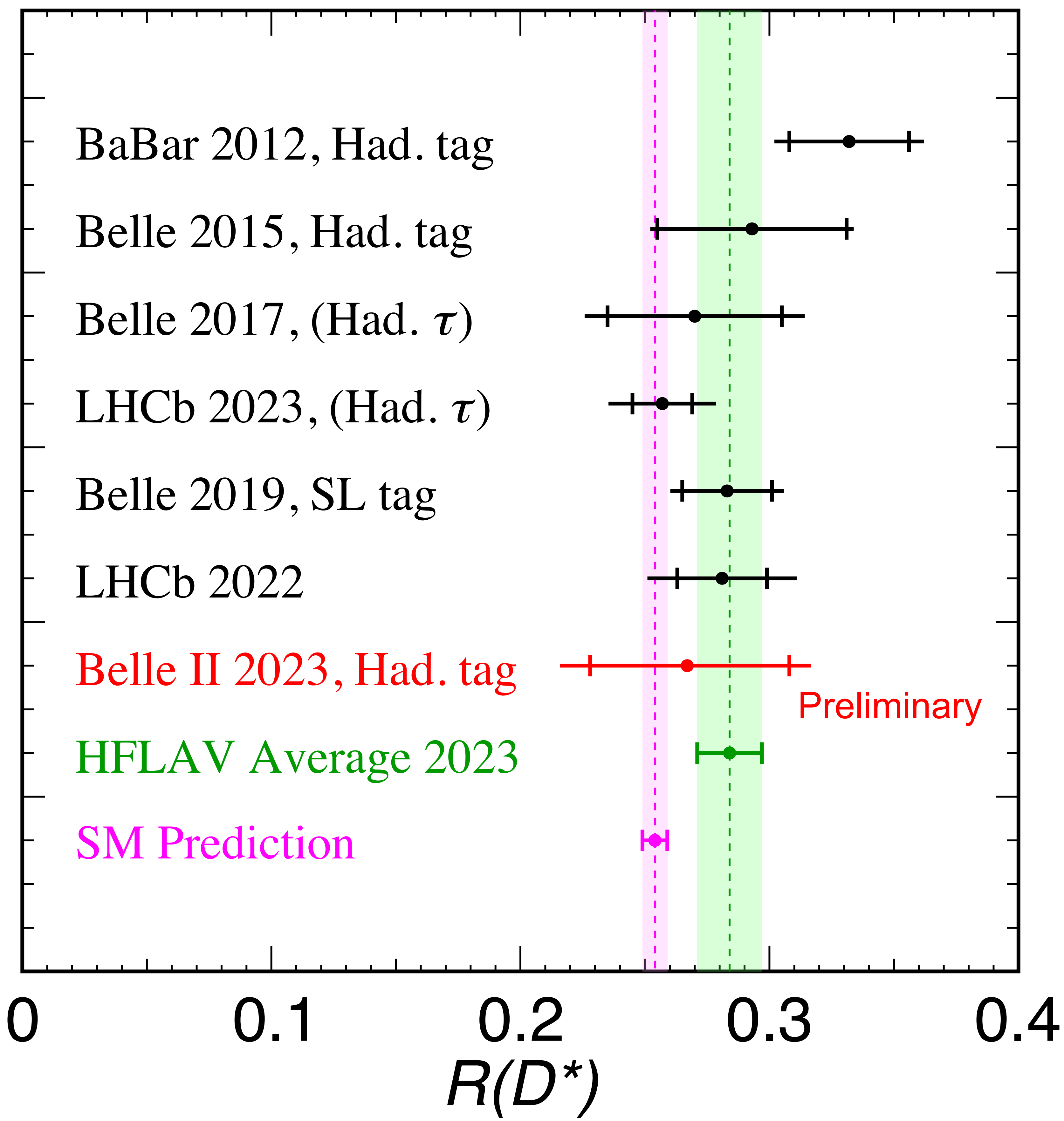

	5 ab^{-1}	50 ab^{-1}
R_D	$(\pm 6.0 \pm 3.9)\%$	$(\pm 2.0 \pm 2.5)\%$
R_{D^*}	$(\pm 3.0 \pm 2.5)\%$	$(\pm 1.0 \pm 2.0)\%$
$P_\tau(D^*)$	$\pm 0.18 \pm 0.08$	$\pm 0.06 \pm 0.04$

Belle II expected precision, from
The Belle II Physics Book, PTEP 2019 (2019) 123C01

new Belle II result is consistent with both the SM and the HFLAV average

$$R(D^*) = 0.267^{+0.041}_{-0.039}{}^{+0.028}_{-0.033}$$

$R(D)$ vs. $R(D^*)$, updated

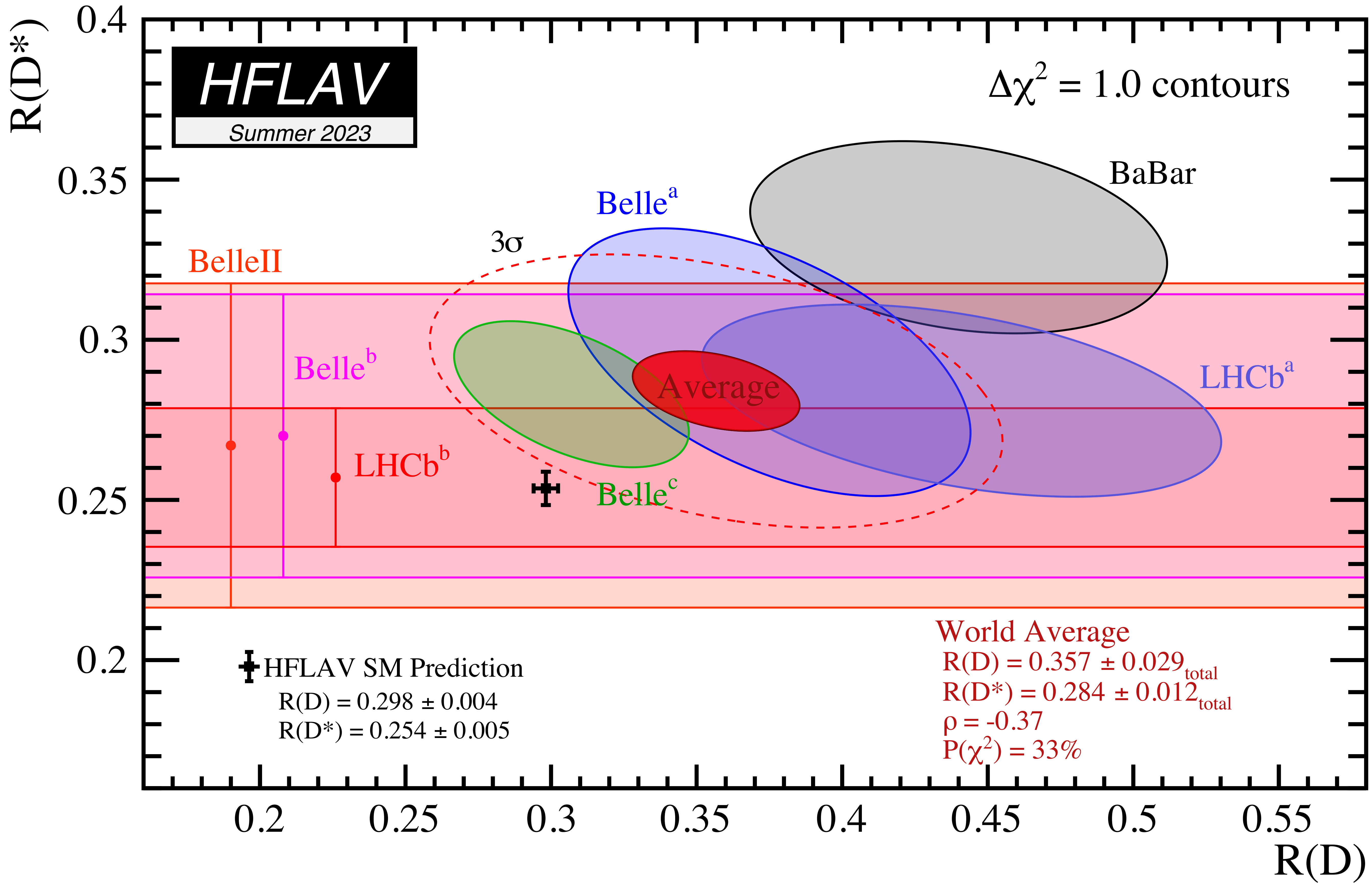

arXiv:2311.07248

Inclusive LFU test w/ $R(X_{\tau/\ell})$

- Why measure $R(X_{\tau/\ell})$?
  - different systematics from $R(D^{(*)})$
  - hence, a complementary test of LFU

$$R(X_{\tau/\ell}) = \frac{\mathcal{B}(B \to X\tau\nu)}{\mathcal{B}(B \to X\ell\nu)}$$

- Procedure
  - use $\tau \to \ell \nu_\tau \bar{\nu}_\ell$ modes
  - select events with $B_{\text{tag}} + \ell$, with remaining particles attributed to X
  - distinguish signal from background by using M^2_{miss} and p^B_ℓ
  - background mostly from $b \to c \to \ell$; some continuum and fake leptons
  - require $p_e > 0.3\ (0.5)$ and $p_e > 0.4\ (0.7)$ in CM (lab)

$R(X_{\tau/\ell})$

arXiv:2311.07248

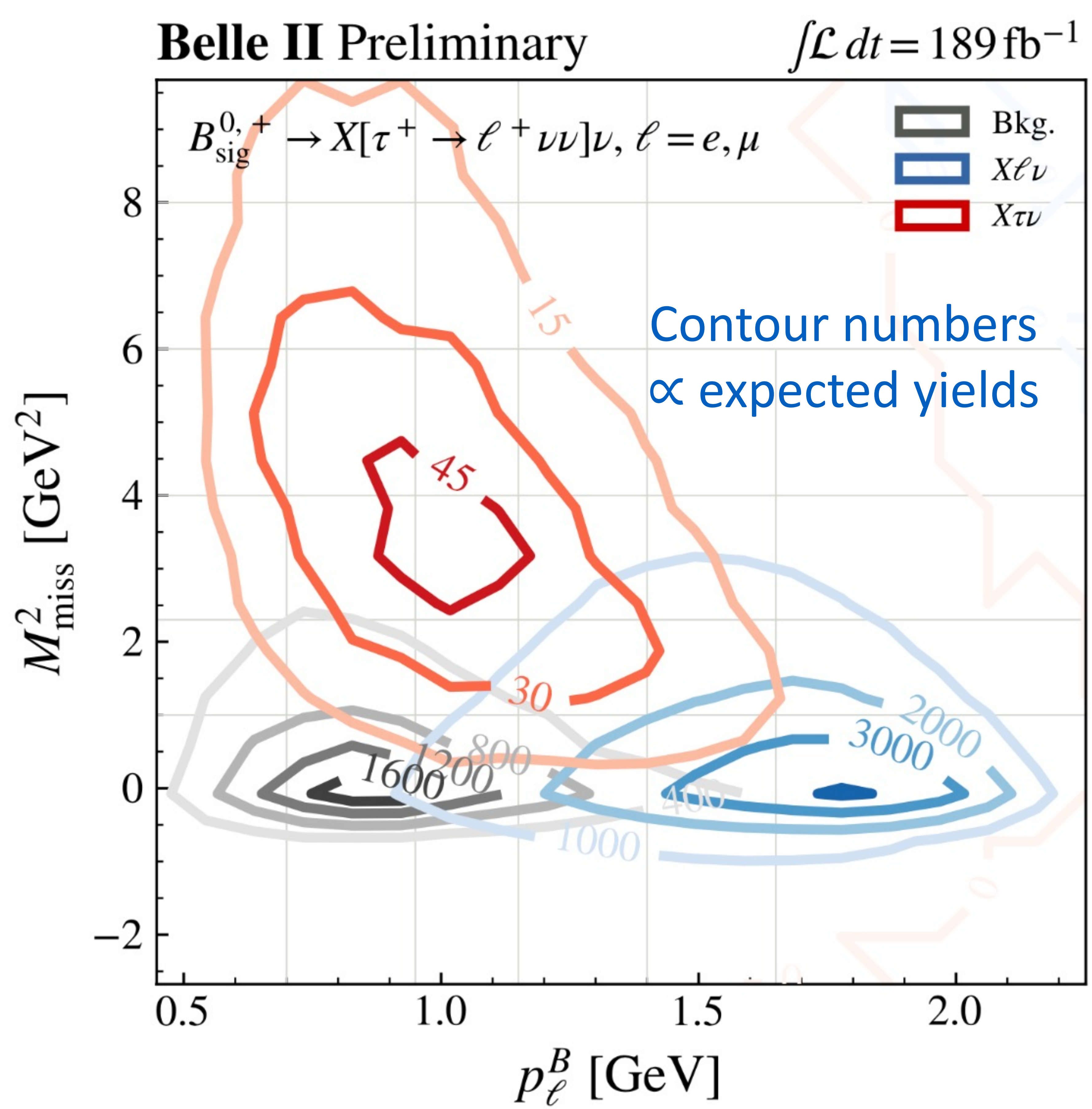

Contour numbers $\propto$ expected yields

$R(X_{\tau/\ell})$, event modeling

- separate templates for e, μ for each of $X\tau\nu$, $X\ell\nu$, other $B\overline{B}$, and continuum ($q\overline{q}$, constrained using off-resonance data)

- for reliable template shapes
  - detailed adjustments to MC (FF's, B and D BF's)
  - corrections by comparison of MC to data in control region: low q^2, low M^2_{miss}, high M_X
  - for instance, adjust M_X in p_ℓ > 1.4 sideband; using these weights also improves modeling in M^2_{miss} and q^2

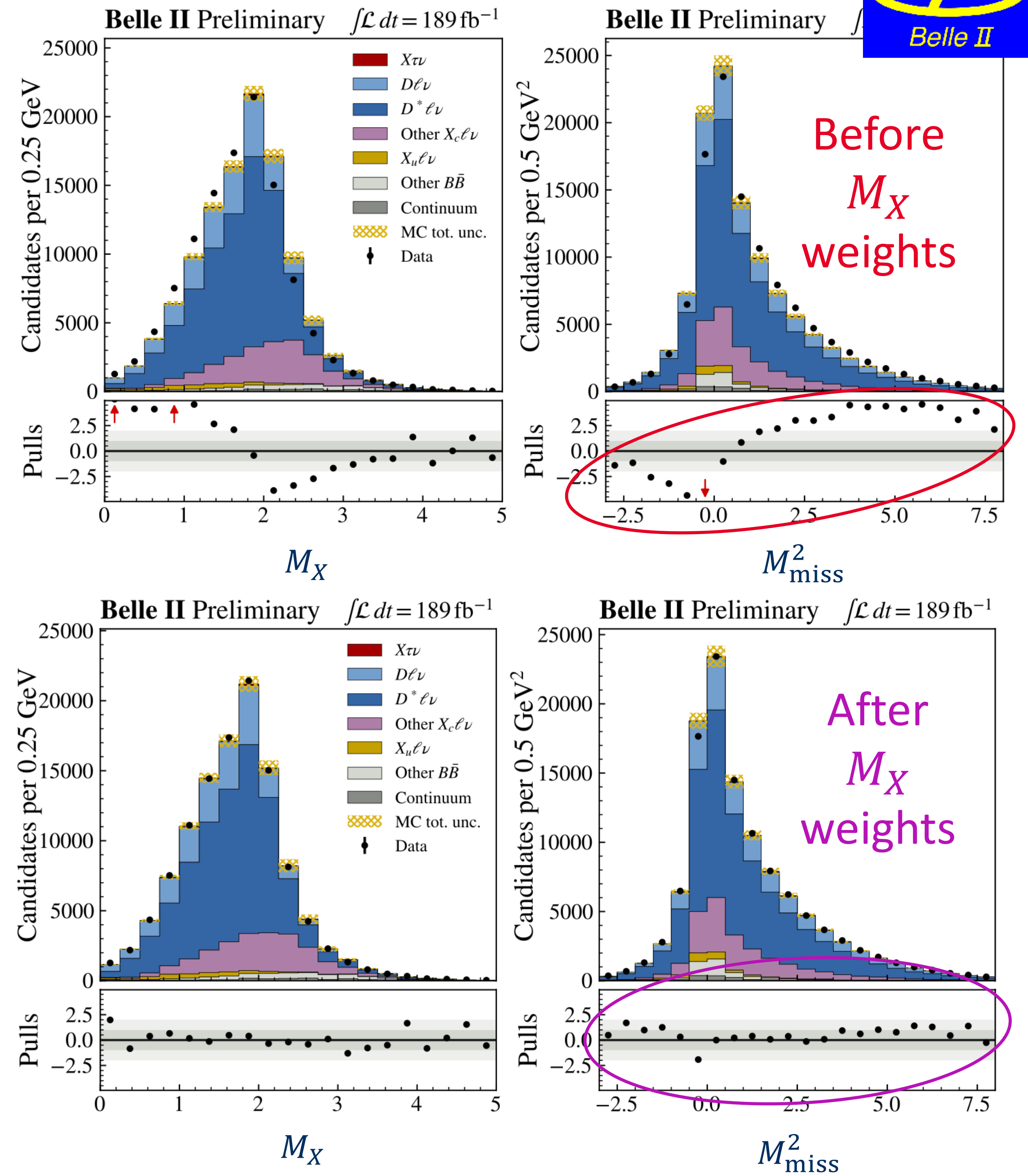

Main sources of systematic uncertainty:

- MC stat ±5.7 %
- Bkg shape ±5.5 %
- M_X modeling ±7.1 %
- $B \to X_c\ell\nu$ BFs ±7.7 %
- $B \to X_c\ell\nu$ FFs ±7.9 %

arXiv:2311.07248

$R(X_{\tau/\ell})$ Results

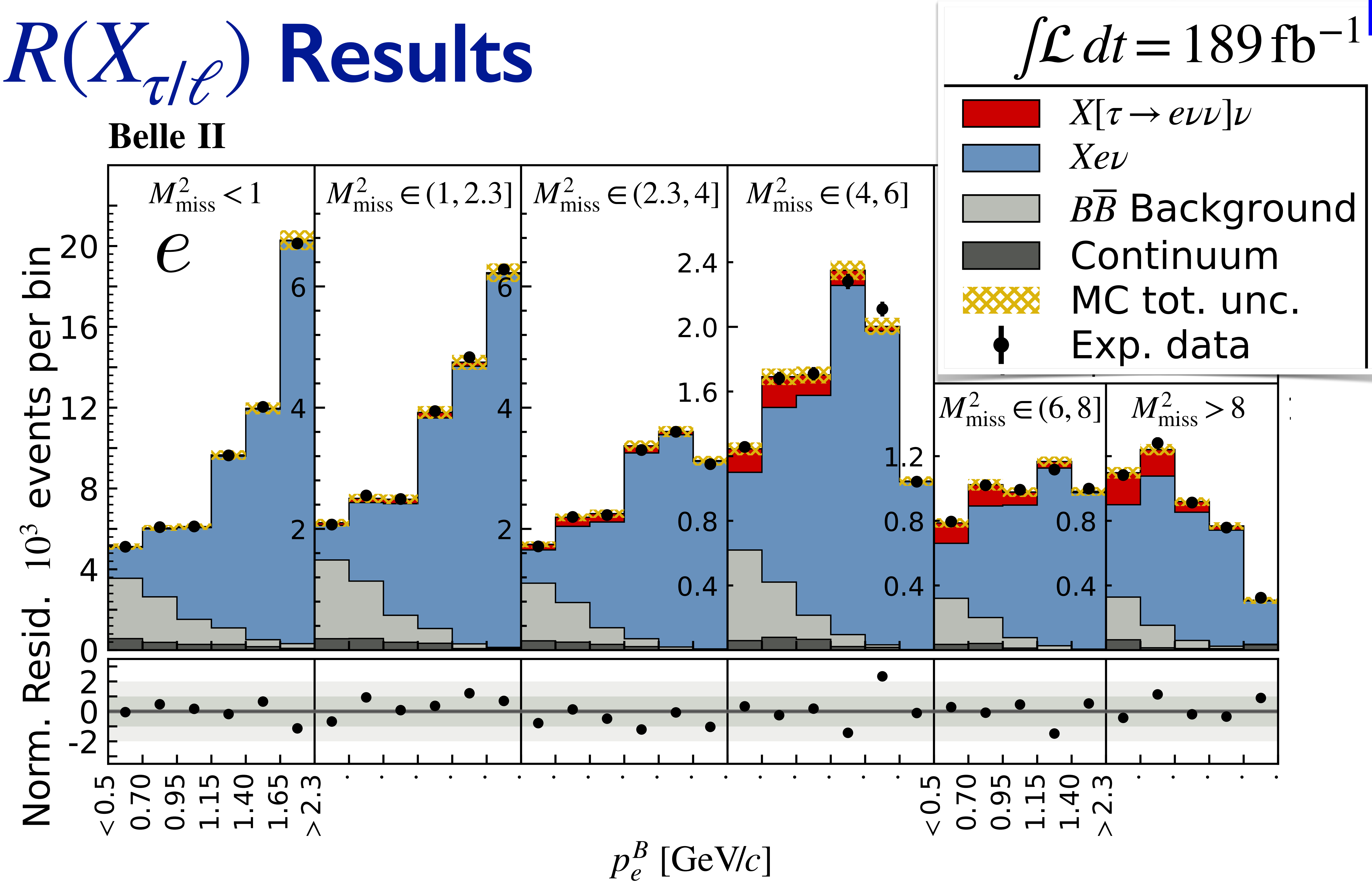

arXiv:2311.07248

$R(X_{\tau/\ell})$ Results

$$R(X_{\tau/\ell}) = 0.228 \pm 0.016 \pm 0.036$$

$$R(X_{\tau/e}) = 0.232 \pm 0.020 \pm 0.037$$

$$R(X_{\tau/\mu}) = 0.222 \pm 0.027 \pm 0.050$$

Consistent with SM: 0.223 ± 0.005

[37] M. Freytsis, Z. Ligeti, and J. T. Ruderman, Flavor models for $\overline{B} \to D^{(*)}\tau\overline{\nu}$, Phys. Rev. D **92**, 054018 (2015).

[38] M. Rahimi and K. K. Vos, Standard Model predictions for lepton flavour universality ratios of inclusive semileptonic B decays, J. High Energ. Phys. **2022**, 7 (2022).

[40] Z. Ligeti, M. Luke, and F. J. Tackmann, Theoretical predictions for inclusive $B \to X_u\tau\overline{\nu}$ decay, Phys. Rev. D **105**, 073009 (2022).

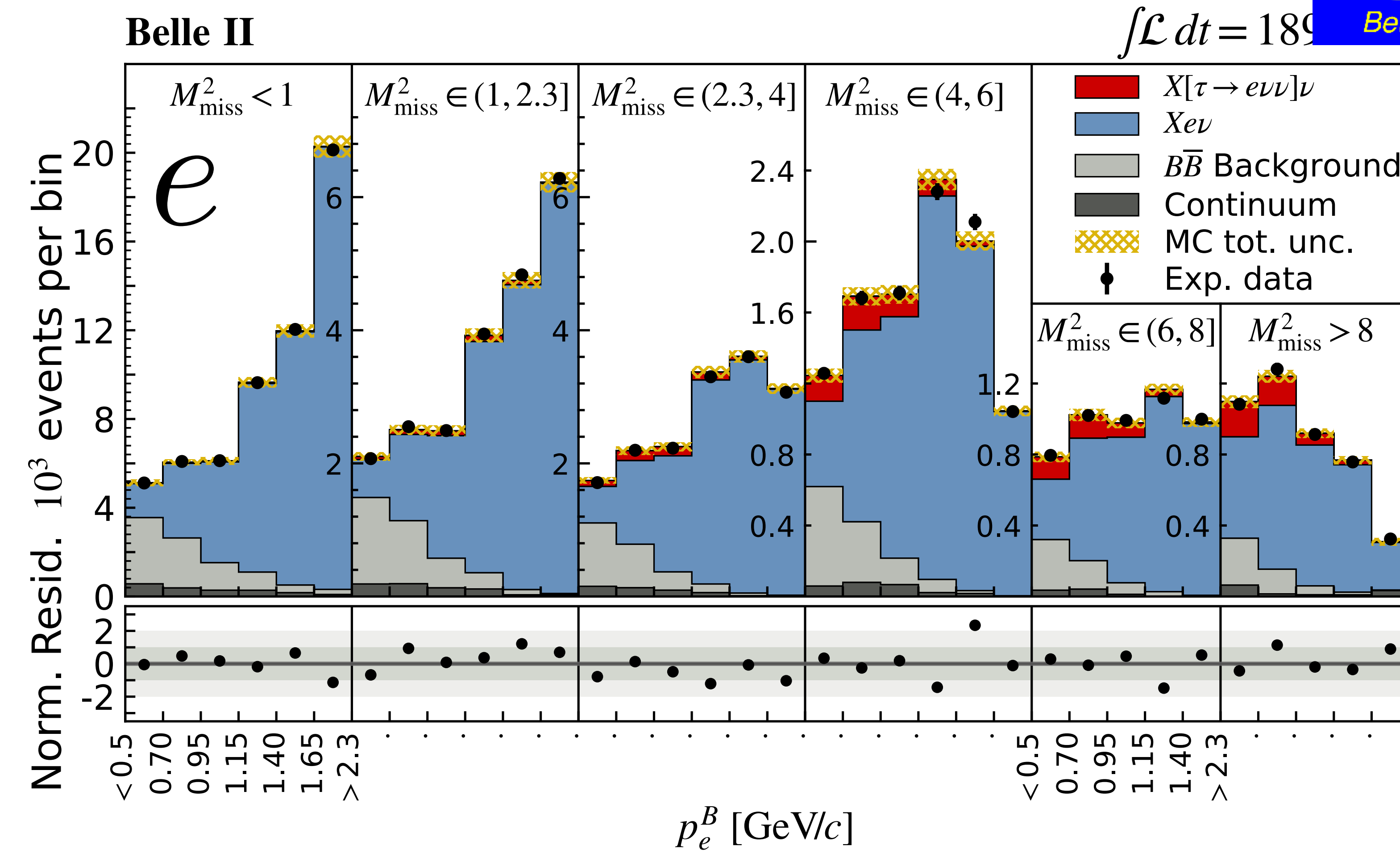

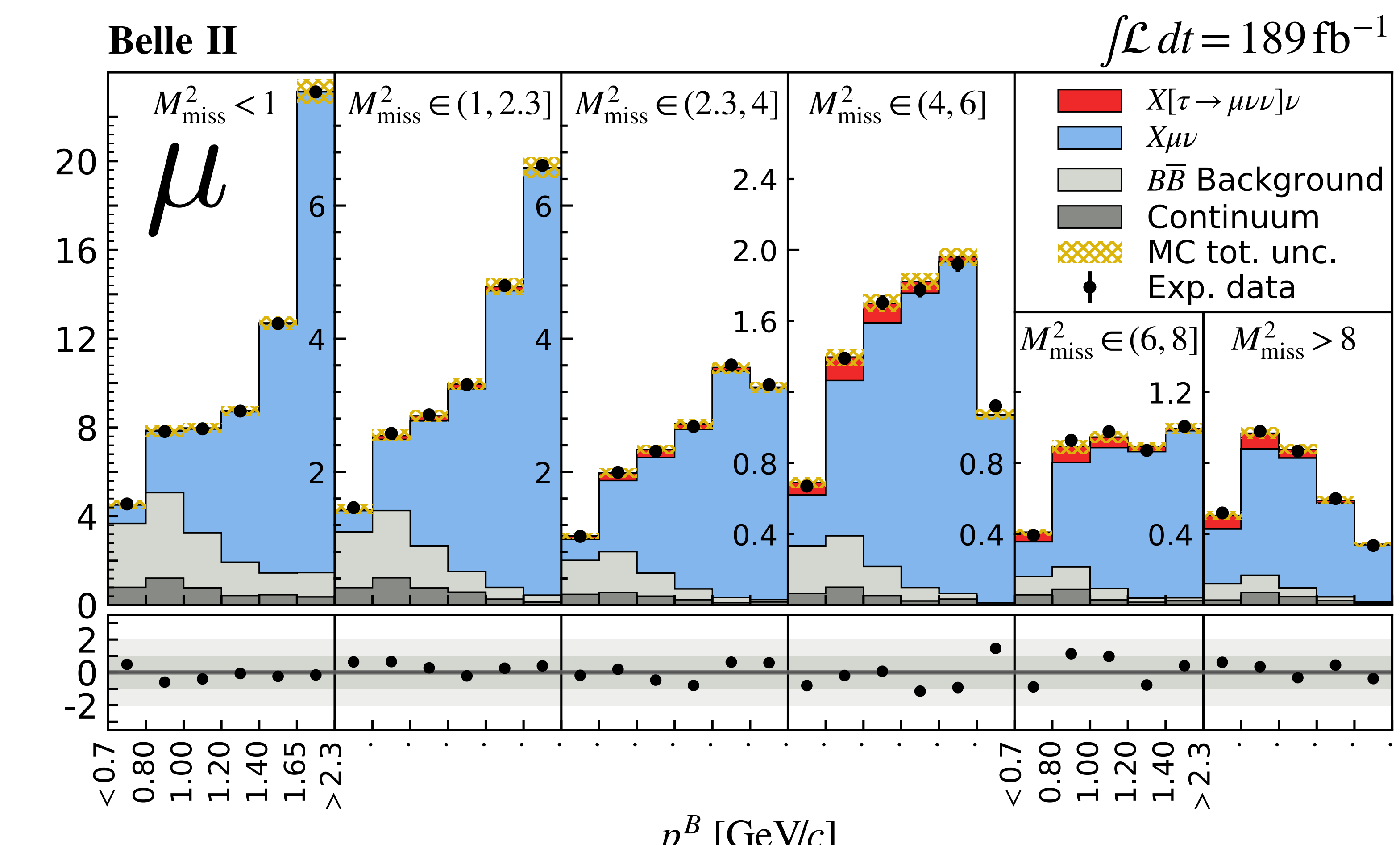

$R(X_{\tau/\ell})$, compared with $R(D^{(*)})$

† = with expected SM contributions of $D^{**}_{(\mathrm{gap})}, X_u$ removed

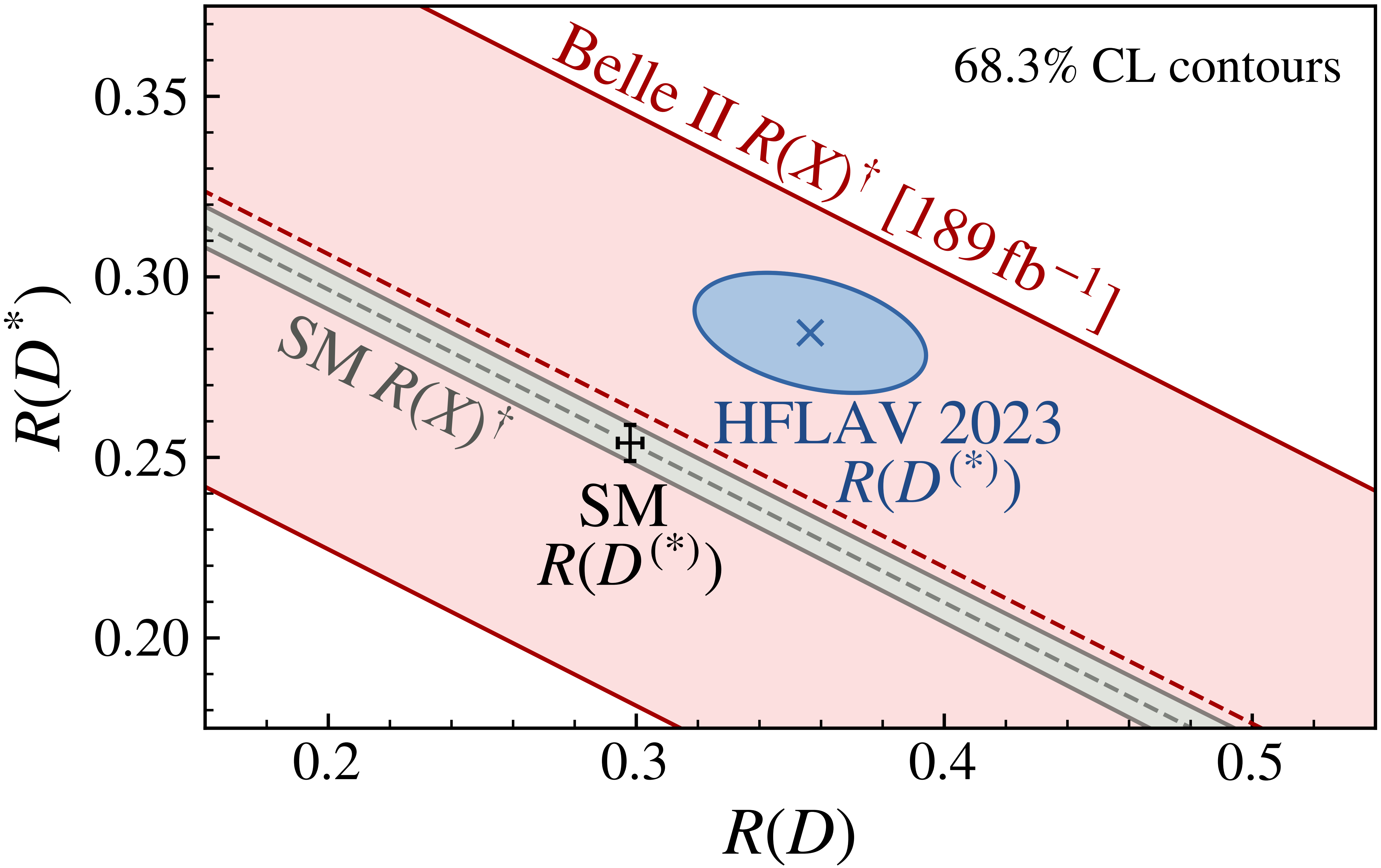

$B^+ \to K^+ \nu\bar{\nu}$ at Belle II

Search for $B^+ \to K^+\nu\bar{\nu}$ at Belle II

- In the SM,
  - $\mathcal{B}(B^+ \to K^+\nu\bar{\nu}) = (4.6 \pm 0.5) \times 10^{-6}$ [4]

[4] T. Blake, G. Lanfranchi, and D. M. Straub, Prog. Part. Nucl. Phys. **92**, 50 (2017).

- sensitive to new physics BSM, e.g.
  - leptoquarks,
  - axions,
  - DM particles, etc.

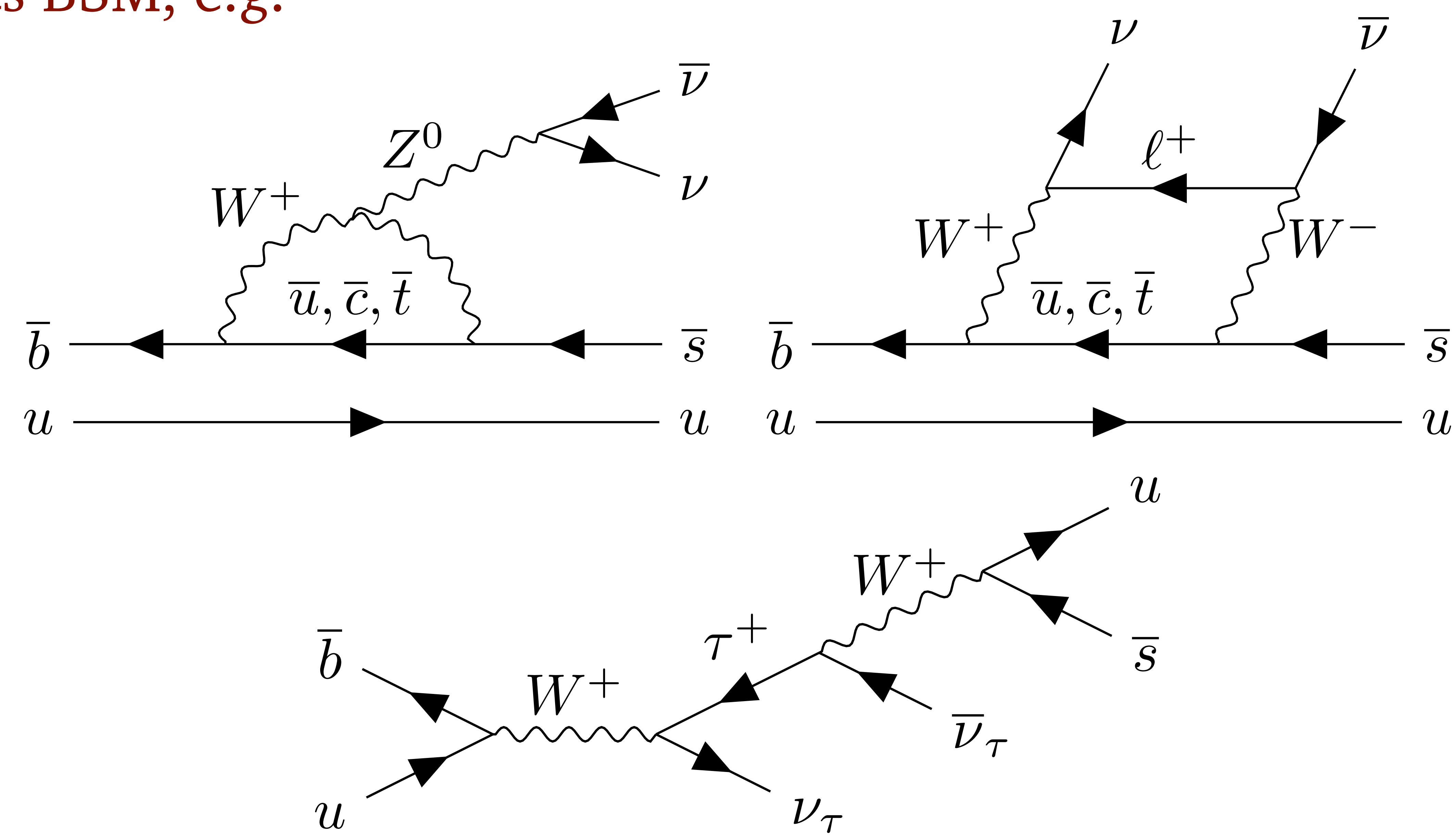

PRL 127, 181802 (2021)

Search for $B^+ \to K^+\nu\bar{\nu}$ at Belle II

- In the SM,
  - $\mathscr{B}(B^+ \to K^+\nu\bar{\nu}) = (4.6 \pm 0.5) \times 10^{-6}$ [4]
- sensitive to new physics BSM, e.g.
  - leptoquarks,
  - axions,
  - DM particles, etc.

[4] T. Blake, G. Lanfranchi, and D. M. Straub, Prog. Part. Nucl. Phys. **92**, 50 (2017).

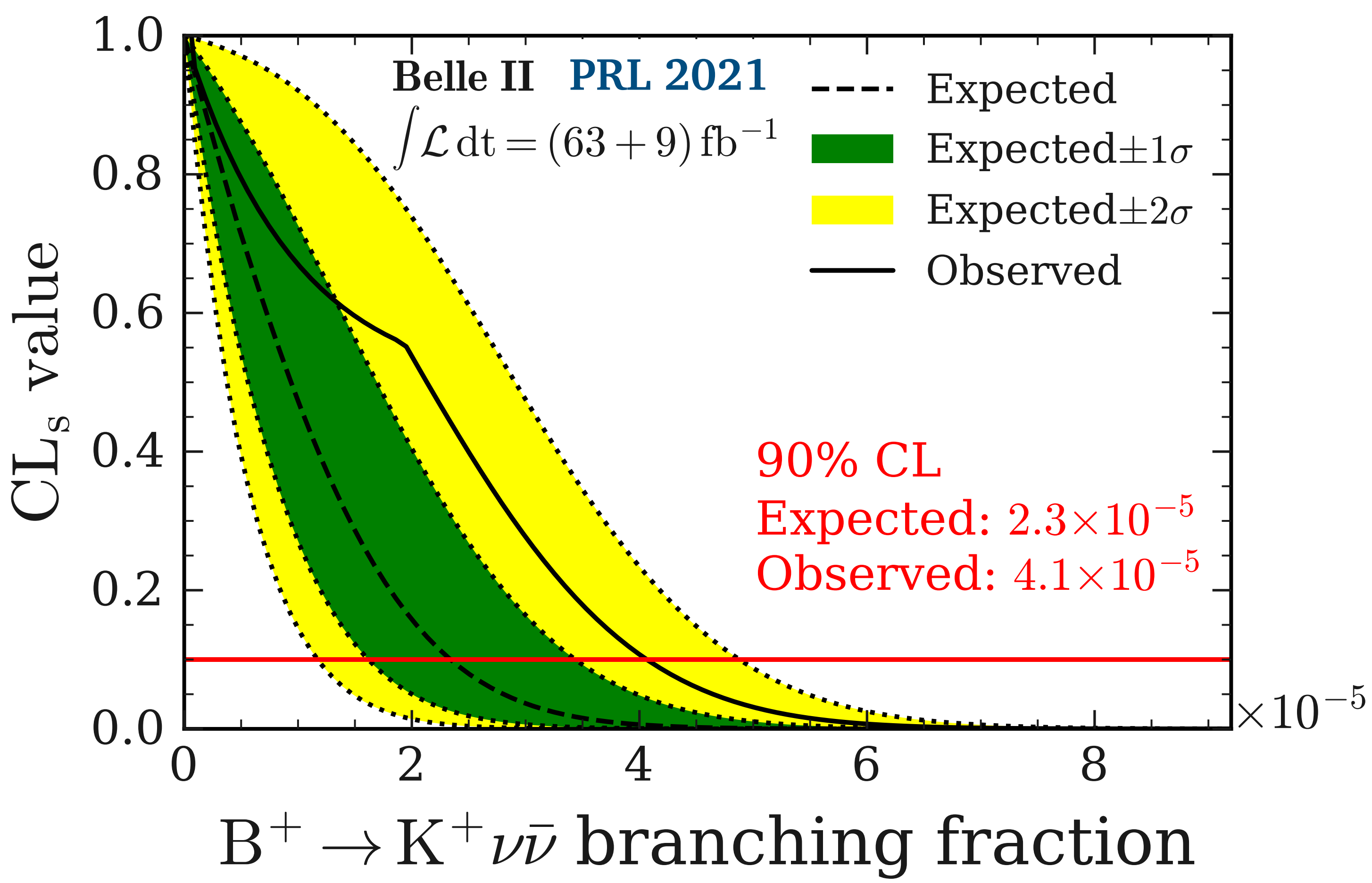

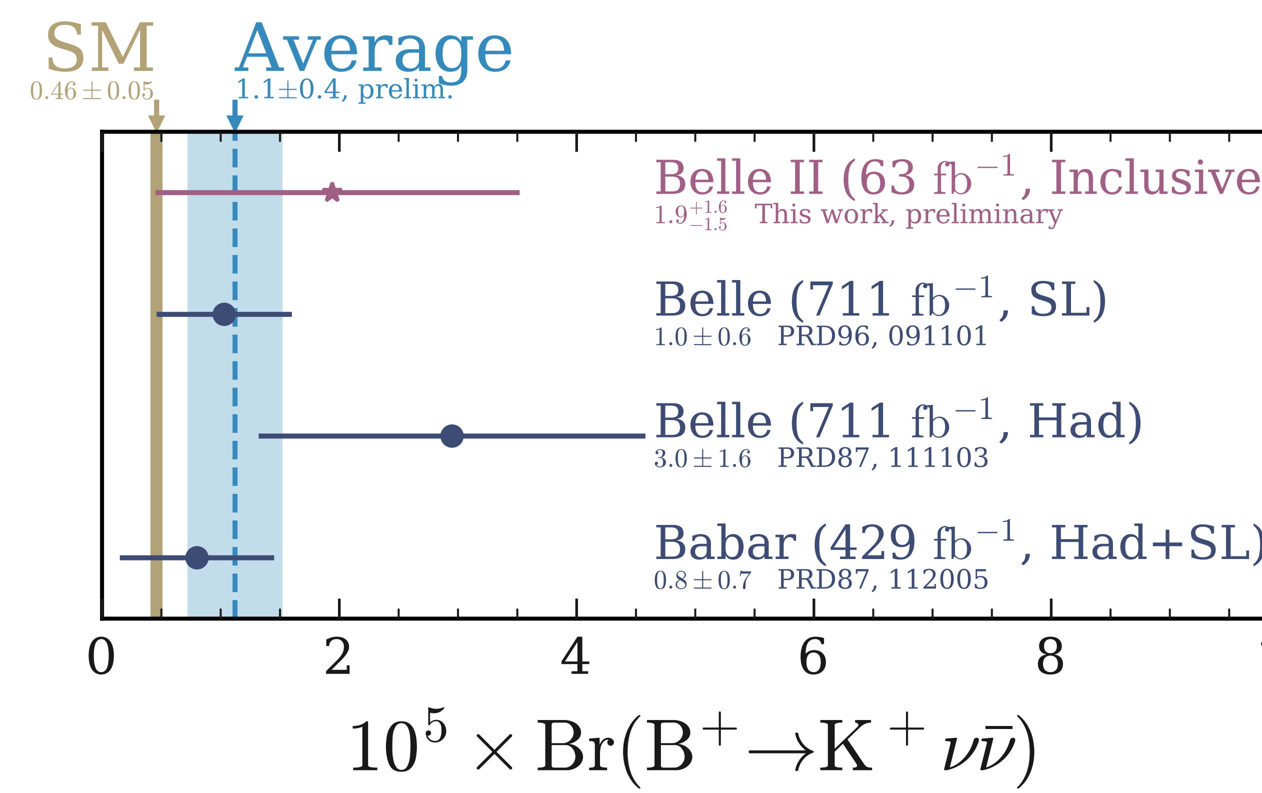

$$\mathcal{B}(B^+ \to K^+\nu\bar{\nu}) = (1.9^{+1.3+0.8}_{-1.3-0.7}) \times 10^{-5}$$

$$< 4.1 \times 10^{-5}$$ @ 90% CL

Search for $B^+ \to K^+ \nu\bar{\nu}$ at Belle II

And, we now have an updated result for 2023!

Two ways of tagging

Hadronic tagging (HTA)

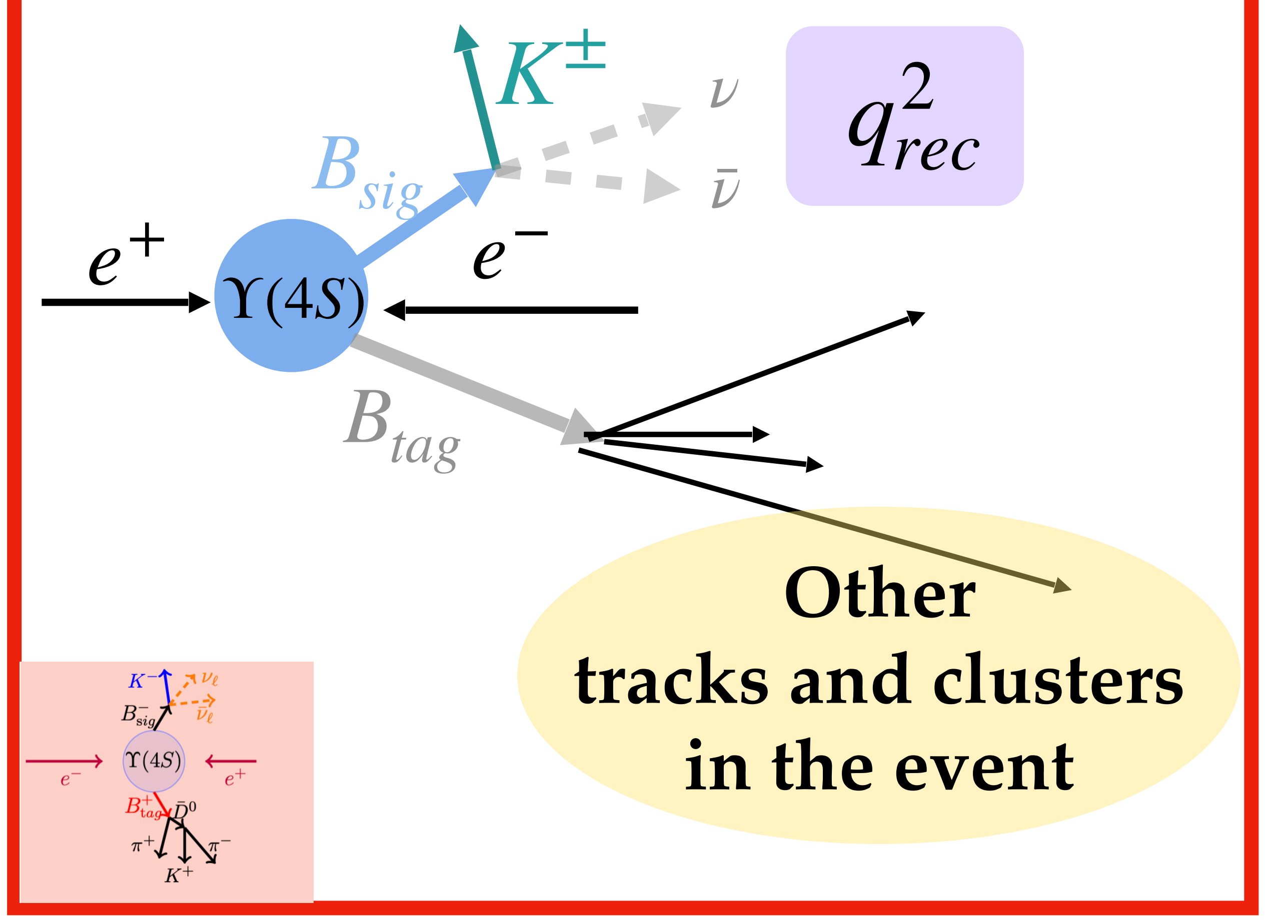

Efficiency →

q^2_{rec} : mass squared of the neutrino pair

← **Purity, Resolution**

Inclusive tagging (ITA)

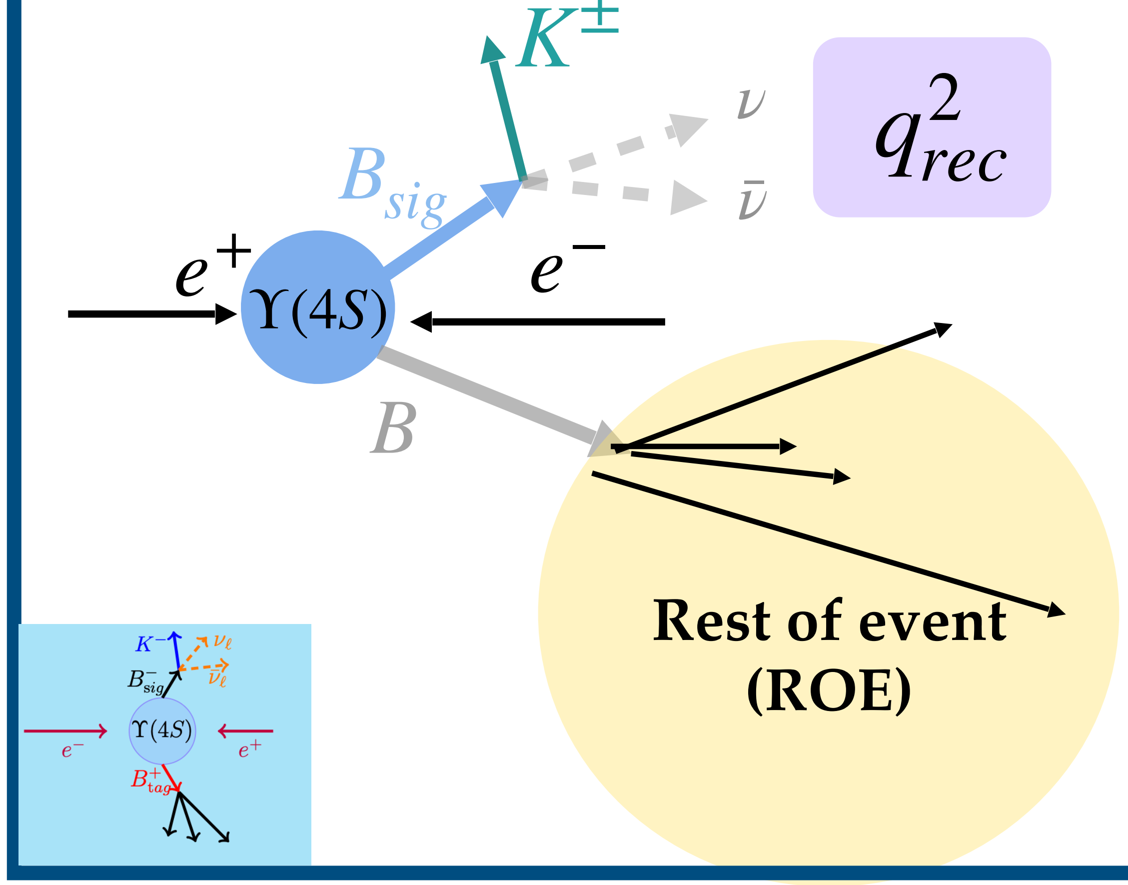

Basic reconstruction of tracks and clusters:

- Charged particles: $E > 100$ MeV/c, close to collision point, in the central part of the detector
- Neutral particles: $E > 100$ MeV **(ITA)**, $E > [60,...,150]$ MeV, ϕ-dependent **(HTA)**
- Signal kaon track candidates required to have high probability to be kaon

Neutral energy validation

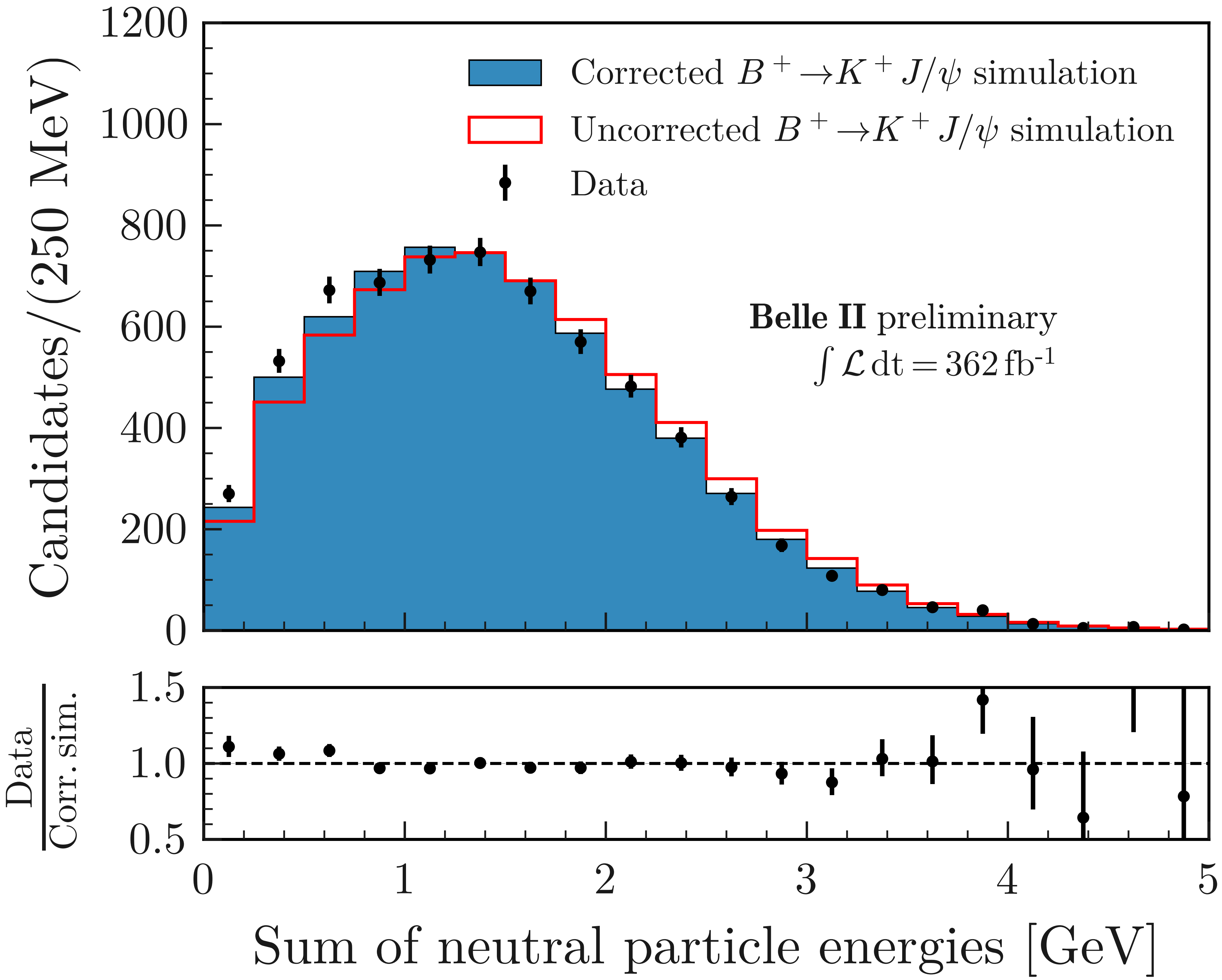

FIG. 2. Summed neutral energy obtained in collision data (points with error bars), uncorrected simulated data (empty histogram), and corrected simulated data (filled histogram), in which a $B^+ \to K^+ J/\psi$ decay is reconstructed. The correction corresponds to a variation of the hadronic energy by -10%. The simulation is normalized to the number of events in data. The ratio shown in the lower panel refers to data over corrected simulation.

Correction for $n_{\gamma\ \mathrm{extra}}$

$$w_{n_{\gamma\ \mathrm{extra}}} = \frac{n_{\mathrm{data}}(n_{\gamma\ \mathrm{extra}})}{n_{\mathrm{simulation}}(n_{\gamma\ \mathrm{extra}})}$$

correction using wrong-sign $K^{\pm}$

validation using pion-enriched sample

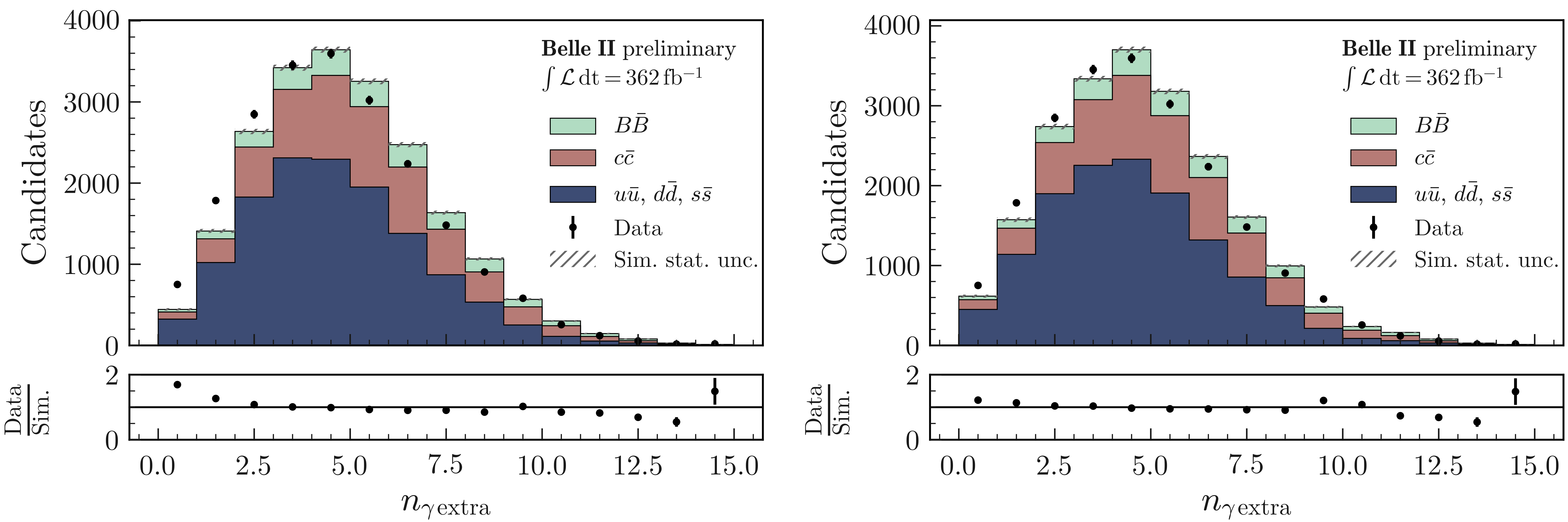

FIG. 3. Distributions of the number of photon candidates in the rest of the event for the HTA after the selection described in Sec. IV in data (points) and simulation (histogram) for the opposite-charge pion-enriched control sample, on the left before the photon multiplicity correction and on the right after the correction. The yields are shown individually for the three background categories ($B\bar{B}$ decays, $c\bar{c}$ continuum, and light-quark continuum). The data to simulation ratio is shown in the bottom panel

K_L^0 efficiency correction

arXiv:2311.14647

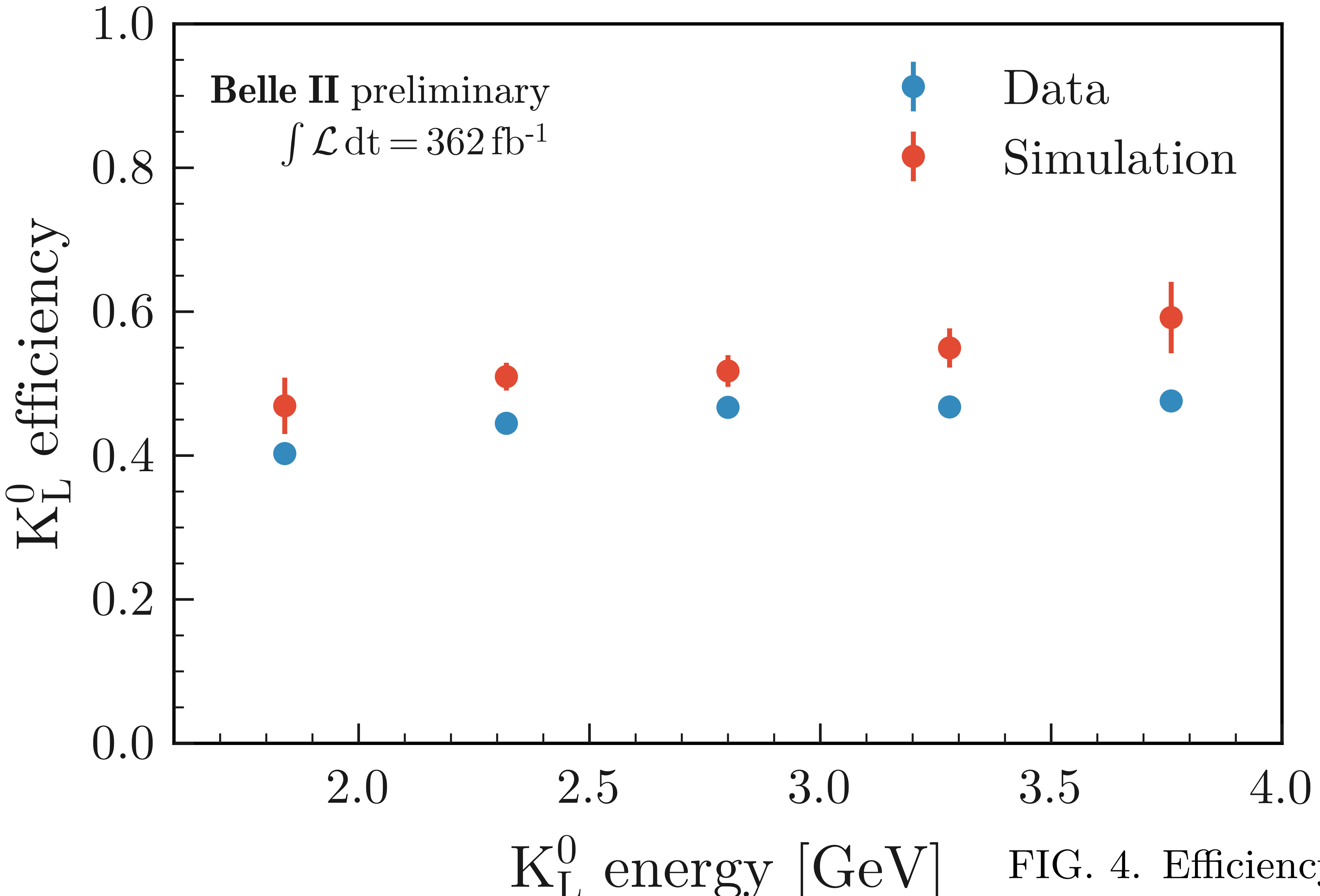

$$e^+e^- \to \gamma\phi(\to K_S^0 K_L^0)$$

FIG. 4. Efficiency of reconstructing an energy deposit in the ECL matched to the K_L^0 direction as a function of the K_L^0 energy for data and simulation selected with the ITA analysis.

PID (K vs. π) validation

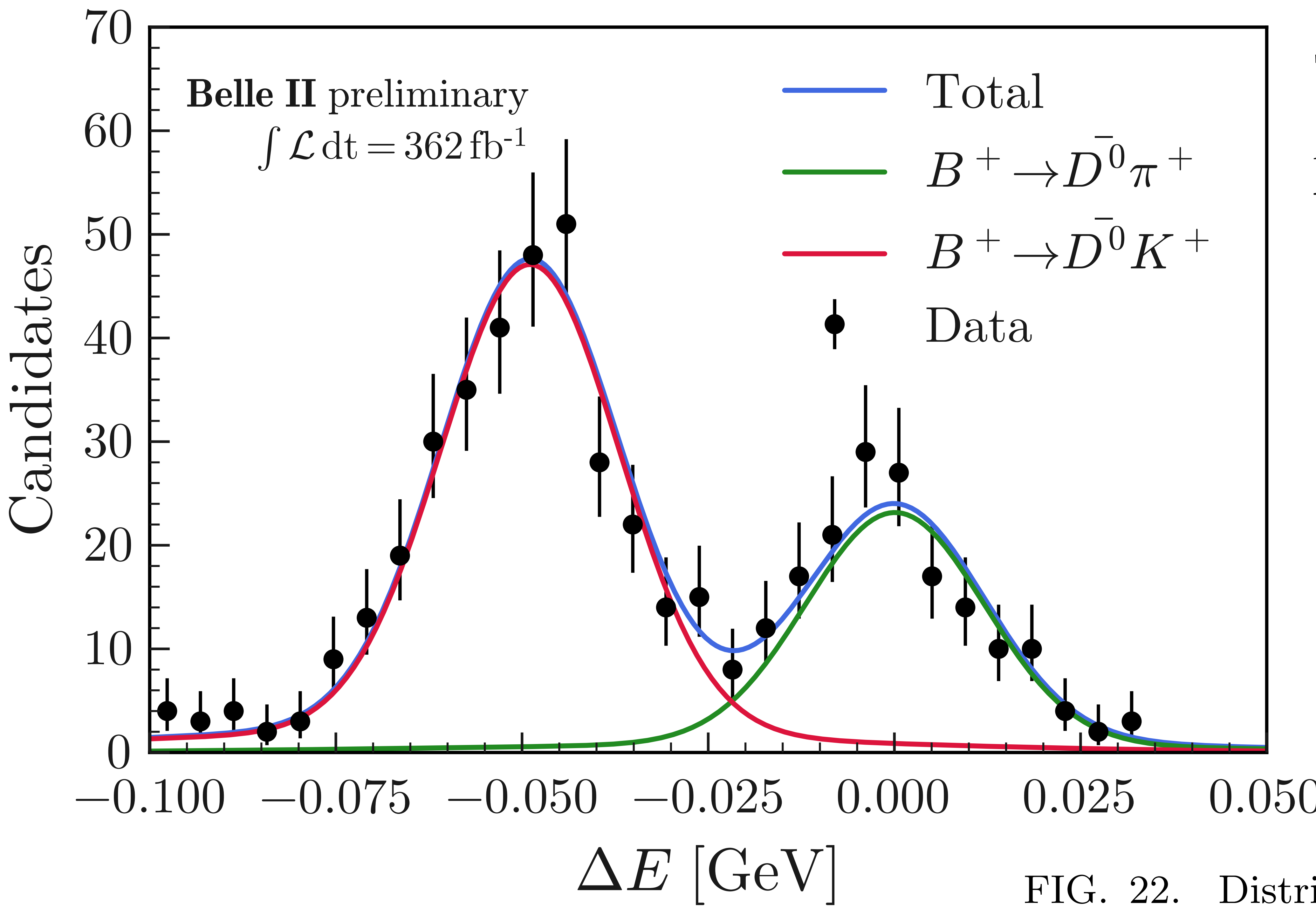

The relative abundance $\overline{D}^0 K^+$ to $\overline{D}^0 \pi^+$ for data vs. MC is found to be consistent w/ expectation with 1.03 ± 0.09

FIG. 22. Distribution of ΔE in data obtained for $B^+ \to (K^+, \pi^+) D^0$ decays reconstructed as $B^+ \to K^+ \nu \bar{\nu}$ events with the daughters from the D^0 decays removed.

arXiv:2311.14647

Signal efficiency (ITA vs. HTA)

after multi-variate analysis for ROE with BDT

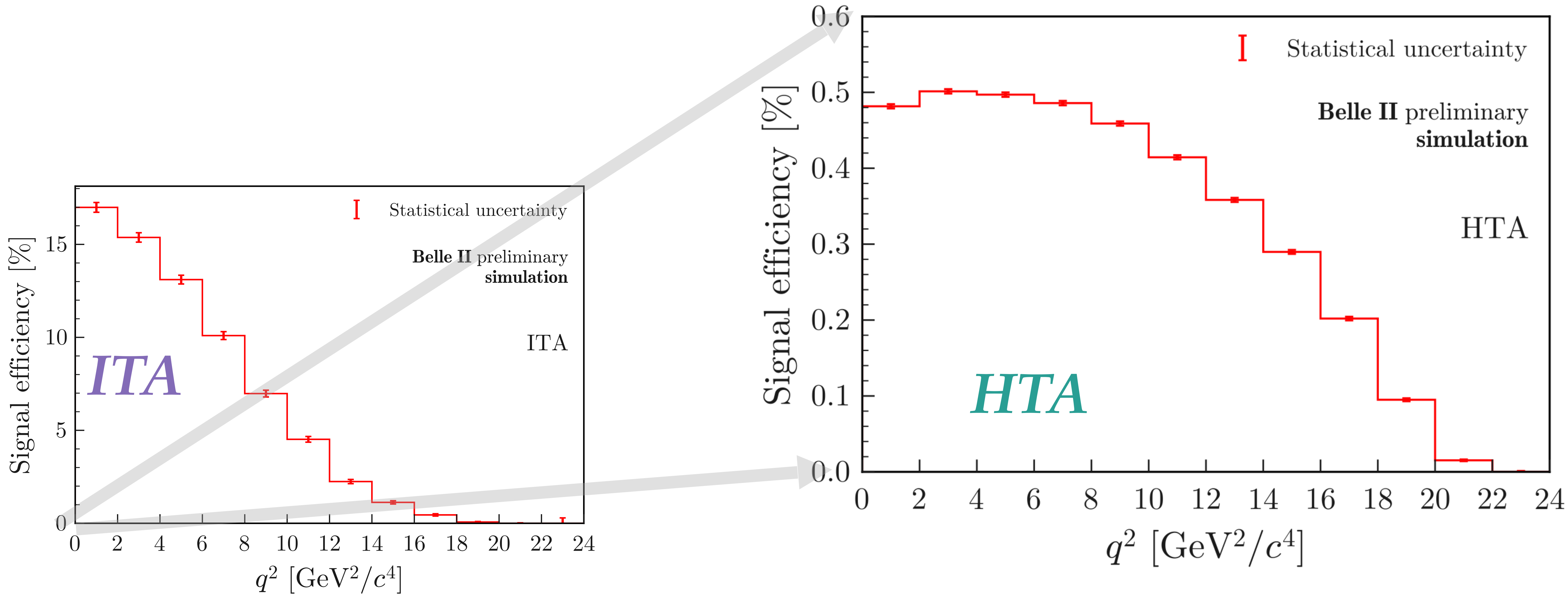

FIG. 5. Signal-selection efficiency as a function of the dineutrino invariant mass squared q^2 for simulated events in the SR for the ITA (left) and HTA (right). The error bars indicate the statistical uncertainty.

Signal efficiency validation (ITA)

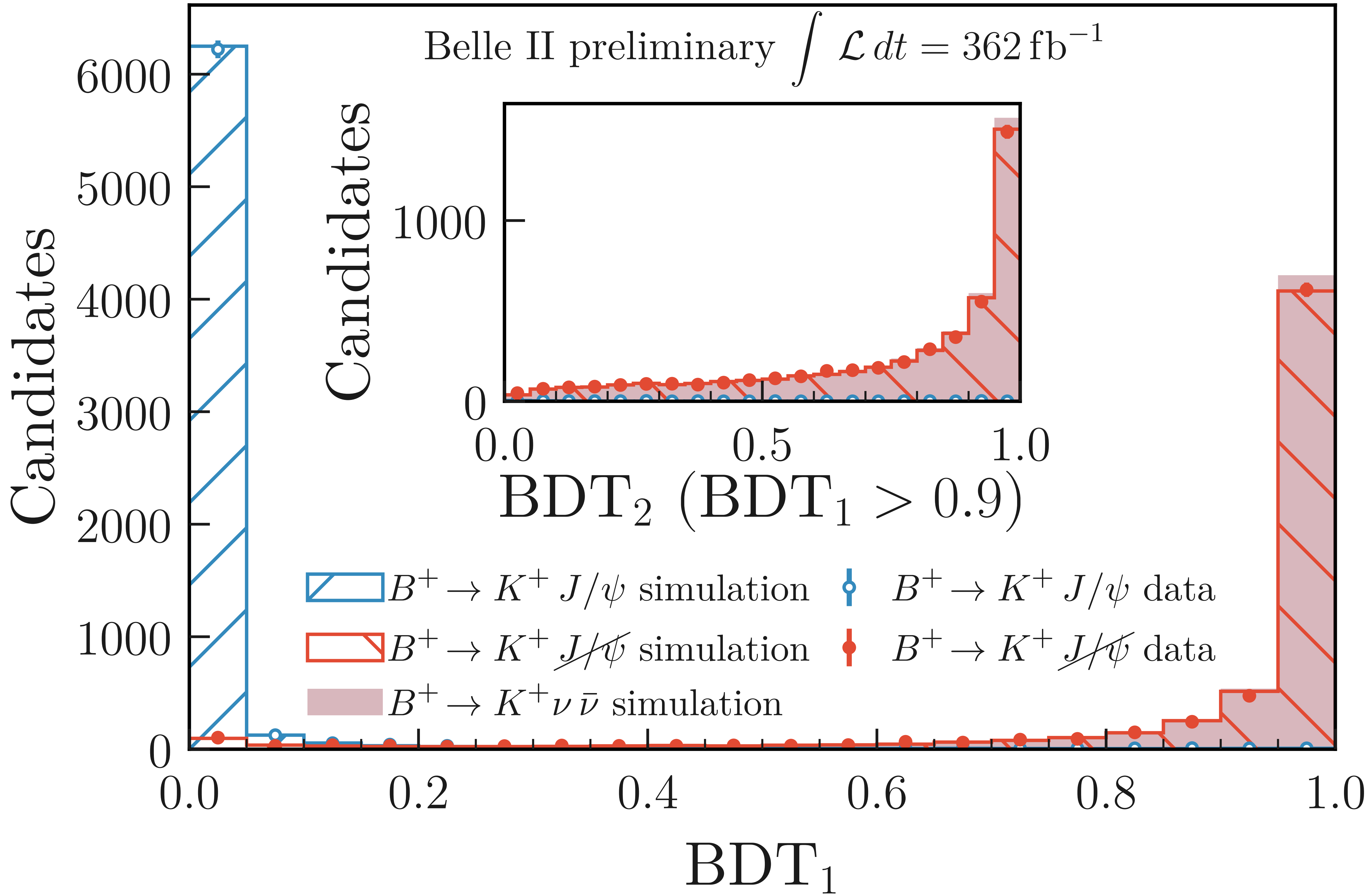

Continuum bkgd. estim. using OFF data

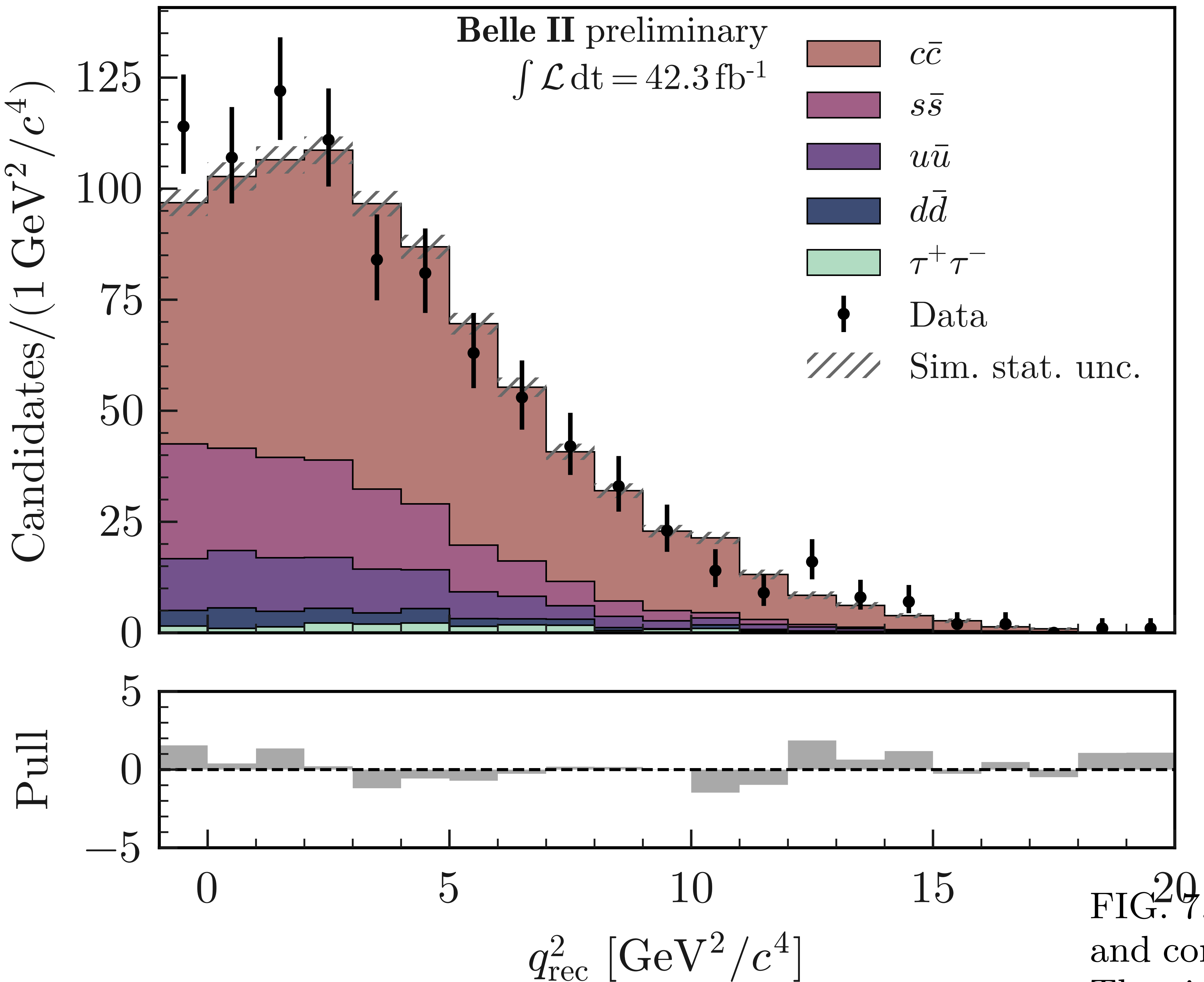

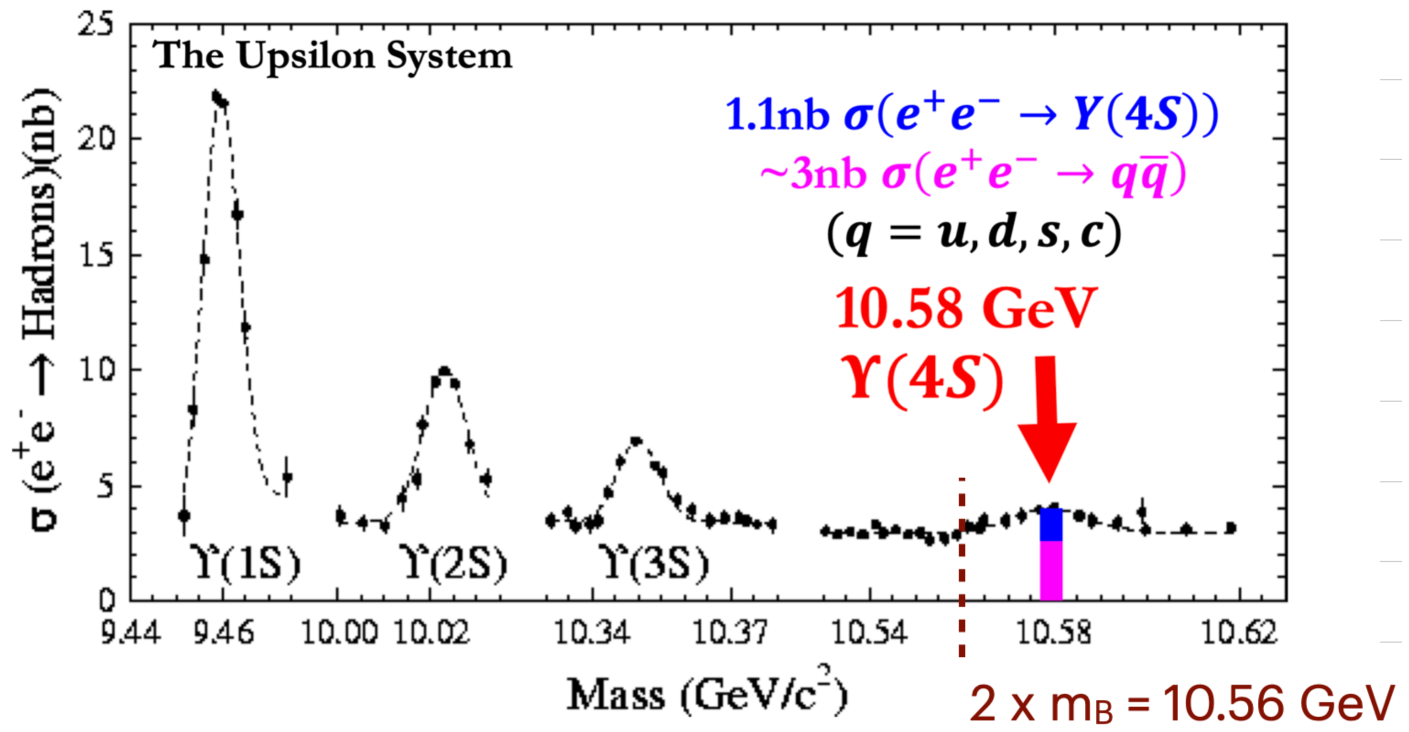

FIG. 7. Distribution of $q^2_{\rm rec}$ for the off-resonance data sample and continuum background simulation in the SR for the ITA. The simulation is normalized to the number of events in the data. The pull distribution is shown in the bottom panel.

$B\overline{B}$ bkgd. mostly for $D \to K^{\pm}X$

arXiv:2311.14647

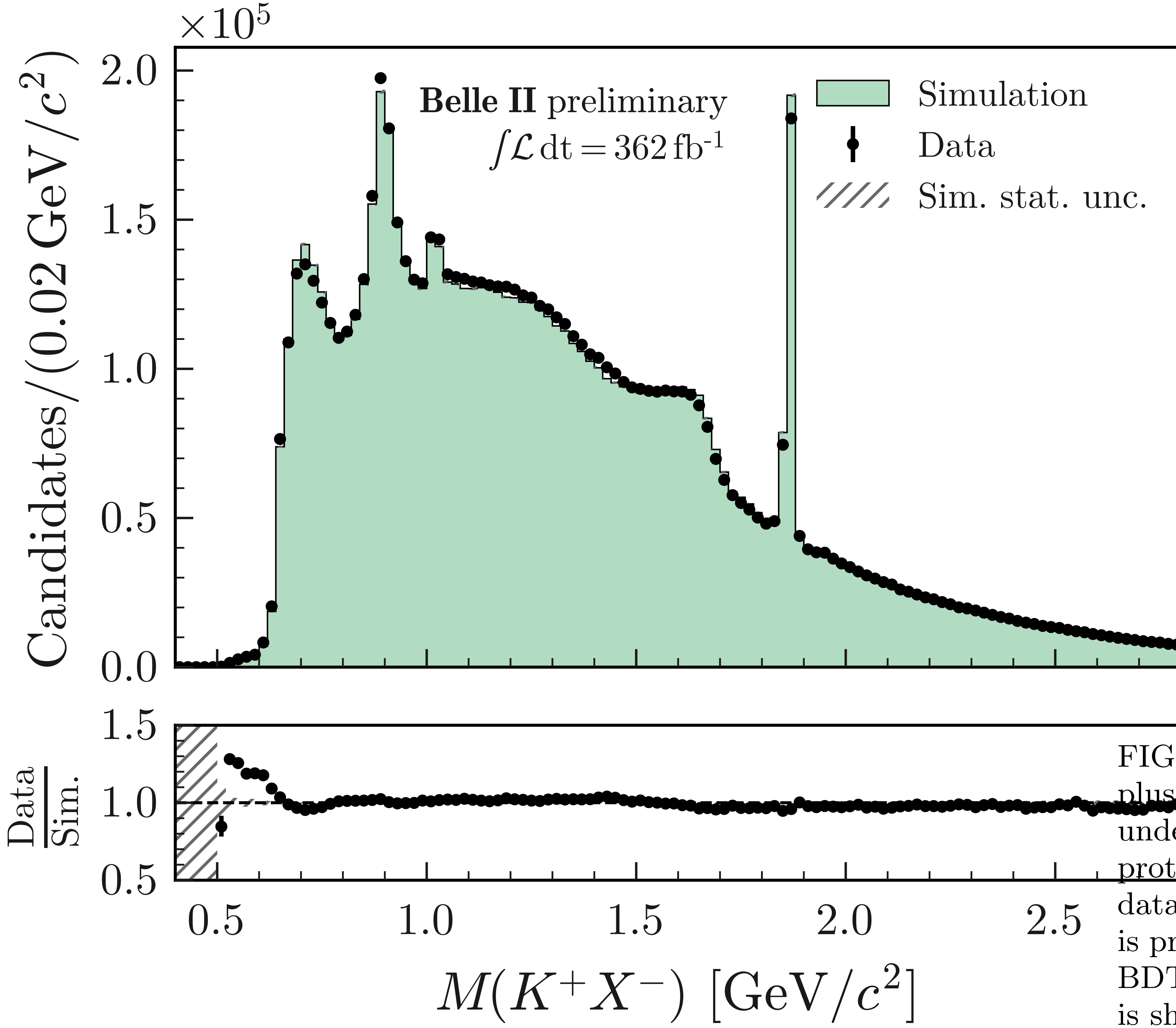

FIG. 8. Distribution of invariant mass for the candidate K^+ plus a charged particle from the ROE, which is reconstructed under the most probable mass hypothesis of a pion, kaon, proton, electron or muon based on the PID information. The data are shown by points with error bars and the simulation is presented as a histogram. The samples are shown after the $BDT_1 > 0.9$ selection in the ITA. The data to simulation ratio is shown in the bottom panel.

$B\overline{B}$ bkgd. estimation using π-enriched sample

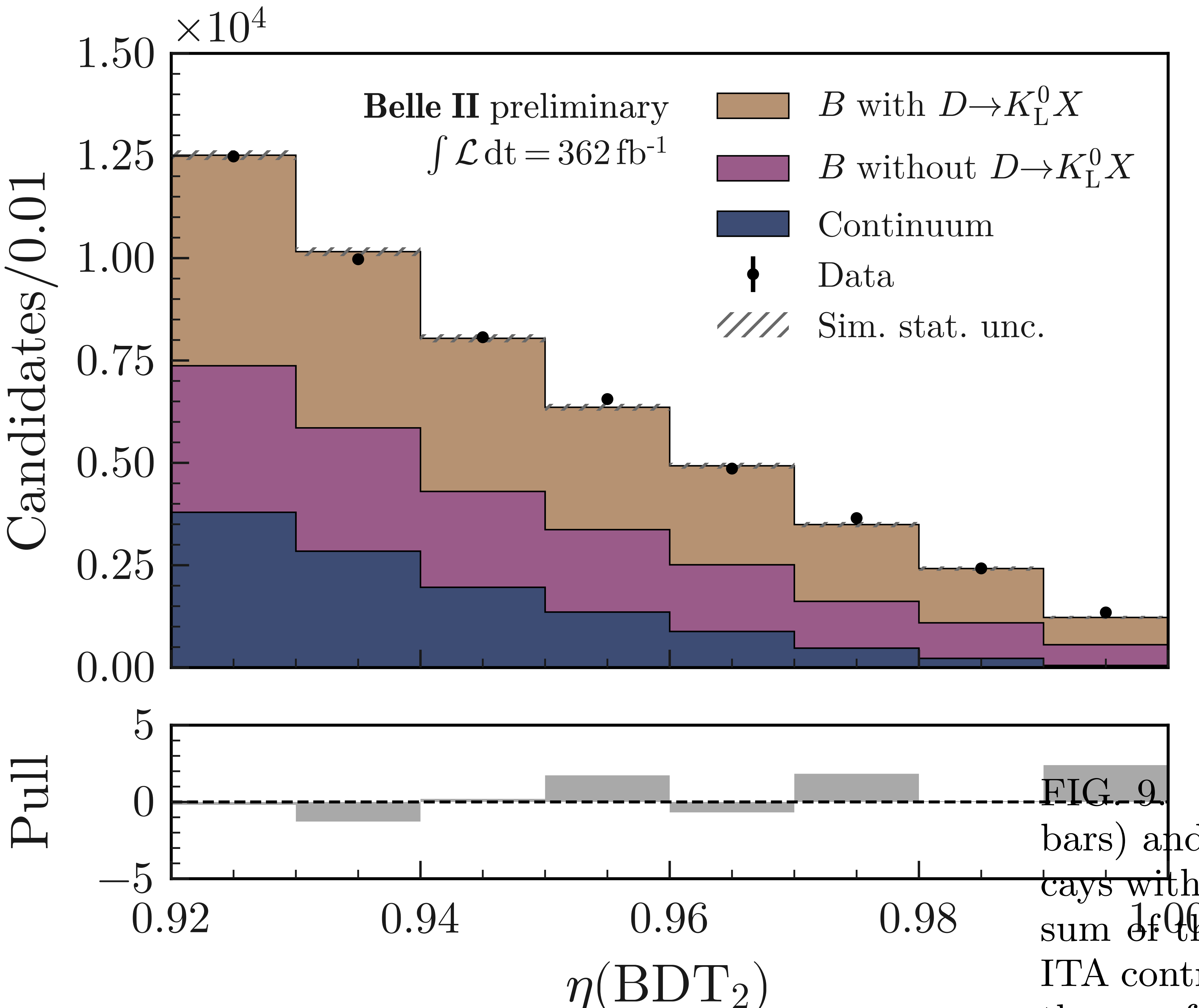

FIG. 9. Distribution of $\eta(\mathrm{BDT}_2)$ in data (points with error bars) and simulation divided into three groups (B-meson decays with and without subsequent $D \to K^0_{\mathrm{L}} X$ decays, and the sum of the five continuum categories), for the pion-enriched ITA control sample. All the corrections are applied, including the one for the contribution involving D mesons decaying to K^0_{L}. The pull distribution is shown in the bottom panel.

Check with lepton-enriched samples

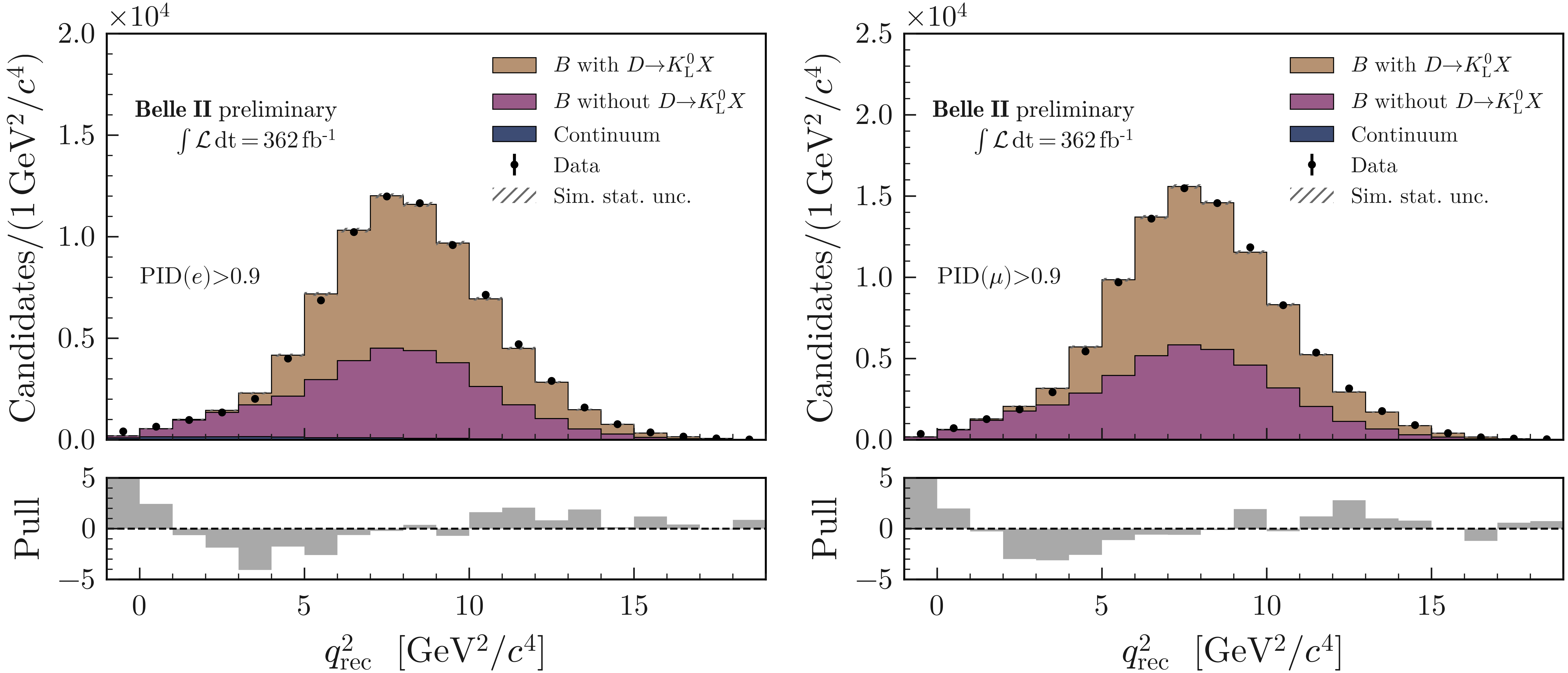

FIG. 10. Distribution of $q^2_{\rm rec}$ in data (points with error bars) and simulation (filled histograms) divided into three groups (B-meson decays with and without subsequent $D \to K^0_{\rm L} X$ decays, and the sum of the five continuum categories), for the electron- (left) and muon-enriched (right) PID control samples with $\eta(\mathrm{BDT}_2) > 0.92$ in the ITA. The pull distribution is shown in the bottom pannel.

Check K_L^0 bkgd. with $B \to K^+ K^0 \overline{K}^0$

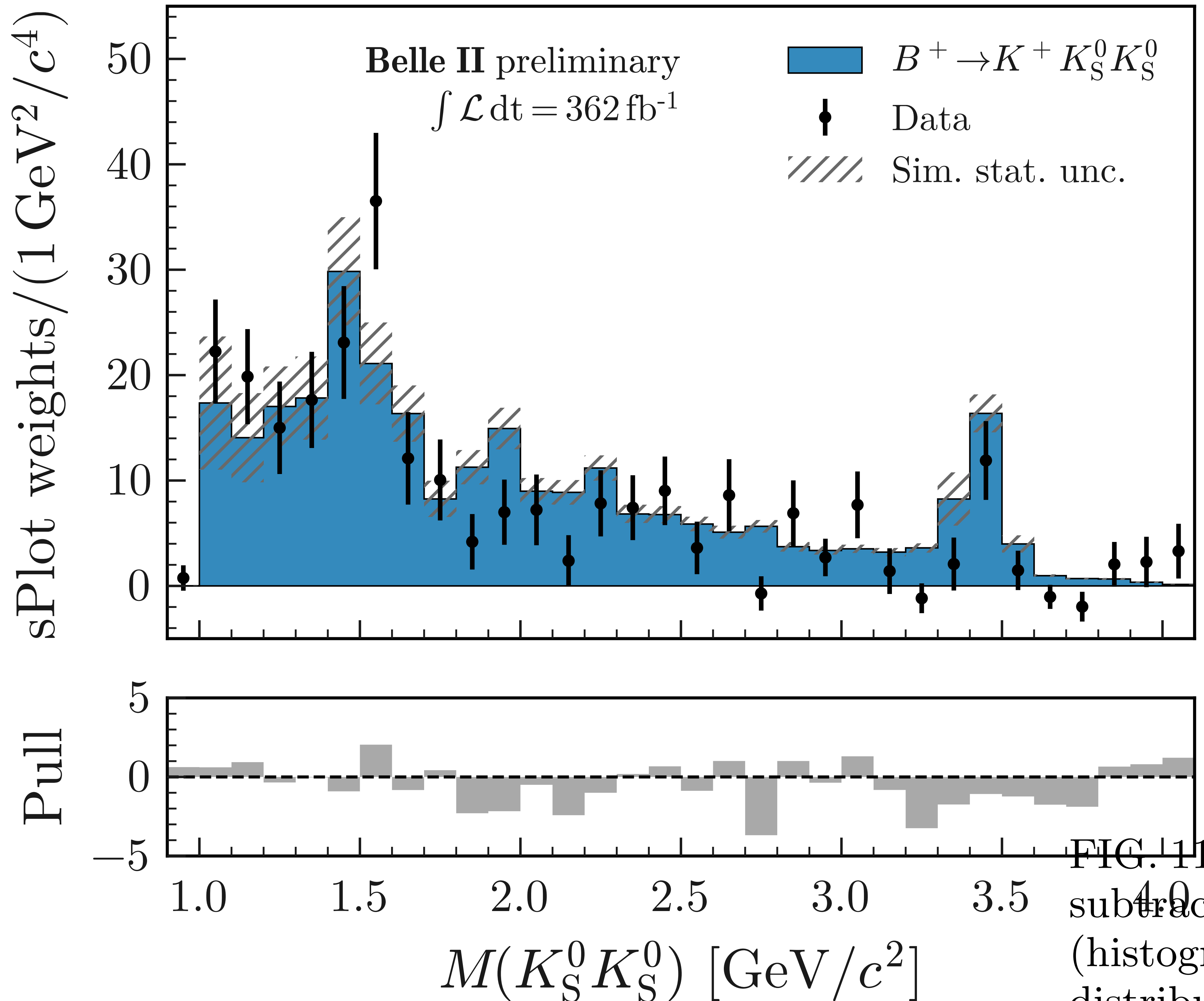

FIG. 11. Distribution of invariant $K_S^0 K_S^0$ mass in background-subtracted data (points with error bars) and signal simulation (histogram) for $B^+ \to K^+ K_S^0 K_S^0$ candidates. The simulated distribution is normalized to the number of $B\bar{B}$ events. The pull distribution is shown in the bottom panel.

Check K_L^0 bkgd. with $B \to K_S^0 K^+ K^-$

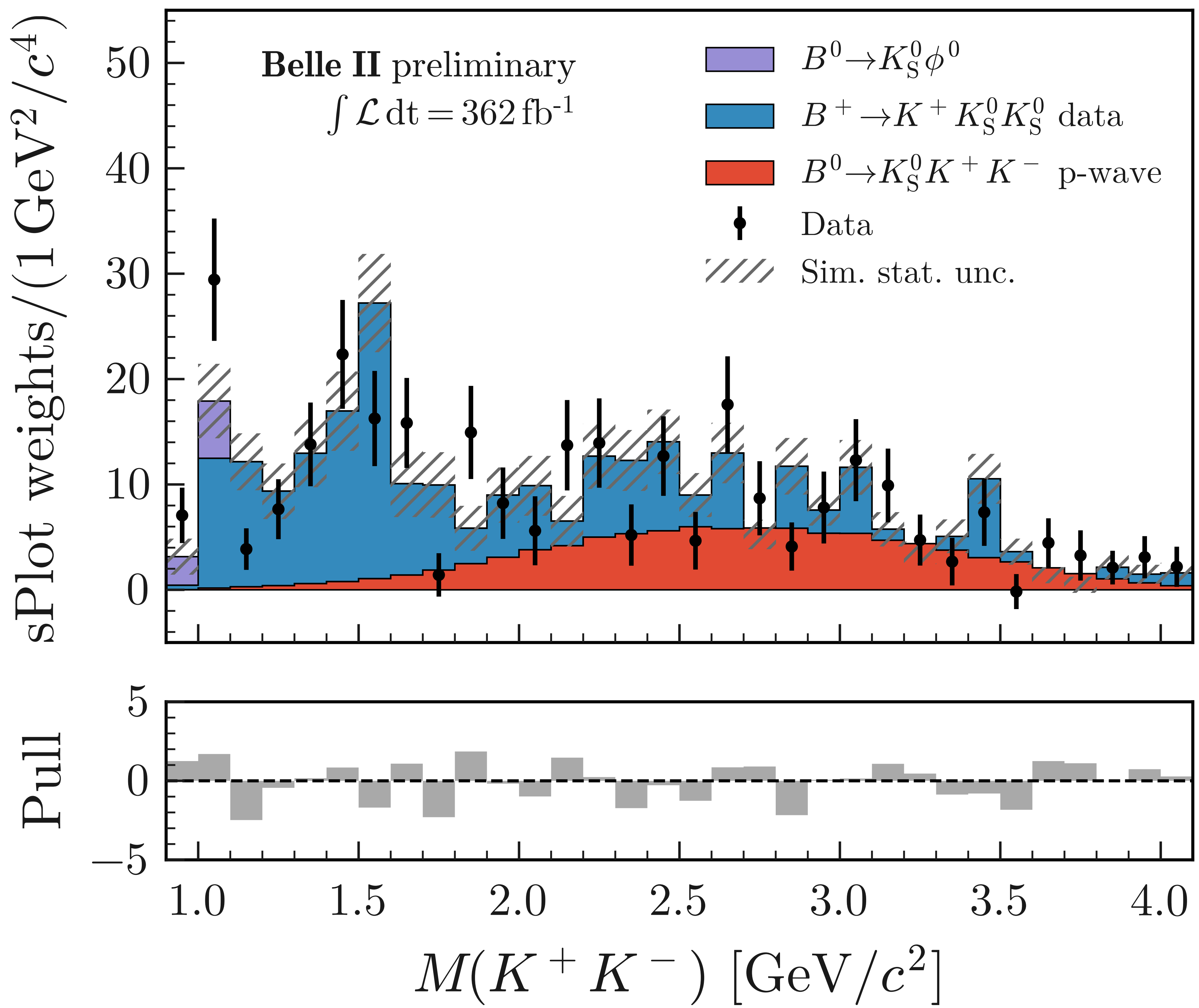

FIG. 12. Distribution of the invariant mass of the K^+K^- pair from $B^0 \to K_S^0 K^+ K^-$ decays in background-subtracted data (points with error bars) and the sum of the simulated p-wave nonresonant component (histogram filled with red), the s-wave contribution estimated using $B^+ \to K^+ K_S^0 K_S^0$ decays in data (histogram filled with blue), and simulated $B^0 \to K_S^0 \phi$, $\phi \to K^+K^-$ decay (histogram filled with purple). The distribution obtained using $B^+ \to K^+ K_S^0 K_S^0$ decays in data is corrected for efficiency and the ratio of the B^+ and B^0 lifetimes. The simulated distributions are normalized to the number of $B\bar{B}$ events. The pull distribution is shown in the bottom panel.

Closure test (ITA)

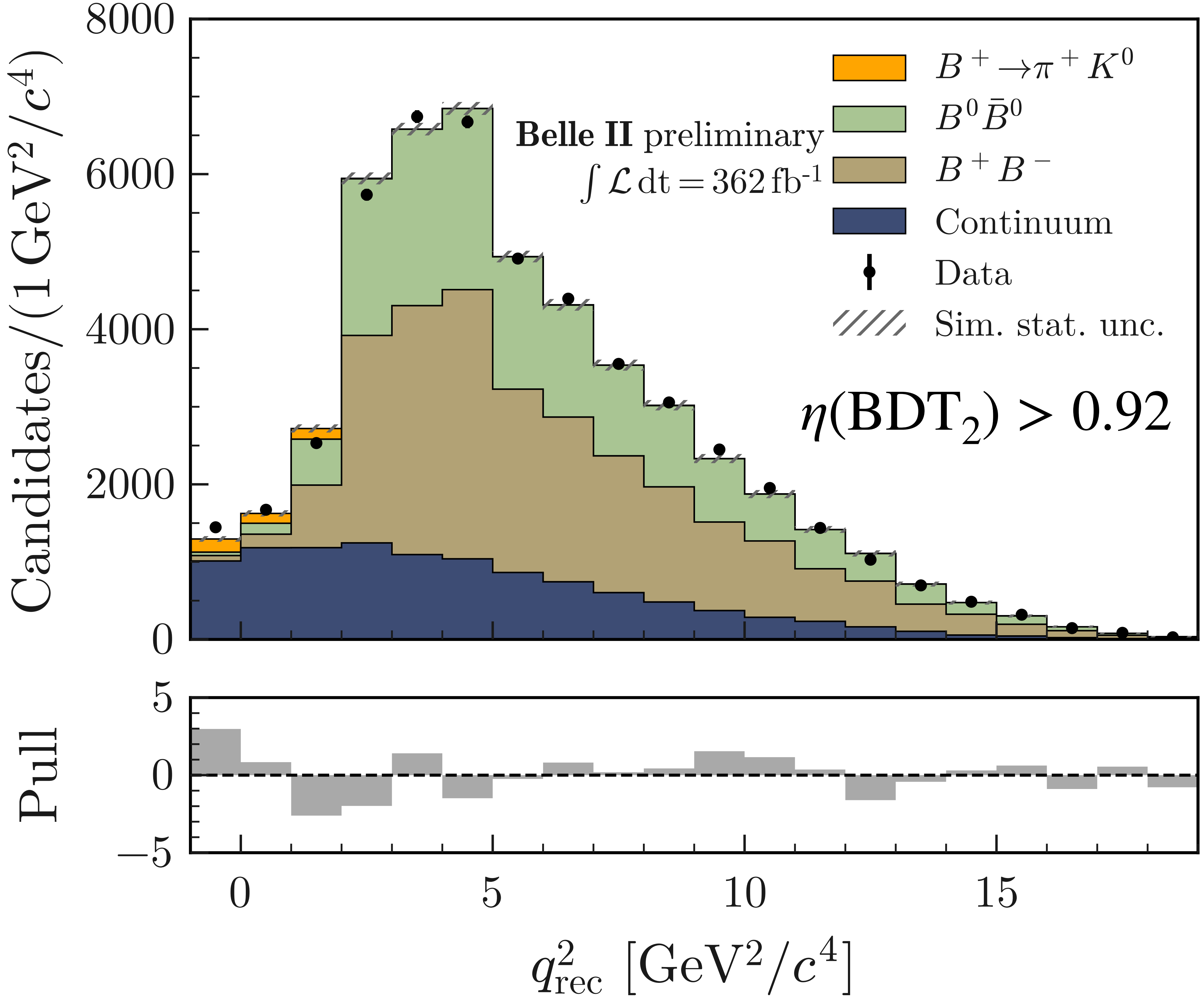

- Pion ID instead of kaon ID
- Different q^2_{rec} bin boundaries
- Only on-resonance data used for fit
- Only normalization systematics included

Result:

- $\mathscr{B}(B^+ \to \pi^+ K^0) = (2.5 \pm 0.5) \times 10^{-5}$

Consistent with PDG:

$\mathscr{B}(B^+ \to \pi^+ K^0) = (2.3 \pm 0.08) \times 10^{-5}$

Search for $B^+ \to K^+ \nu\bar{\nu}$ at Belle II

Results

$B^+ \to K^+\nu\bar{\nu}$ result (ITA)

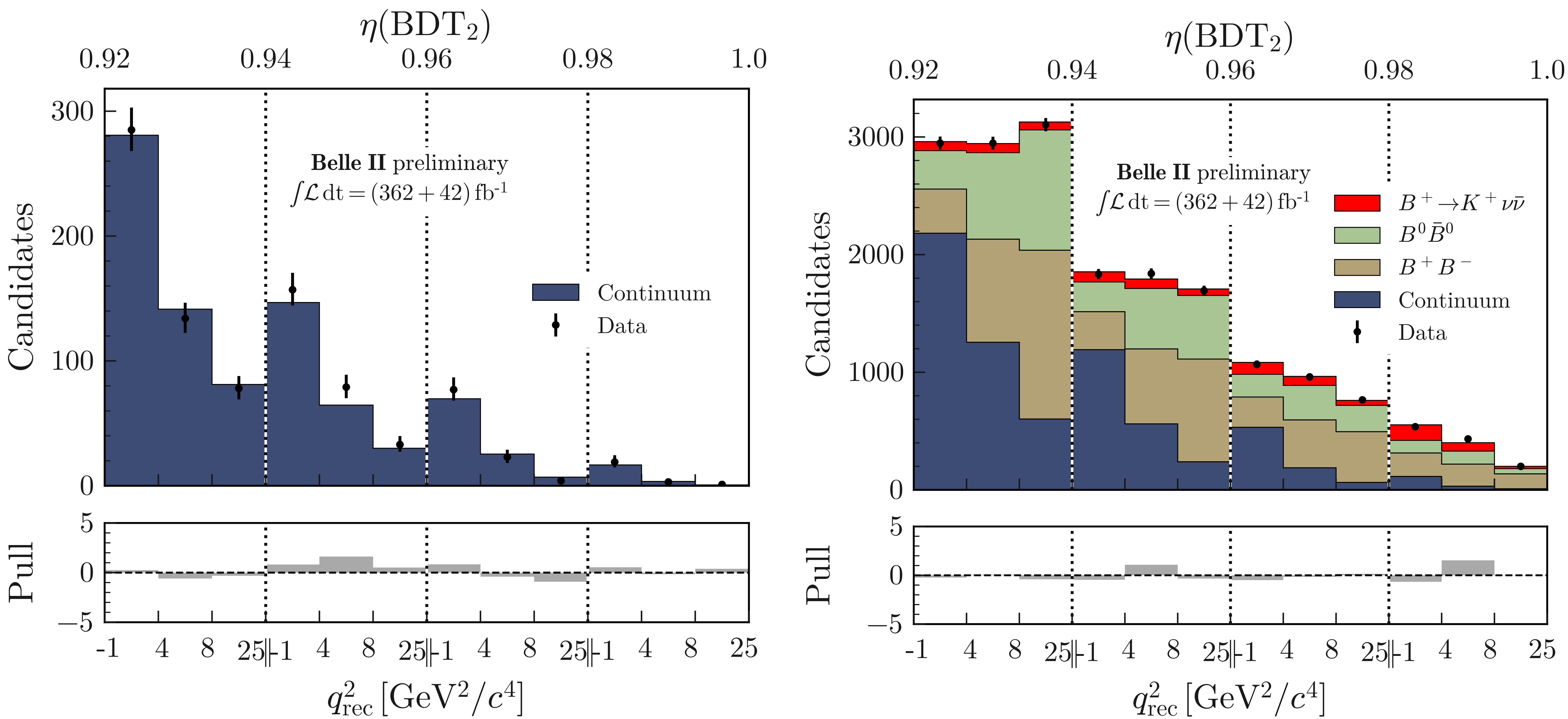

FIG. 13. Observed yields and fit results in bins of the $\eta(\mathrm{BDT}_2) \times q^2_{\mathrm{rec}}$ space obtained by the ITA simultaneous fit to the off- and on-resonance data, corresponding to an integrated luminosity of 42 and $362\,\mathrm{fb}^{-1}$, respectively. The yields are shown individually for neutral and charged B-meson decays and the sum of the five continuum categories. The yields are obtained in bins of the $\eta(\mathrm{BDT}_2) \times q^2_{\mathrm{rec}}$ space. The pull distribution is shown in the bottom panel.

arXiv:2311.14647

$B^+ \to K^+ \nu\bar{\nu}$ post-fit distributions (ITA)

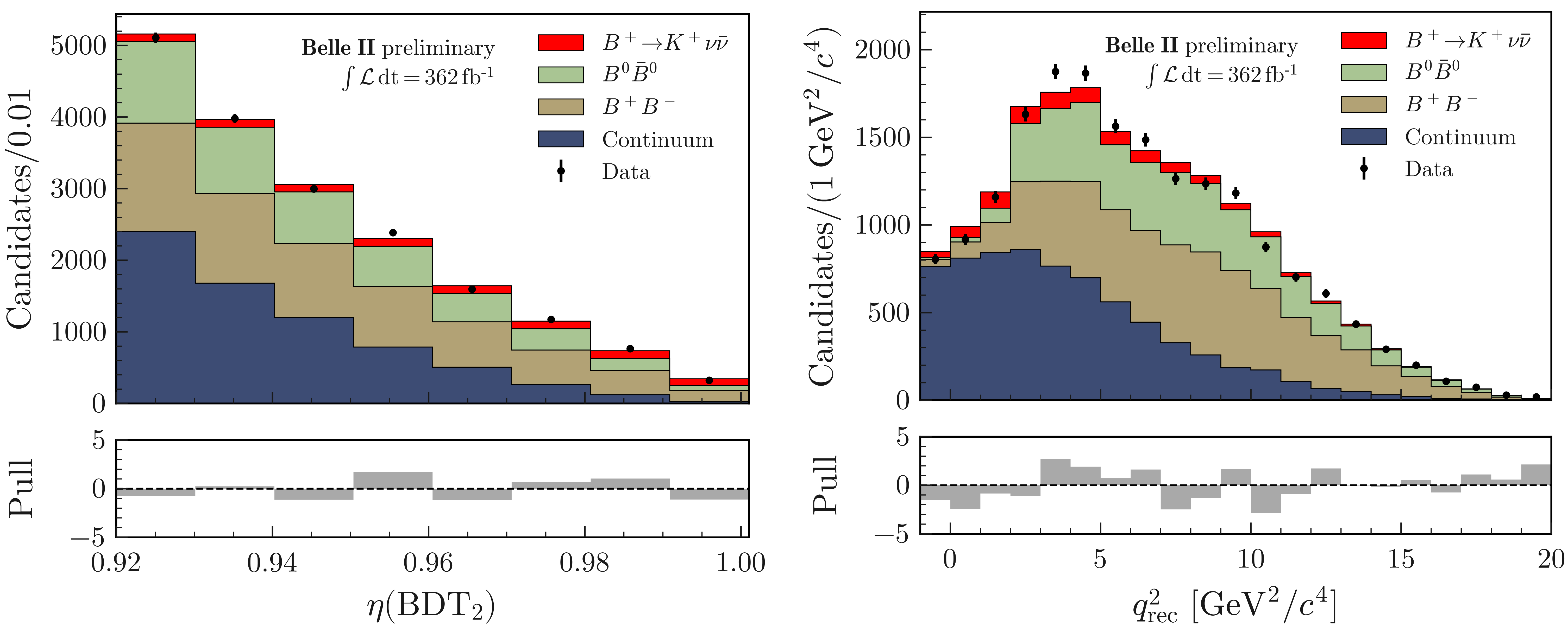

$$\eta(BDT_2) > 0.92$$

$B^+ \to K^+\nu\bar{\nu}$ post-fit distributions (ITA)

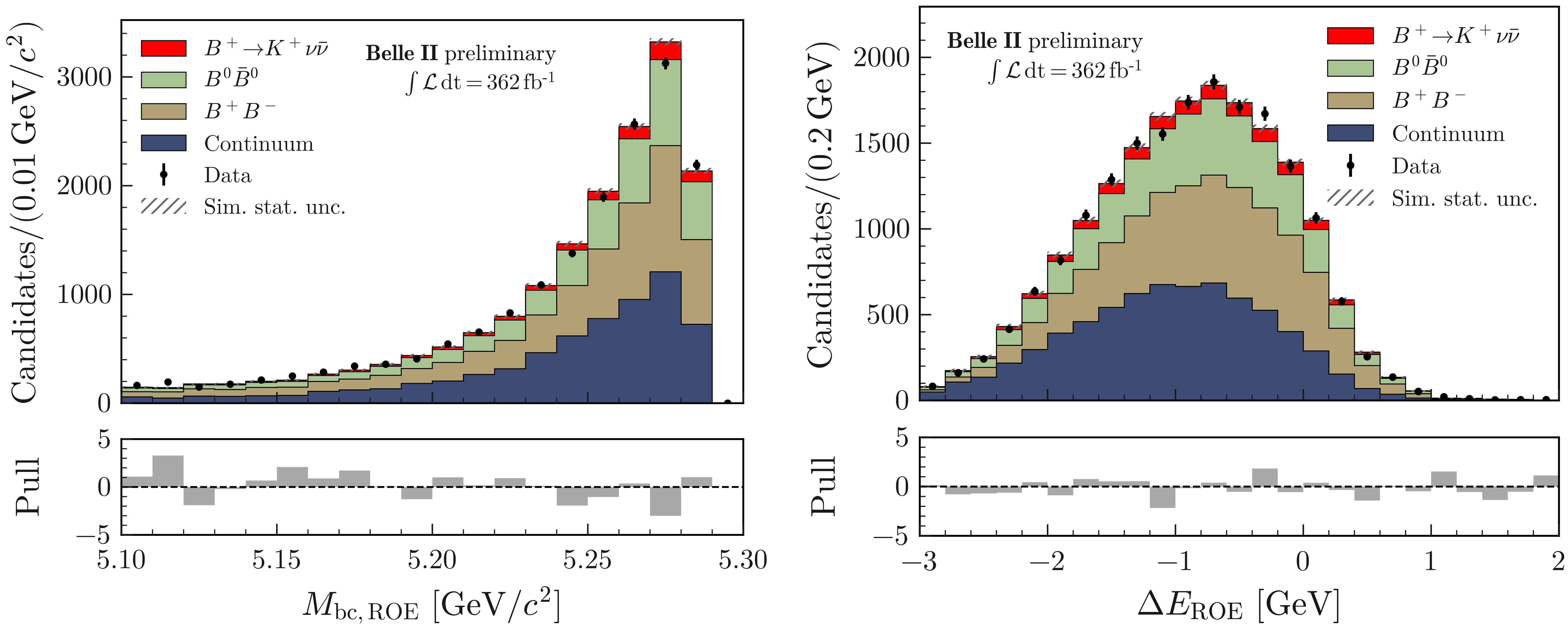

$\eta(\mathrm{BDT}_2) > 0.92$

arXiv:2311.14647

$B^+ \to K^+\nu\bar{\nu}$ post-fit distributions (ITA)

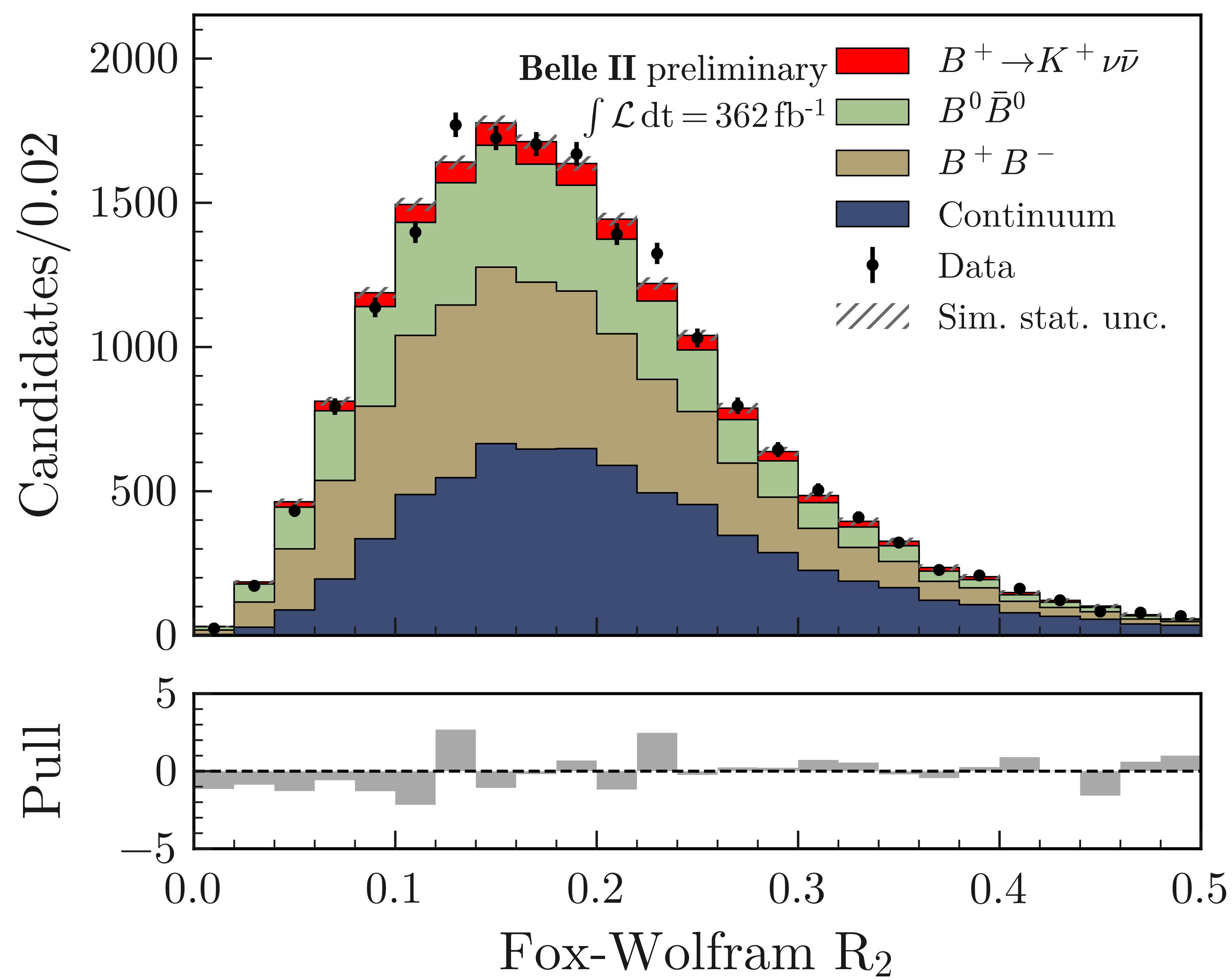

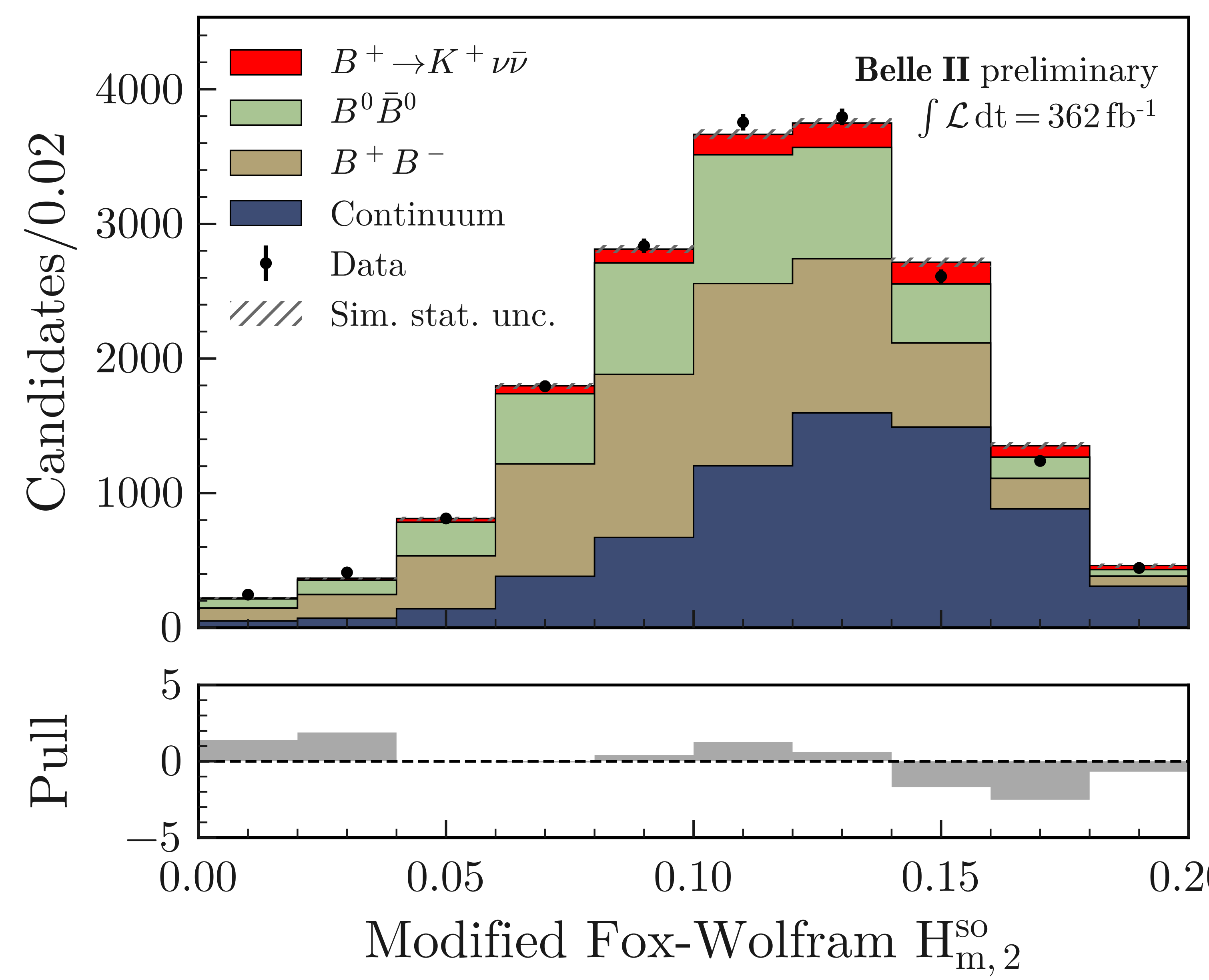

$\eta(\text{BDT}_2) > 0.92$

arXiv:2311.14647

$B^+ \to K^+\nu\bar{\nu}$ post-fit (SE) distributions (ITA)

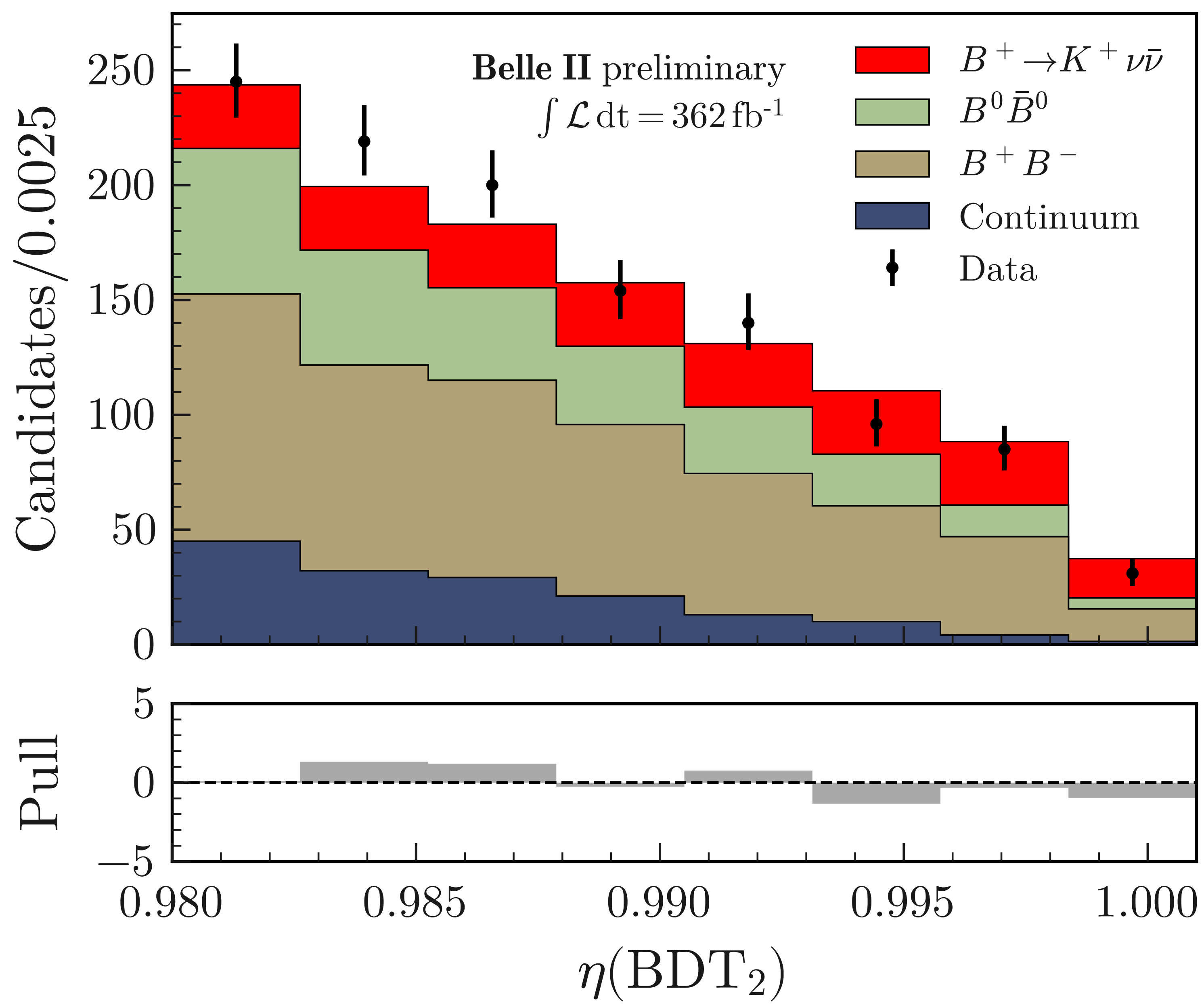

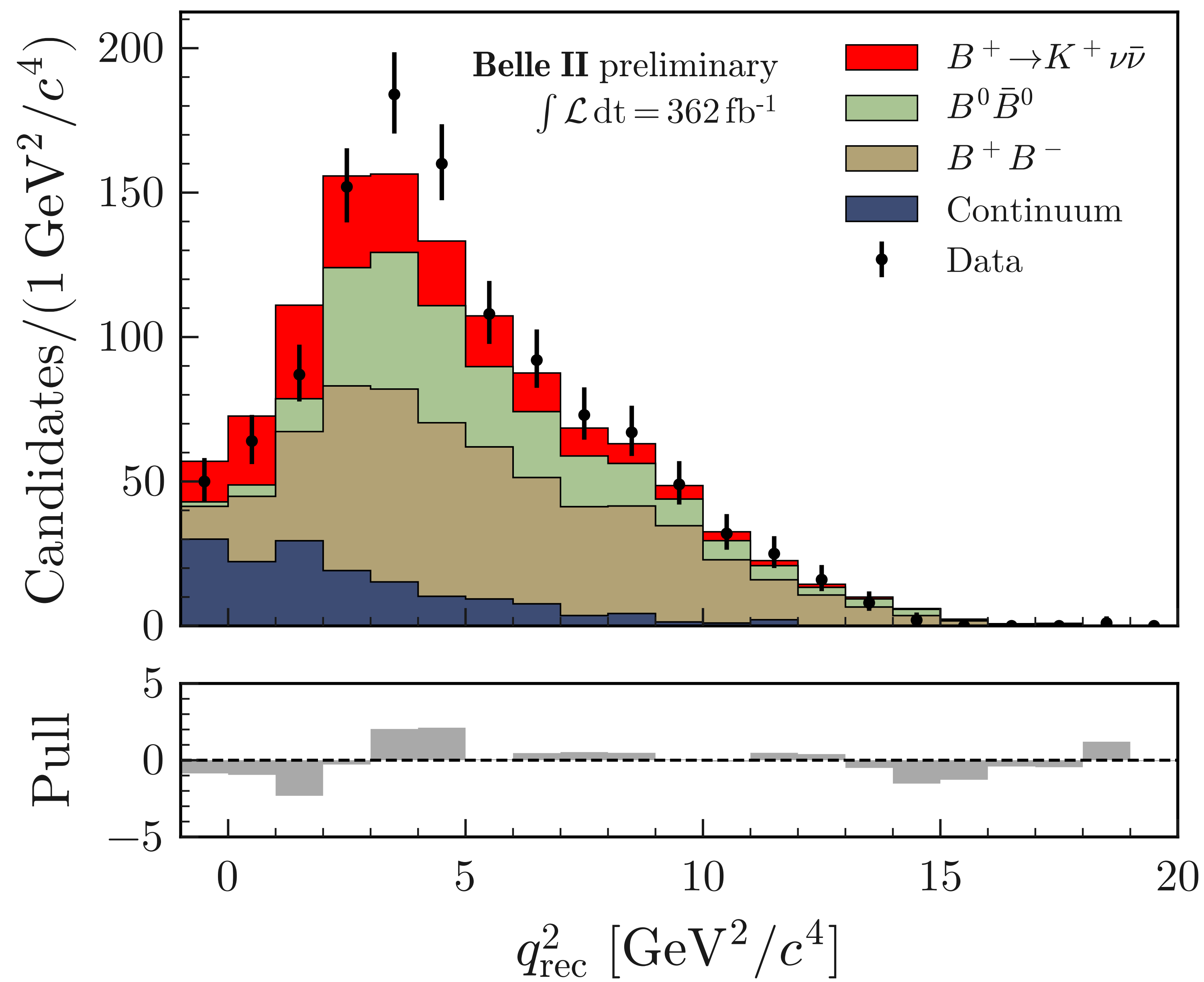

$$\eta(BDT_2) > 0.98$$

$B^+ \to K^+\nu\bar{\nu}$ post-fit (SE) distributions (ITA)

arXiv:2311.14647

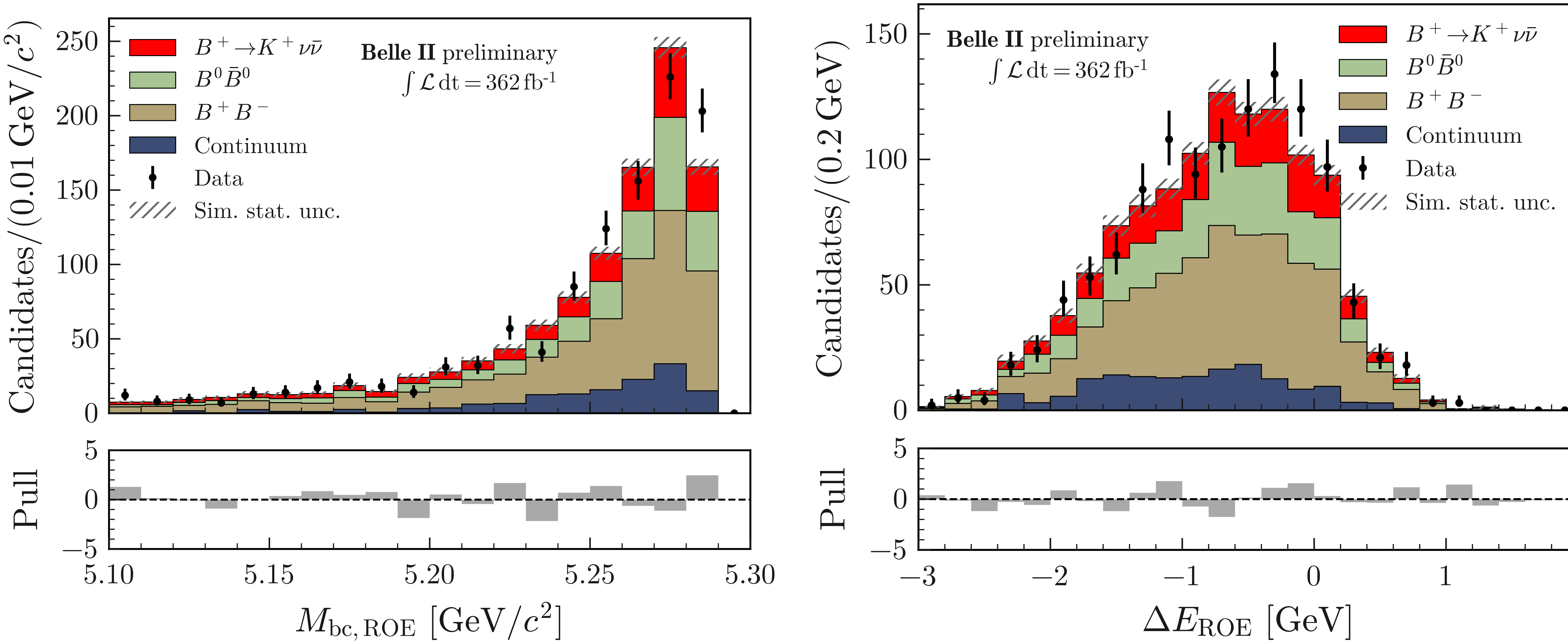

$$\eta(\text{BDT}_2) > 0.98$$

$B^+ \to K^+\nu\bar{\nu}$ post-fit (SE) distributions (ITA)

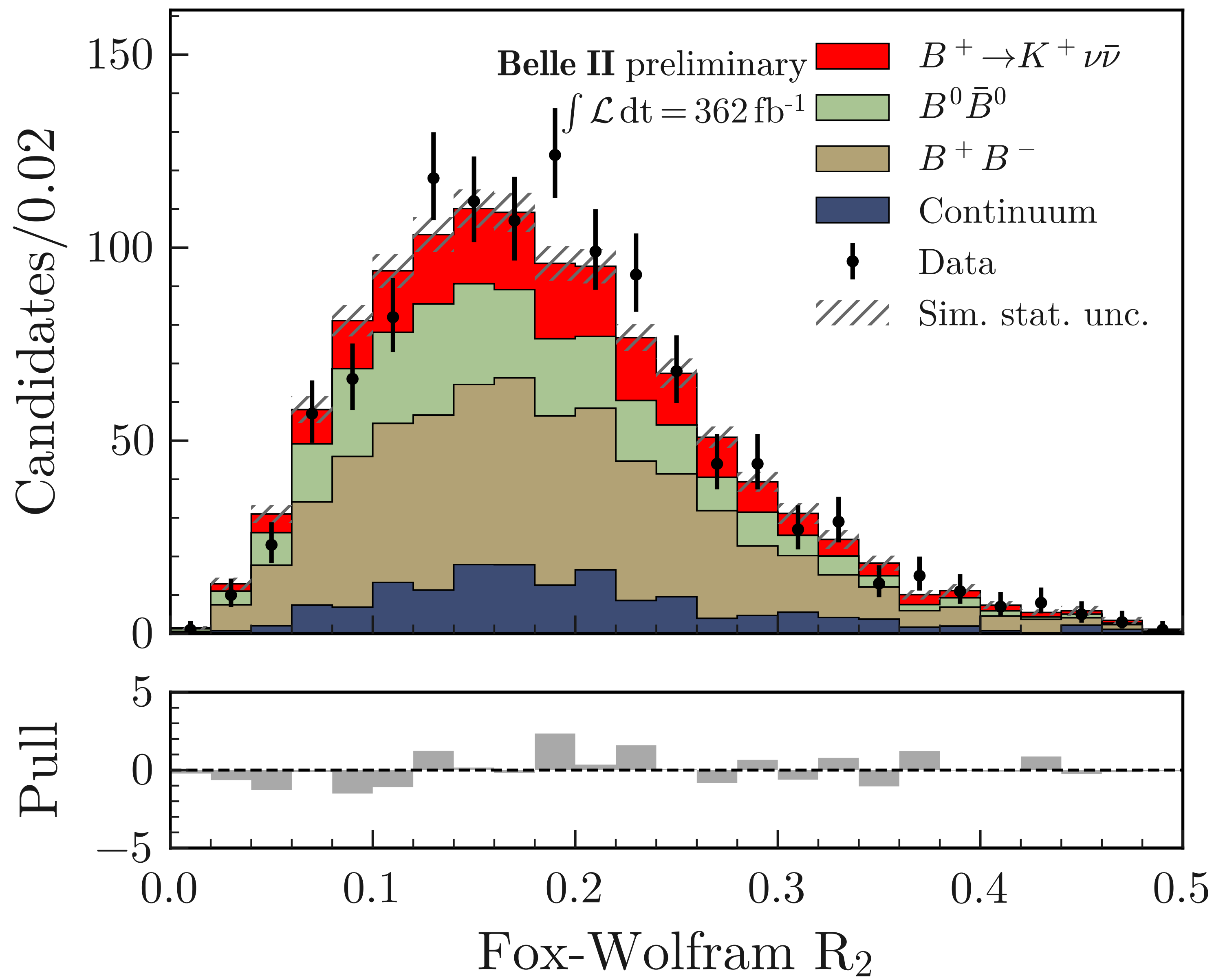

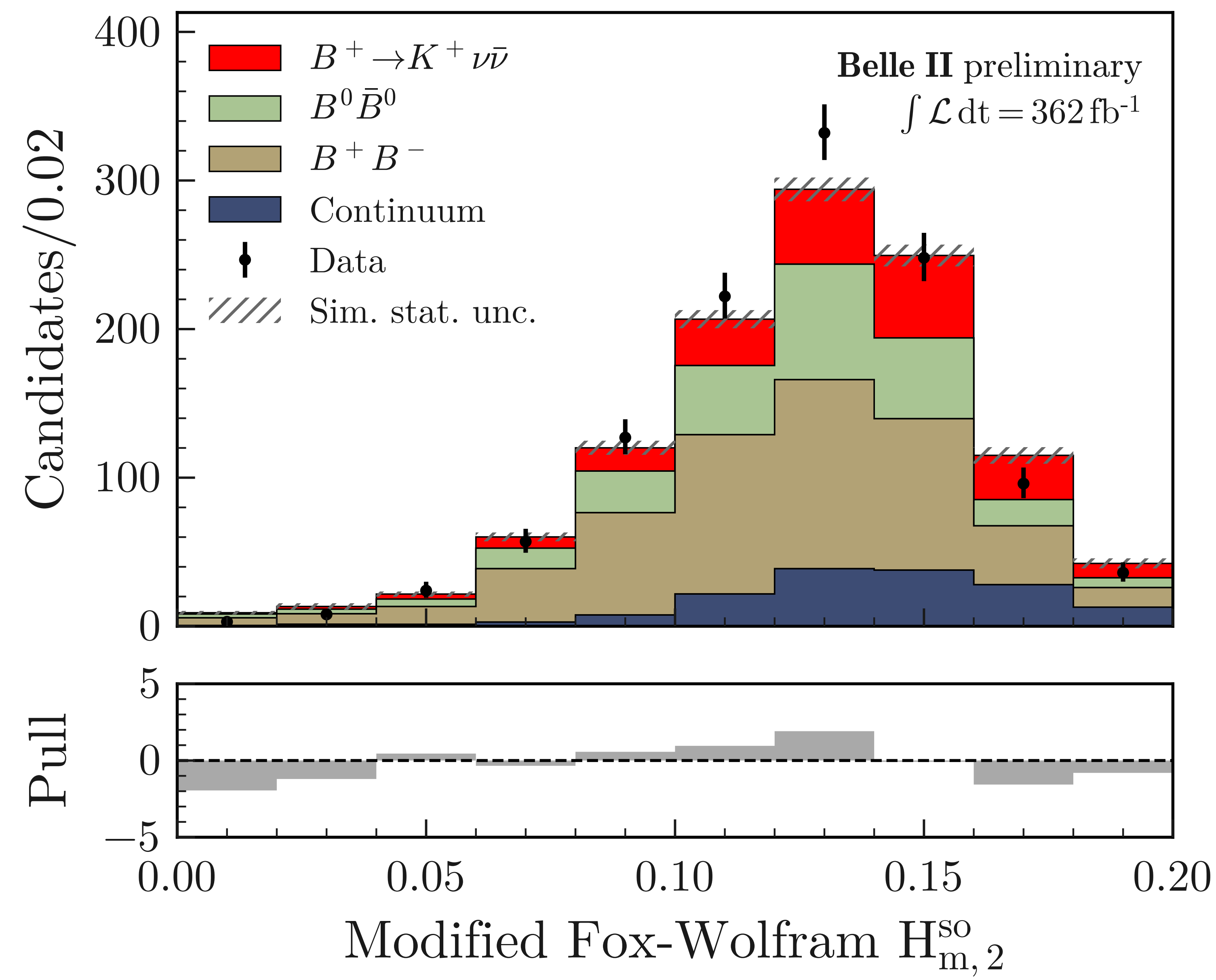

$$\eta(\mathrm{BDT}_2) > 0.98$$

$B^+ \to K^+ \nu\bar{\nu}$ result (HTA)

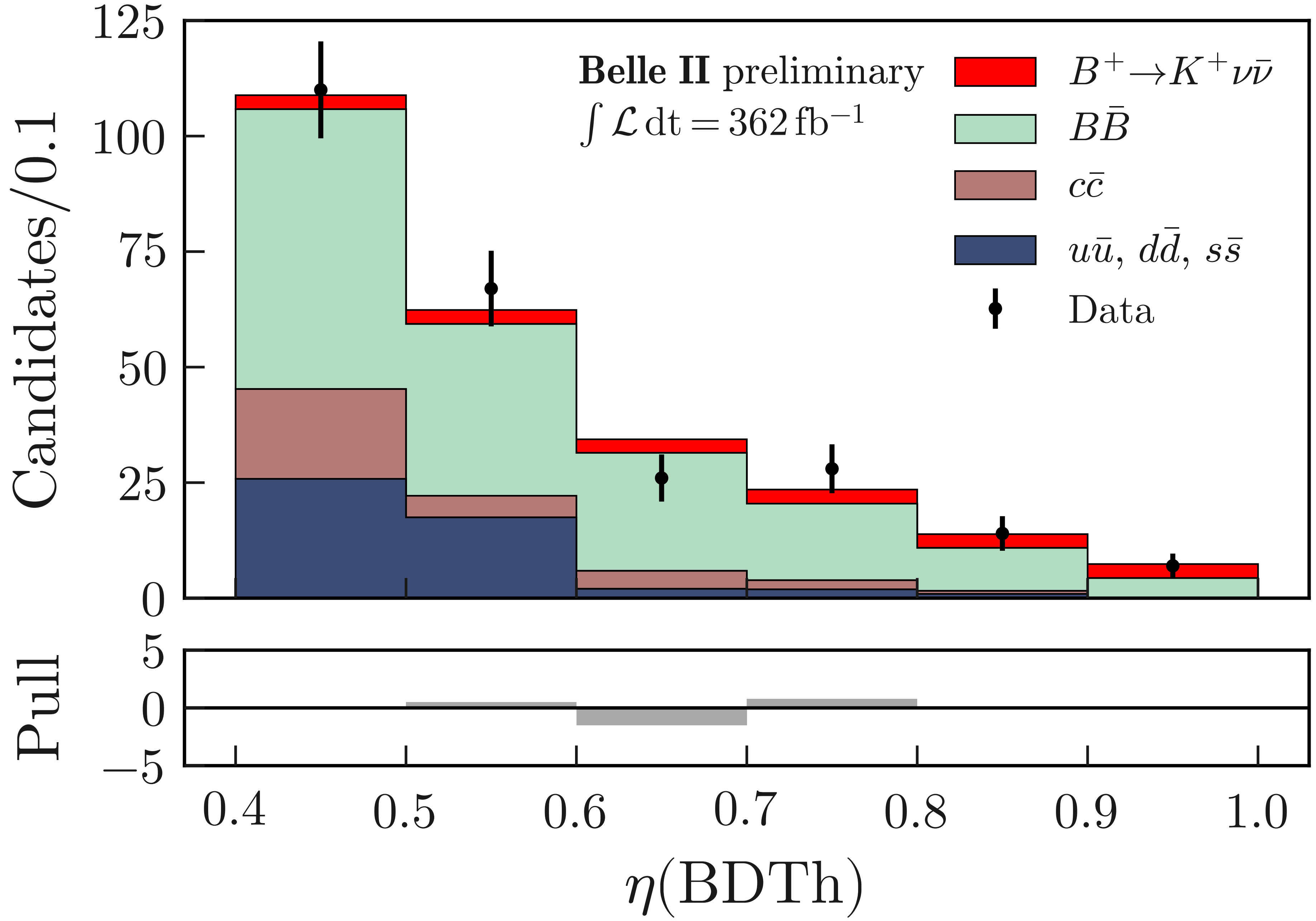

FIG. 17. Observed yields and fit results in bins of η(BDTh) as obtained by the HTA fit, corresponding to an integrated luminosity of 362 fb^{-1}. The yields are shown for the signal and the three background categories ($B\bar{B}$ decays, $c\bar{c}$ continuum, and light-quark continuum). The pull distribution is shown in the bottom panel.

arXiv:2311.14647

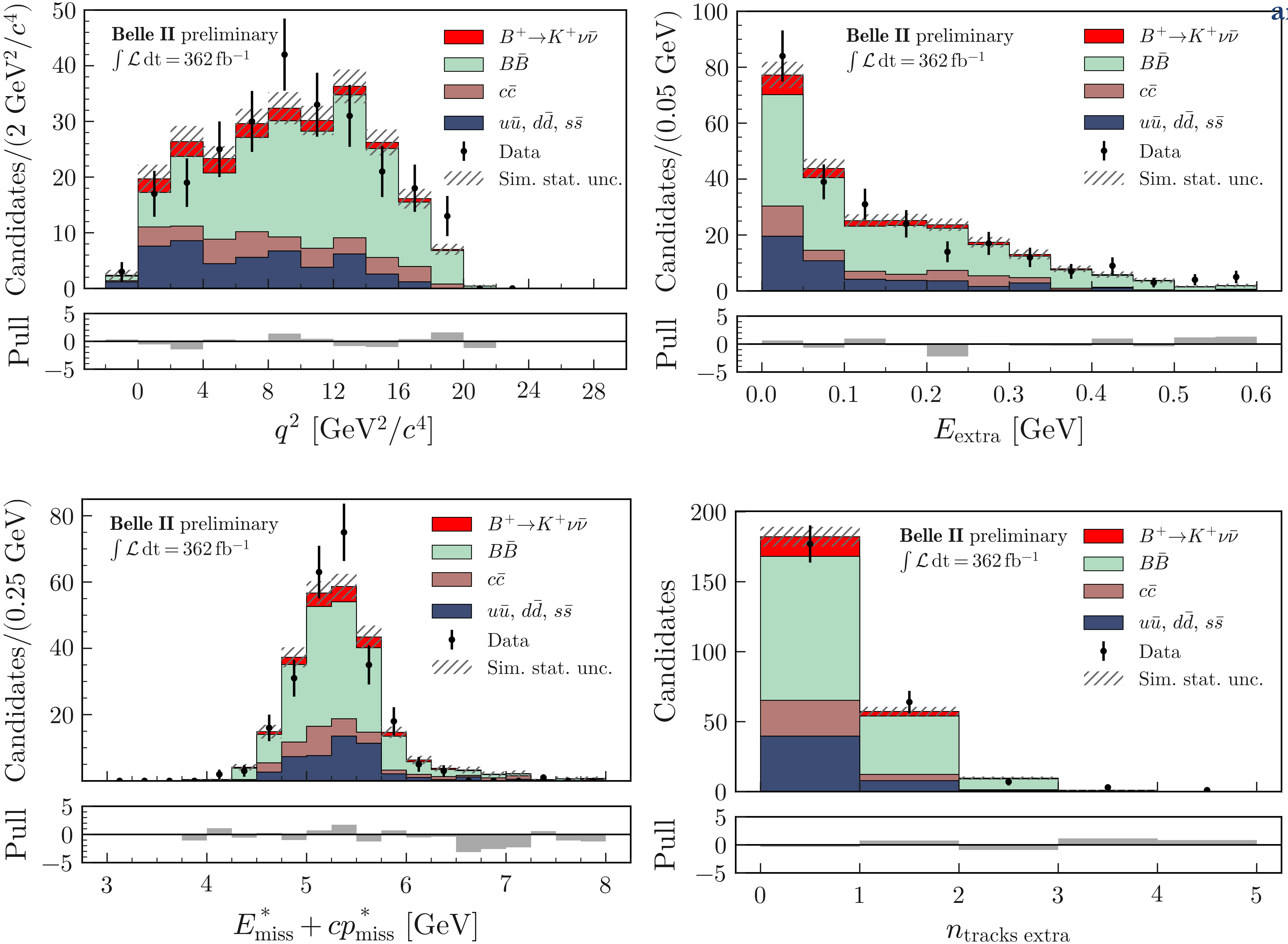

HTA post-fit

$\mu(\mathrm{BDT}_h) > 0.4$

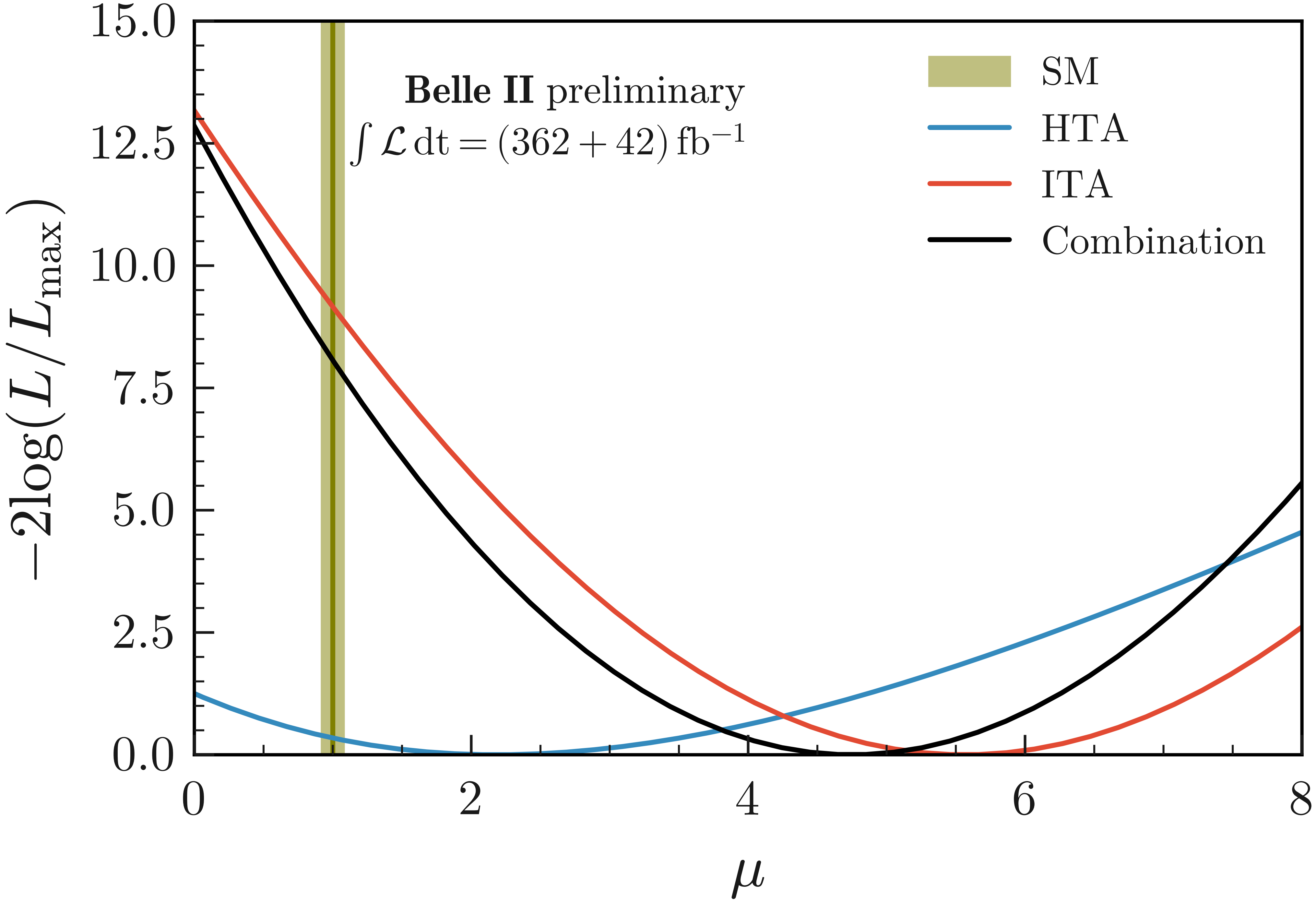

FIG. 16. Twice the negative log-likelihood ratio as a function of the signal strength μ for the ITA, the HTA, and the combined result. The value for each scan point is determined by fitting the data, where all parameters but μ are varied.

$B^+ \to K^+\nu\bar{\nu}$ (combined)

- Prob(null signal of $B^+ \to K^+\nu\bar{\nu}$) = 0.012% (3.5σ)
- Prob($B^+ \to K^+\nu\bar{\nu}$ from SM only) = 0.17% (2.7σ)

arXiv:2311.14647

Stability checks

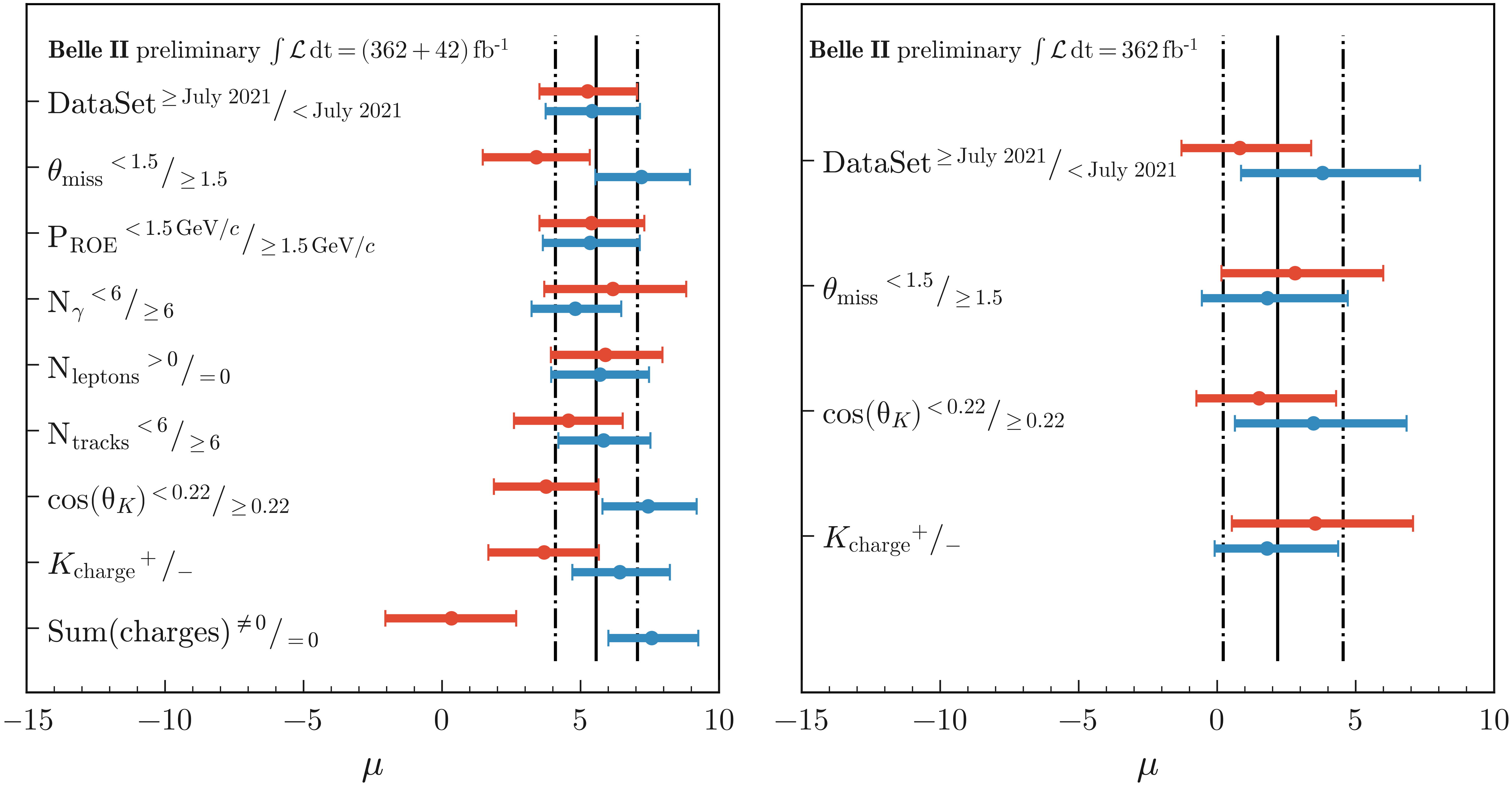

arXiv:2311.14647

$\mathcal{B}(B^+ \to K^+\nu\bar{\nu})$ global picture

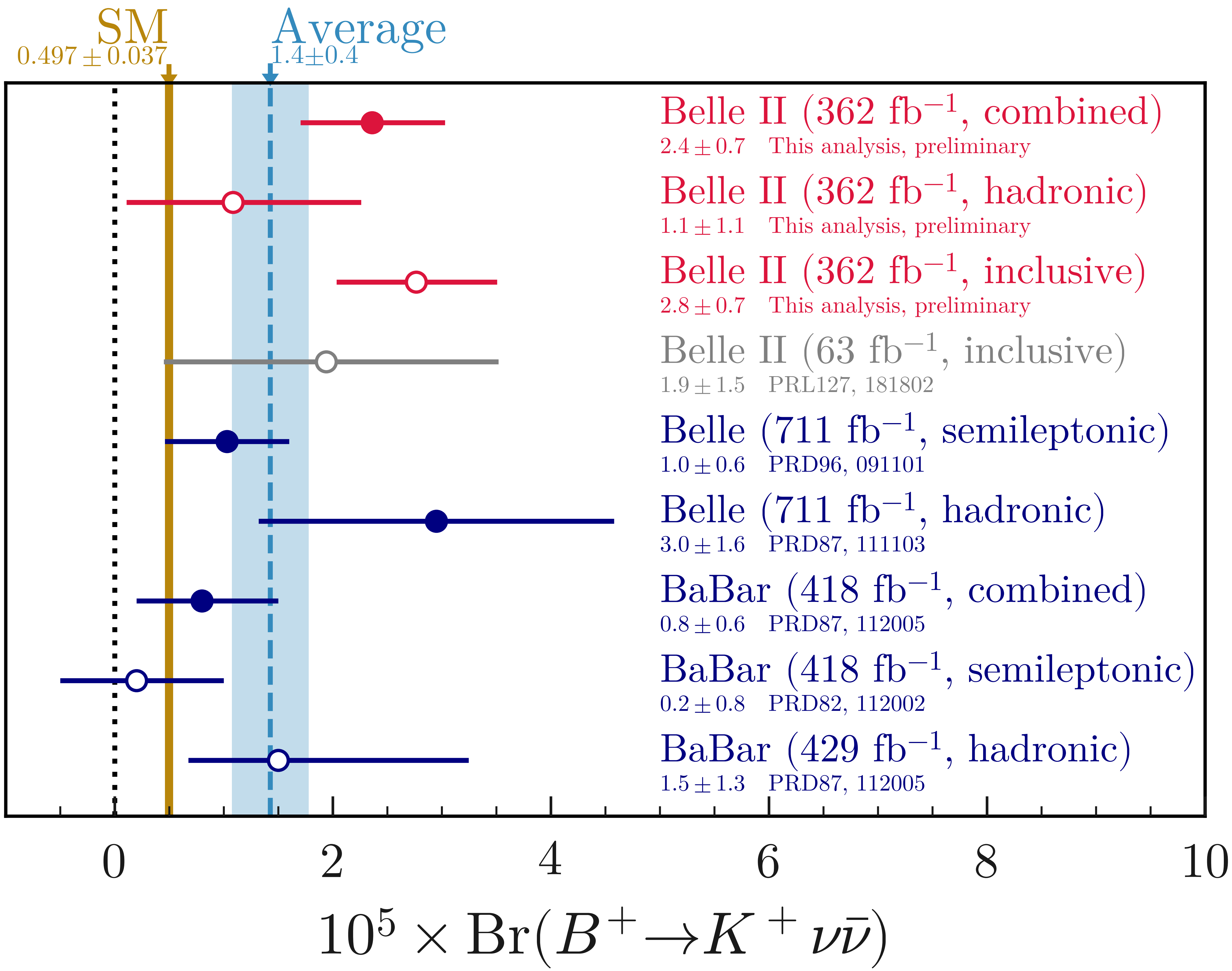

Closing

- With a very clean initial state of e^+e^- collision, equipped with a hermetic Belle II detector covering near 4π around the interaction point, we can study many subjects involving final states with missing particles by using $(E, \vec{p})$ conservation.
- In this talk, we have presented just a few selected topics including ALP search (2020), test of LFU with $\tau \to \ell\nu\bar{\nu}$, and $B^+ \to K^+\nu\bar{\nu}$.
- By combining two (nearly independent) analysis methods, Belle II has observed evidence for $B^+ \to K^+\nu\bar{\nu}$ at 3.5σ, which is above SM prediction by 2.7σ.

Thank you!

Appendices

$e^+e^- \to \Upsilon(4S)$ as a B-factory

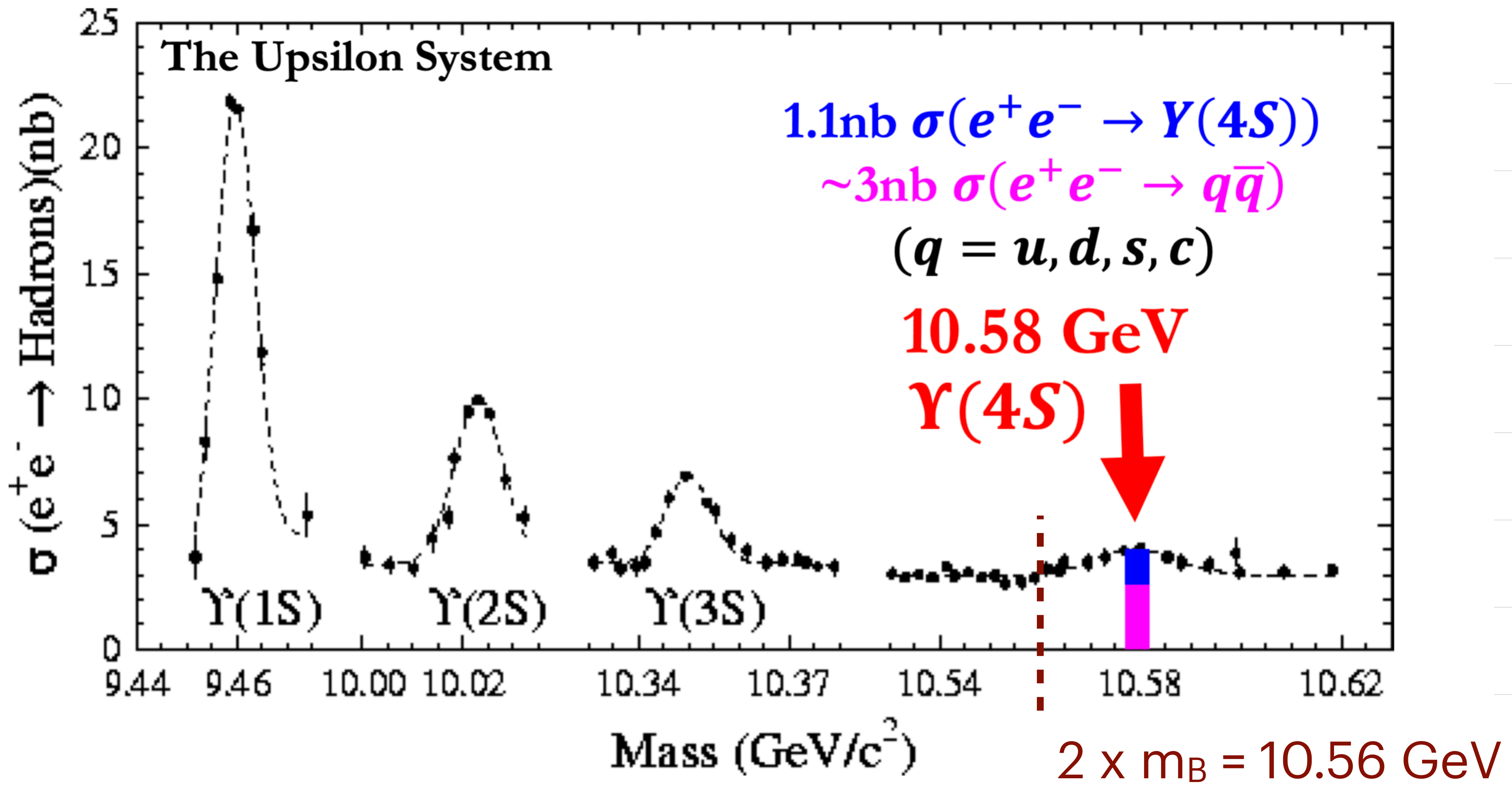

- $\mathcal{B}(\Upsilon(4S) \to B\overline{B}) > 96\%$, with $p_B^{CM} \sim 0.35$ GeV/c
- nothing else but $B\overline{B}$ in the final state
  $\therefore$ if we know $(E, \vec{p})$ of one B, the other B is also constrained

Key variables of B decays

$$\Delta E = E_B^* - \sqrt{s}/2$$

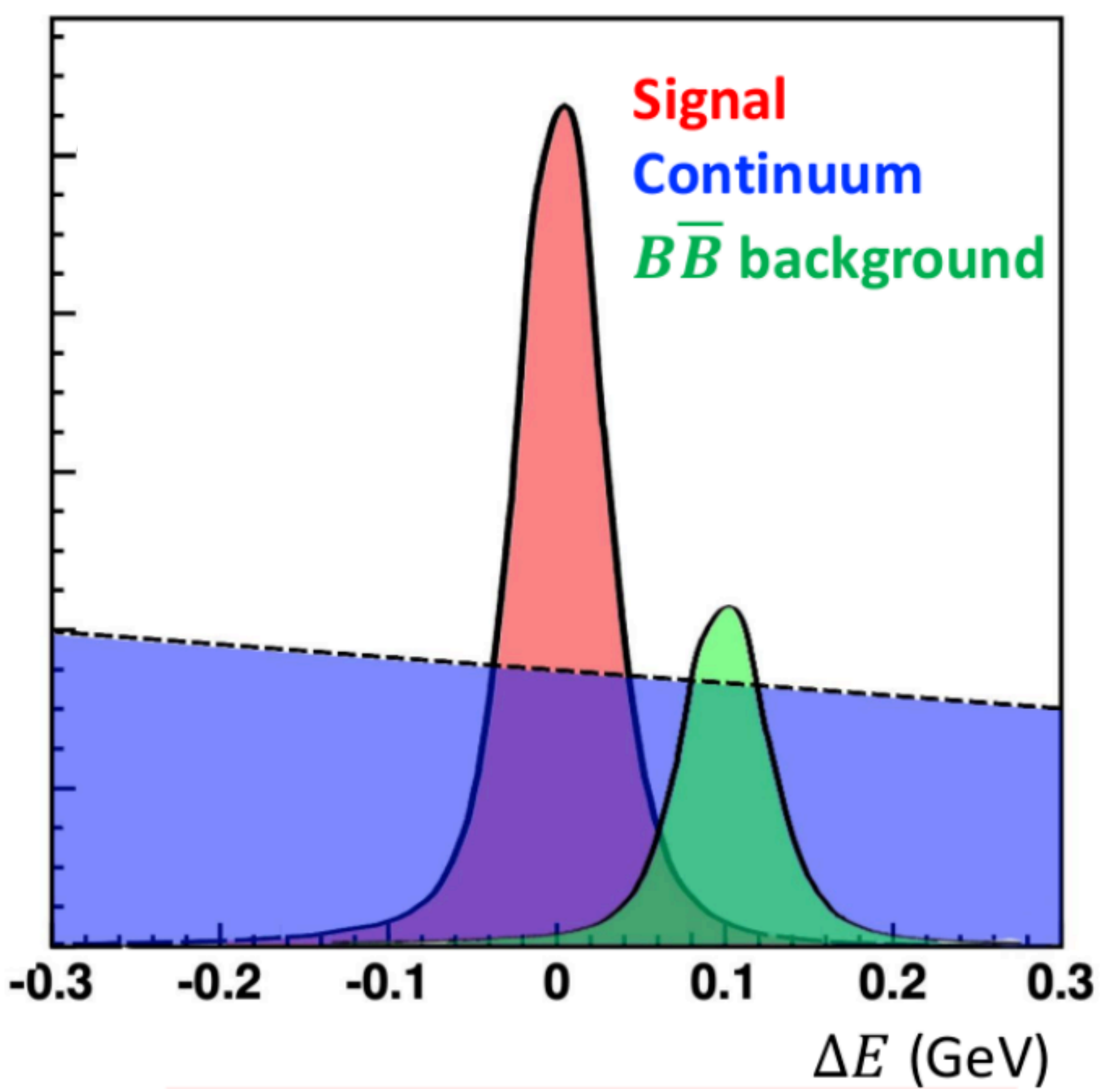

$$M_{bc} = \sqrt{(\sqrt{s}/2)^2 - \vec{p}_B^{\,*2}}$$

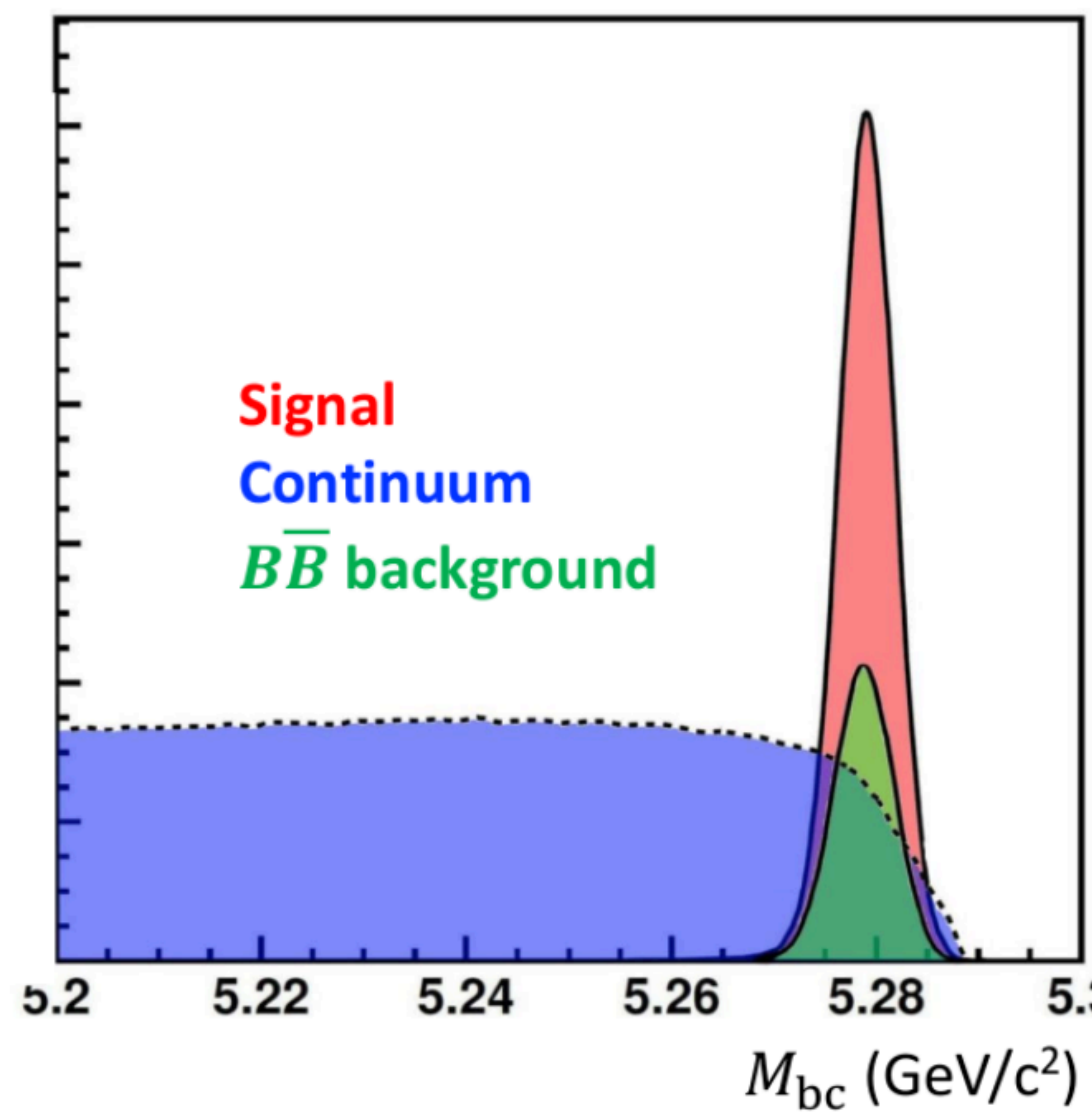

Full Event Interpretation (FEI)

- FEI algorithm to reconstruct B_{tag}
  - uses ~200 BDT's to reconstruct $\mathcal{O}(10^4)$ different B decay chains
  - assign signal probability of being correct B_{tag}

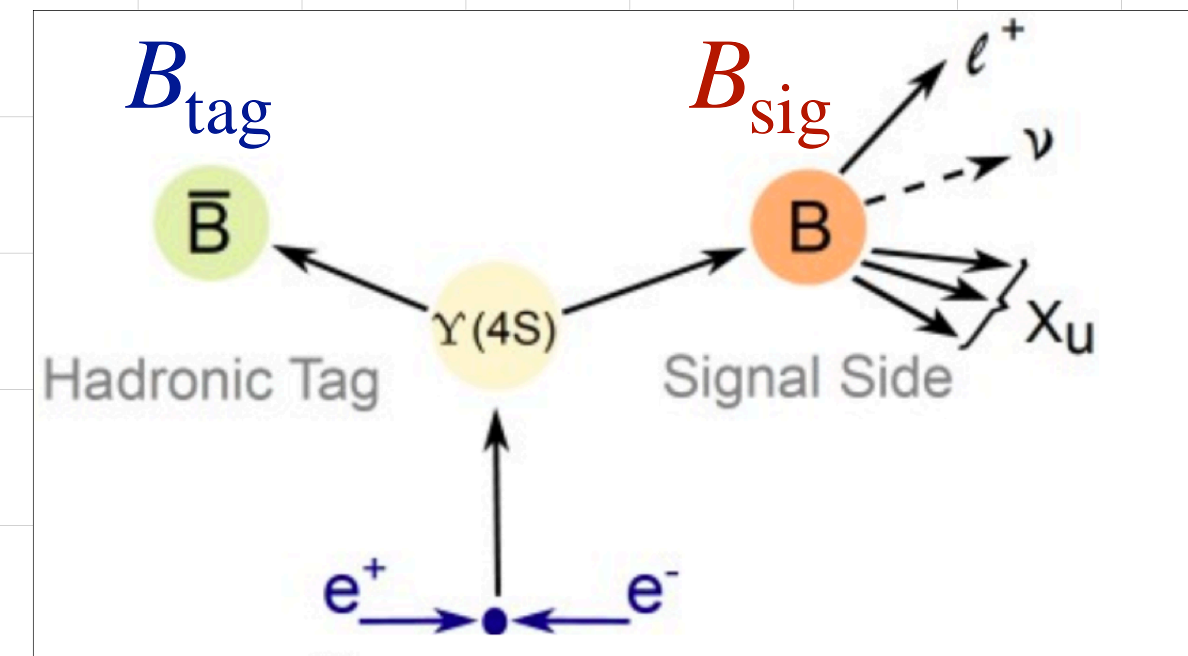

Comput Softw Big Sci 3, 6 (2019)

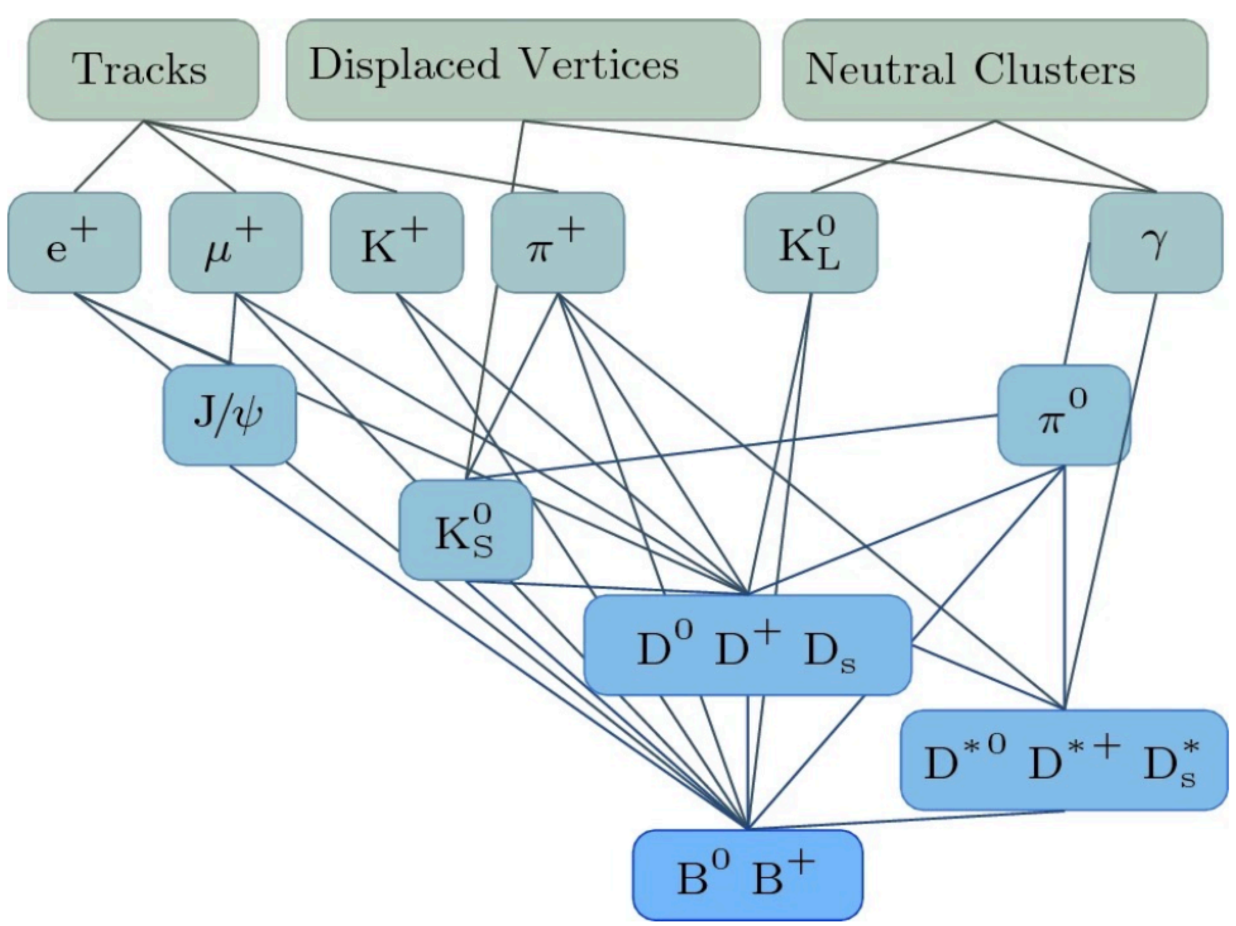

arXiv:2008.060965